

**Honeybee visual cognition: a miniature brain's
simple solutions to complex problems**

Mark Roper

Thesis submitted in partial fulfilment of the
requirements of the Degree of Doctor of Philosophy

Queen Mary University of London

July 2017

Preface

To begin this thesis, it is seemingly appropriate to start with a quote that beautifully exemplifies why we should study honeybees.

“The bee's life is like a magic well: the more you draw from it, the more it fills with water.”

This statement by Nobel laureate Karl von Frisch, a pioneer of honeybee research, is as true today, as it was in the 1920's when he first theorised that honeybees could communicate between nest mates (v. Frisch 1927). In the many decades since von Frisch began his experiments we have seen an amazing escalation in mankind's comprehension of animal psychology, biology, and the fundamental neuroscience of how the brain works. Yet, despite all this scientific knowledge, not to mention our technological advancements, we are still, as scientists, bewildered by how these tiny insects with less than a million neurons in their brains are able to accomplish the rich behavioural and cognitive abilities they exhibit in their daily lives.

In this thesis, I ‘draw a few more drops from the well’, and provide novel insights into just part of the grander endeavour of understanding honeybee cognition. Using both theoretical models, and behavioural experiments with real honeybees, I describe how the miniature brains of these insects may efficiently utilise visual cues to help identify and select potentially rewarding foraging resources. These findings, although focused on the intricacies of honeybee behaviour, may have much wider implications for animal cognition, as well as intriguing future industrial applications.

Statement of Originality

I, Mark Roper, confirm that the research included within this thesis is my own work or that where it has been carried out in collaboration with, or supported by others, that this is duly acknowledged below and my contribution indicated. Previously published material is also acknowledged below.

I attest that I have exercised reasonable care to ensure that the work is original, and does not to the best of my knowledge break any UK law, infringe any third party's copyright or other Intellectual Property Right, or contain any confidential material.

I accept that the College has the right to use plagiarism detection software to check the electronic version of the thesis.

I confirm that this thesis has not been previously submitted for the award of a degree by this or any other university.

The copyright of this thesis rests with the author and no quotation from it or information derived from it may be published without the prior written consent of the author.

Signature:

A handwritten signature in blue ink, appearing to be 'M. Roper', written in a cursive style.

Date: February 2017

Details of collaboration and publications:

In collaborations with my supervisors Prof Lars Chittka and Dr Chrisantha Fernando, and my colleagues Dr Stephan Wolf and Nikolaos Katsaros, I have published the following research papers during my PhD studentship.

Insect Bio-Inspired Neural Network Provides New Evidence on How Simple Feature Detectors Can Enable Complex Visual Generalization and Stimulus Location Invariance in the Miniature Brain of Honeybees

Mark Roper, Chrisantha Fernando and Lars Chittka

PLoS Computational Biology (2017), 13(2): e1005333

The data and models presented in the following two publications did not contribute towards my thesis, nor does the research in this thesis appear in these publications.

Voxel Robot: A Pneumatic Robot with Deformable Morphology

Mark Roper, Nikolaos Katsaros, and Chrisantha Fernando

From Animals to Animats 13, Volume **8575** of the series Lecture Notes in Computer Science

Bumblebees utilize floral cues differently on vertically and horizontally arranged flowers

Stephan Wolf*, **Mark Roper***, and Lars Chittka

Behavioral Ecology (2015), **26** (3):773-781.

*These authors contributed equally to this work.

The following publication was the result of a neuroscience project, under the guidance of Dr Gregory Gage, during my Methods in Computational Neuroscience 2013 summer school in Woods Hole, Boston. The data presented in this publication did not contribute towards my thesis.

Grasshopper DCMD: An Undergraduate Electrophysiology Lab for Investigating Single-Unit Responses to Behaviorally-Relevant Stimuli

Dieu My. Nguyen, **Mark Roper**, Stanislav Mircic, Robert M. Olberg, Gregory J. Gage

The Journal of Undergraduate Neuroscience Education (JUNE), Spring 2017, 15(2): A162-A173

Abstract

In recent decades we have seen a string of remarkable discoveries detailing the impressive cognitive abilities of bees (social learning, concept learning and even counting). But should these discoveries be regarded as spectacular because bees manage to achieve human-like computations of visual image analysis and reasoning? Here I offer a radically different explanation. Using theoretical bee brain models and detailed flight analysis of bees undergoing behavioural experiments I counter the widespread view that complex visual recognition and classification requires animals to not only store representations of images, but also perform advanced computations on them. Using a bottom-up approach I created theoretical models inspired by the known anatomical structures and neuronal responses within the bee brain and assessed how much neural complexity is required to accomplish behaviourally relevant tasks. Model simulations of just eight large-field orientation-sensitive neurons from the optic ganglia and a single layer of simple neuronal connectivity within the mushroom bodies (learning centres) generated performances remarkably similar to the empirical result of real bees during both discrimination and generalisation orientation pattern experiments. My models also hypothesised that complex ‘above and below’ conceptual learning, often used to exemplify how ‘clever’ bees are, could instead be accomplished by very simple inspection of the target patterns. Analysis of the bees’ flight paths during training on this task found bees utilised an even simpler mechanism than anticipated, demonstrating how the insects use unique and elegant solutions to deal with complex visual challenges. The true impact of my research is therefore not merely showing a model that can solve a particular set of generalisation experiments, but in providing a fundamental shift in how we should perceive visual recognition problems. Across

animals, equally simple neuronal architectures may well underlie the cognitive affordances that we currently assume to be required for more complex conceptual and discrimination tasks.

Table of contents

Abstract	6
Table of contents	7
Figures and tables	10
Chapter 1: Introduction	12
1.1 Honeybees as a model system.....	12
1.1.1 Honeybee compound eyes, optic lobes and mushroom bodies.....	13
1.1.2 Neuronal minimalism and response specificity	20
1.2 The study of honeybee visual cognition	23
1.2.1 Y-Maze flight arena	25
1.2.2 PER, SER & virtual reality arenas.....	29
1.3 Structure of the thesis	31
Chapter 2: Theoretical models of how honeybees may discriminate and generalise simple bars and gratings	35
2.1 Abstract.....	35
2.2 Introduction	36
2.3 Methods.....	38
2.3.1 Pre-processing of patterns.....	38
2.3.2 Calculating lobula neuronal responses	39
2.3.3 Calculating mushroom body Kenyon cell responses.....	45
2.3.4 Calculating Kenyon cell similarity ratios and experiment performances.....	52

2.3.5 Evaluating honeybee and model experimental performances	53
2.4 Results.....	55
2.4.1 Experiment set 1: simple bar and grating pattern discrimination	55
2.4.2 Experiment set 2: fine angle discrimination	61
2.4.3 Experiment set 3: eidetic imagery and orientation discrimination.....	65
2.4.4 Experiment set 4: oriented grating generalisation	69
2.5 Discussion	76
2.5.1 Minimising connections between neuropiles	77
2.5.2 Neuronal response specificity	79
2.5.3 Parallel processing	82
Chapter 3: Theoretical models of how honeybees may discriminate and generalise multi-oriented bar and grating patterns.....	86
3.1 Abstract.....	86
3.2 Introduction	87
3.3 Methods.....	89
3.4 Results.....	94
3.4.1 Experiment set 1: discrimination of multi-oriented bar patterns	94
3.4.2 Experiment set 2: generalisation of multi-oriented bar and grating patterns	101
3.5 Discussion	112
Chapter 4: Theoretical models of how honeybees could solve the ‘above and below’ conceptualisation task	118
4.1 Abstract.....	118
4.2 Introduction	119
4.3 Methods.....	121
4.3.1 Stimuli	121
4.3.2 Simulated experiments – phase 1	122

4.3.3 Simulated experiments – phase 2	123
4.3.4 Simulation procedure	123
4.4 Results.....	125
4.4.1 Simulation results – ‘above and below’ phase 1.....	125
4.4.2 Simulation results – ‘above and below’ phase 2.....	127
4.5 Discussion	131
Chapter 5: High-speed videography analysis of honeybee flight trajectories provides new evidence on how bees solve the ‘above and below’ conceptualisation task....	137
5.1 Abstract.....	137
5.2 Introduction	138
5.3 Methods.....	140
5.3.1 Apparatus.....	140
5.3.2 Stimuli	143
5.3.3 Experiment trial procedure.....	144
5.3.4 Pre-training – ‘above and below’ phase 1.....	145
5.3.5 Main training – ‘above and below’ phase 2	146
5.3.6 Video analysis – annotation	147
5.4 Results.....	149
5.4.1 Experimental issues (sample size and video analysis)	149
5.4.2 Individual performances	150
5.4.3 Flight analysis.....	152
5.4.4 Hypotheses comparison.....	157
5.5 Discussion	159
5.6 Individual flight transition details	166
Chapter 6: General discussions	172
6.1 Main findings	172

6.2 Model limitation and future work	175
6.3 Thesis implications for behavioural experiments	179
6.3 Final thoughts	186
Acknowledgments	188
References.....	189

Figures and tables

Figure 1.1 Schematic view of the honeybee brain	14
Figure 1.2 Top-down schematic view of the Y-Maze flight arena.	26
Figure 2.1 Schematic representation of the stimuli pre-processing	39
Figure 2.2 Schematic representation of the model neuron responses	42
Figure 2.3 Simplified example of the lobula orientation-sensitive neuron (LOSN) type A and type B firing rate response calculations.....	44
Figure 2.4 Schematic representation of SEO and EAI models.	47
Figure 2.5 Summary of honeybee empirical results and model performances for discrimination tasks of simple bars and gratings	57
Figure 2.6 Summary of model performances for discrimination tasks of simple bars and gratings when scaled	58
Figure 2.7 Model Kenyon cell activation for scaled bar patterns	60
Figure 2.8 Summary model performances for discrimination of fine angle differences	63
Figure 2.9 Performance of EAI_AB with differing edge lengths	64
Figure 2.10 Summary of honeybee behaviour and model performance for discrimination of two horizontal gratings	67
Figure 2.11 Summary of honeybee behaviour and model performance for discrimination of training grating patterns	70
Figure 2.12 Summary of honeybee behaviour and model performance for generalisation between training patterns	72
Figure 2.13 Summary of honeybee behaviour and model performance for generalisation to novel stimuli tasks.....	74
Figure 2.14 Analysis of SEO_AB and EAI_AB model performance for generalisation between vertical gratings.....	76
Figure 3.1 Schematic representation of DISTINCT and MERGED models	91
Figure 3.2 Exemplary summary of honeybee behaviour and model performance for discrimination of multi-oriented patterns.....	96
Figure 3.3 Model performance for discrimination of multi-oriented patterns when horizontally offset	97
Figure 3.4 Model Kenyon cell activation for offset grating quadrant pattern	100
Figure 3.5 Honeybee behaviour and model performance for simple generalisation of quadrant multi-oriented bar patterns	103

Figure 3.6 Honeybee behaviour and model performance when generalising to a modified CS+ quadrant pattern	104
Figure 3.7 Honeybee behaviour and model performance when generalising to patterns when there is only a single quadrant different between CS+/ TS ^{COR} and TS ^{INC} ..	105
Figure 3.8 Honeybee behaviour and model performance when generalising to a mirror image or left right reversed quadrant patterns.....	107
Figure 3.9 Honeybee behaviour and model performance when generalising to a chequerboard pattern	108
Figure 3.10 Model Kenyon cell activation for generalization experiments Batch 2	110
Figure 3.11 Summary of honeybee behaviour and model performance for generalisation of quadrant patterns.....	111
Figure 3.12 Honeybee behaviour and model performance for the discrimination of simple cross patterns	117
Figure 4.1 Model performance for discrimination of referent in ‘above and below’ phase 1 simulations	126
Figure 4.2 Summary of model performances for ‘above and below’ phase 2 simulations when target shape is the same on all patterns	128
Figure 4.3 Summary of model performances for ‘above and below’ phase 2 simulations when target shape is different on the CS+ stimulus to those on the TS ^{COR} / TS ^{INC} stimuli.....	129
Figure 4.4 Summary of model performances for ‘above and below’ phase 2 simulations when referents are in different locations and target shape is different on the CS+ stimulus to those on the TS ^{COR} / TS ^{INC} stimuli	130
Figure 4.5 Schematic representation of the honeybee field of view when observing ‘above and below’ patterns	135
Figure 5.1 Y-Maze apparatus used for ‘above and below’ experiments.....	142
Figure 5.2 Pictures of honeybees approaching feeder tubes during the ‘above and below’ pilot study.....	143
Figure 5.3 Tracking of honeybees approaching a pattern	148
Figure 5.4 Individual honeybee performances for the ‘above and below’ experiments	151
Figure 5.5 Honeybee initial arm choice and subsequent decision	154
Figure 5.6 Honeybee initial fixation point during above and below experiments	156
Figure 6.1 Example graphs displaying bumblebee discrimination task learning curves.	183
Figure 6.2 Example of combined discrimination and generalisation feature patterns ..	185
Table 2.1 EAI_AB LOSN to Kenyon cell configuration types	49
Table 2.2 EAI_ABC LOSN to Kenyon cell configuration types.....	51
Table 2.3 LOSN type A, B responses in each quadrant to scaled single bar patterns	59
Table 2.3 LOSN type A, B and C responses in each quadrant to grating patterns	68
Table 3.1 LOSN type A & type B responses in each quadrant of spiral, cross and grating patterns	98
Table 3.2 LOSN type A & type B responses in each image quadrant of the quadrant grating patterns offset horizontally	99
Table 5.2 Flight transition counts for honeybee ‘above and below’ experiments	157
Table 5.2 Individual flight transitions for honeybee Above_A	168
Table 5.3 Individual flight transitions for honeybee Below_A.....	169
Table 5.4 Individual flight transitions for honeybee Below_B.....	171

Chapter 1: Introduction

1.1 Honeybees as a model system

Mankind has a long-standing fascination with honeybees, their social structure, their proverbial work ethic, and of course their commercial importance as crop pollinators and honey producers. In recent decades they have also started to play a fundamentally different role. The old viewpoint of ‘lower life forms’ as mindless automatons has slowly been replaced with a realisation that learning, memory and cognition is important to all animals (Dukas 2004). Here, honeybees have proved to be extremely useful to the study of animal cognition. Not only do they exhibit their own complex dance “language” (v. Frisch 1927), astounding olfactory learning abilities (Bitterman, Menzel et al. 1983, Laska, Galizia et al. 1999), but, more applicable to this thesis, they also possess remarkable visual learning capabilities. This, combined with their relentless appetite for collecting nectar, means that these visual cognitive abilities can be easily tested under laboratory conditions.

In this thesis I primarily focus on modelling the worker honeybee (*Apis mellifera*) brain and its ability to discriminate and generalise achromatic patterns. Before describing some of the earlier behavioural work conducted in this area, I begin with an overview of the honeybee eyes and the subsequent visual processing within the bee brain.

1.1.1 Honeybee compound eyes, optic lobes and mushroom bodies

Compound eyes

The worker honeybee has two compound eyes, each composed of ~5,500 individual optical units (ommatidia), whose lenses are arranged in a quasi-hexagonal grid (Streinzer, Brockmann et al. 2013). Each ommatidium contains a biconvex cuticle lens, formed from two primary pigment cells and a crystalline cone formed from four Semper cells. The lens guides the received light to the top of a central light channel (rhabdom), which is subsequently surrounded by two more secondary pigment cells that prevents light escaping into adjoining ommatidia (Varela and Wiitanen 1970). In this way each ommatidium receives ~2.5° of the visual field, with an approximate ½° overlap of the respective visual fields of each of its six adjacent neighbours (Laughlin and Horridge 1971, Seidl and Kaiser 1981). Each rhabdom is composed of eight long retinal cells and a ninth retinal cell adjoining at the base (Skrzipek and Skrzipek 1974, Ribi 1975). Each of the eight retinal cells has ~40,000 highly oriented microvilli that align towards the centre of the rhabdom. The microvilli contain 500 to 2,000 rhodopsin visual pigments that react maximally to photons at either the ultraviolet (~350nm), blue (~440nm), or green (~540nm) wavelengths (Menzel and Blakers 1976, Peitsch, Fietz et al. 1992). Photons, of the correct wavelengths, interacting with the rhodopsin cause a cascade of protein translations that induces a depolarising effect of 1-2mV per reaction (Land and Chittka 2012), it is the summation of these reactions that subsequently gets transmitted to the bee brain as electrical signals. Each ommatidium extends its nine retinal cell axons to the optic lobes, six of these, called short visual fibres, are maximally sensitive to the green wavelengths. Of the other three retinal cells, named long visual fibres, two are either sensitive to blue or ultraviolet (uv) wavelengths (with a higher distribution of the uv types in the dorsal regions of the eye (Wakakuwa, Kurasawa et al. 2005)).

Regrettably, there is still no conclusive evidence, although considerable debate (Menzel and Snyder 1974, Wakakuwa, Kurasawa et al. 2005), for the wavelength sensitivity of the third long visual fibre.

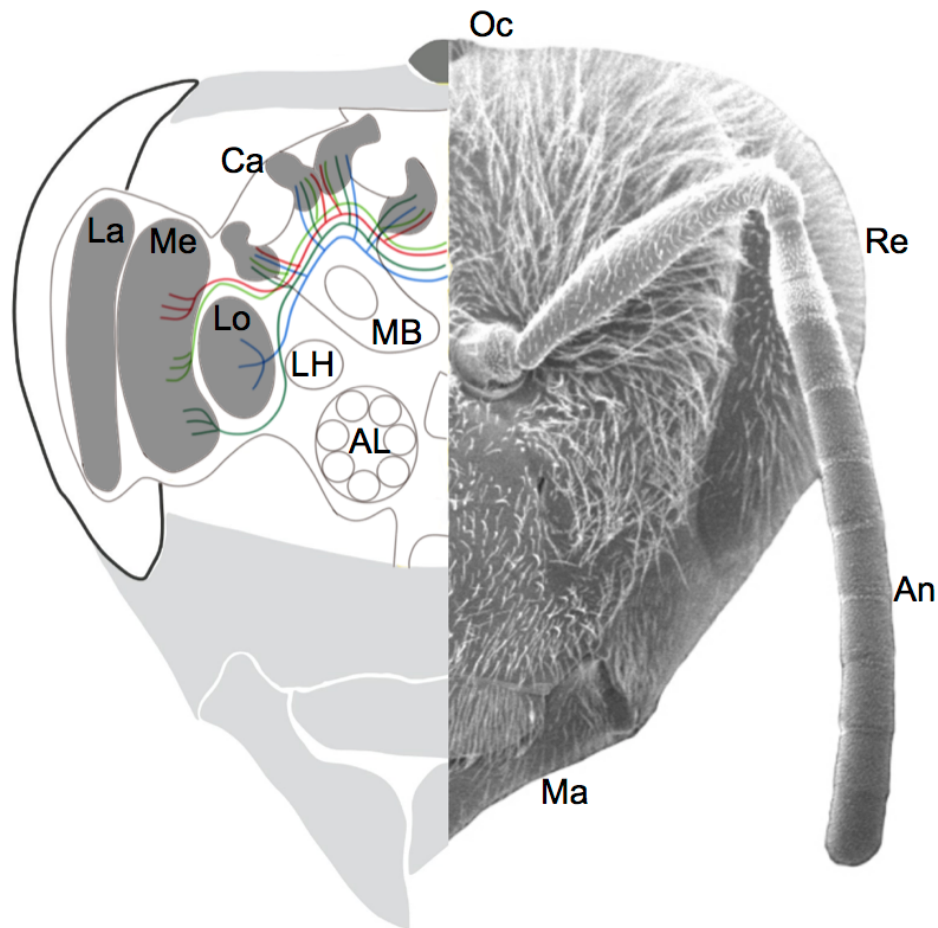


Figure 1.1 Schematic view of the honeybee brain. **Left:** Representation of the optic lobes (La: lamina, Me: medulla, Lo: lobula) and the neuronal pathways to the mushroom bodies (MB) learning centres. Both the medulla (red and green lines) and lobula (blue lines) extend fibres to the calyxes (Ca) of both the ipsilateral and contralateral hemisphere mushroom bodies. Mushroom bodies also receive olfactory information from the ipsilateral antenna lobe (AL) and lateral horn (LH). Adapted from (Ehmer and Gronenberg 2002). **Right:** Front view of the bee head showing the compound eyes / retina (Re), ocelli: three small lens eyes on the top of the bees head (Oc), the antennae (An) and mandibles (Ma). Adapted from (Chittka and Brockmann 2005).

Optic lobes

Beneath the retina the honeybee has three optic lobes, the lamina, medulla and lobula (Fig 1.1). Within the first of these, the lamina, each of the nine retinal axons from an ommatidium is confined within a single lamina cartridge. Here, the short visual fibres (green channel retinal cells) connect to three distinct lamina monopolar cells present in each cartridge (with consistent synaptic connections between the cell types throughout the eye (Ribi 1975)). These short visual fibres subsequently terminate within the lamina substrate. In contrast, the long visual fibres, which make only occasional connections to the monopolar cells, extend through the lamina to the medulla (2nd optic ganglion). One of the monopolar cells provides excitatory synapses to, and receives synaptic input from, the same monopolar cell type in each of the immediately adjacent lamina cartridges. A fourth monopolar cell, being present in about one in every four cartridges, provides inhibitory synaptic connections to adjacent cartridge monopolar cells (Ribi 1975). Each of these three or four monopolar cells per cartridge extends an axonal like fibre, alongside the three long visual fibres, into the medulla.

The medulla maintains the highly columnar structure seen in the retina and lamina, however, the deeper into the eight, easily identifiable, substrate layers within the medulla the sparser these columnar neurons become (Ribi and Scheel 1981). Indeed, both the long visual fibres and lamina monopolar cells that provide the initial visual information to the medulla, extend no lower than the third definable layer (Ribi and Scheel 1981). In addition to these columnar neurons, the medulla contains a large number of tangential (amacrine) inter-neurons. These neurons extend dendritic fibres perpendicular to the columns with a large variety of morphologies. Different neuron types extend arborisations into specific combinations of the different medulla layers, as well as spanning a multitude of different regions and widths of the columnar array (Ribi

and Scheel 1981, Ehmer and Gronenberg 2002). Unfortunately, unlike the lamina, no detailed connectomics of the medulla synapses are available for honeybees. 3D reconstruction of a single complete medulla column surrounded by its six neighbouring columns in the fruit fly (*Drosophila*), showed that of the ~900 neurons detected, a remarkable ~315,500 postsynaptic sites existed, and over 2,500 presynaptic sites within the central column's neurons alone (Takemura, Xu et al. 2015). Regrettably, this research wasn't able to detail where the neurons' dendritic fibres originated from, or extended to, once outside of the reconstruction zone. This does however suggest that a huge amount of neuronal processing is being done as visual information is being transmitted through the medulla. Electrophysiology on the bumblebee (*Bombus impatiens*) brain has shown that both the firing characteristics, and visual stimuli sensitivities, of the different medulla neurons change depending on their respective layers. Those with arborisations in the early layers responded mostly to either broad band colour ranges (i.e. sensitive to a large range of wavelengths) or very narrow bands, with the neurons typically having distinct on / off responses to stimuli (Paulk, Dacks et al. 2009). Neurons from later layers showed much more complex colour opponent responses, responding for example to green wavelengths, but being inhibited if ultraviolet light was also present. These neurons also exhibited much more complex firing rate characteristics, producing either phasic or tonic responses, or in some instances both, depending on the particular visual stimuli provided (Paulk, Dacks et al. 2009). Similar, but limited, recordings of colour opponent neurons have also been made in honeybees (Kien and Menzel 1977). Recordings of orientation selective medulla neurons are unavailable to date in honeybees, although, several classes of neurons maximally sensitive to particular edge orientations have been found in the medulla of numerous other insects (McCann and Dill 1969, James and Osorio 1996, Okamura and

Strausfeld 2007, Spalthoff, Gerdes et al. 2012). The final class of medulla neurons, transmedulla neurons, extend dendritic fibres outside of the medulla substrate and convey information to the posterior protocerebrum (thought to be involved in processing motion) (Paulk, Dacks et al. 2009), the mushroom bodies (learning centres) (Gronenberg 2001), as well as to the lobula (the 3rd and final optic ganglion) (Witthöft 1967).

The lobula is the smallest of the three optic lobes, receiving only half as many inputs from the medulla, as the medulla does from the lamina (Witthöft 1967). In the first four layers of the lobula, the columnar structure seen throughout the optic lobes is, for the most part, continued (Ribi and Scheel 1981). Although some large field neurons extending over whole eye regions have been reported in bumblebees (Paulk, Phillips-Portillo et al. 2008). In layers 5 and 6, this structure is abandoned with a ‘spaghetti’ web of very wide-field and large-field neurons, each with individually branched dendritic fibres extending and displaying arborisations over large regions of the columnar inputs on the layer 4-5 border. Extracellular recordings from the lobula indicate wide-field neurons, responding to stimuli in particular sub-regions of the eye, characterised as either colour opponent neurons or non-colour opponent (i.e. broad band and narrow band) neurons (Kien and Menzel 1977, Yang, Lin et al. 2004), as well as the very large-field neurons that are either direction or edge orientation sensitive; these respond to stimuli moving anywhere across large regions of the eye (Bishop 1970, Maddess and Yang 1997, Maddess, Davey et al. 1999). Recent bumblebee recordings again provide similar, and more detailed results (Paulk, Phillips-Portillo et al. 2008), although some differences may exist between the species: in bumblebees, the layer 1-4 neurons respond mostly to achromatic motion cues (moving bars or gratings), whereas layer 5-6 neurons respond to colour cues. Neurons extending through all layers 1-6 are columnar

(only receiving input from a small region of the medulla) and respond selectively to combinations of colour and: motion, direction or orientation of the stimuli. Layer 1-4 extrinsic neurons leave the lobula and extend axons to the posterior protocerebrum; these neurons reliably fire when stimuli are presented, but exhibit inconsistent firing rates or variances in firing initiation after a stimulus onset. Layer 5-6 neurons extend to the mushroom bodies (Fig 1.1) and the dorsal and lateral protocerebrum; these neurons have much higher spiking precision (consistent firing patterns and precise response firing times to a given stimulus) and appear highly phasic in nature (Paulk, Phillips-Portillo et al. 2008) (see also (Hertel and Maronde 1987) for a review of the corresponding honeybee lobula optic tracts).

Mushroom bodies

In this thesis I investigated the honeybees ability to learn and identify achromatic patterns, as such, the theoretical models produced (Chapter 2 and Chapter 3) concentrated on a particular class of large-field neurons from the lobula, and their connections within the mushroom bodies. The mushroom bodies are thought to be the primary site for associative learning and memory, with supporting evidence at least for olfactory learning (Hammer 1993, Hammer 1997, Heisenberg 2003, Devaud, Papouin et al. 2015). However, visual learning has also been implicated in other brain regions in fruit flies (dorsal and lateral protocerebrum (Liu, Seiler et al. 2006), central complex (Seelig and Jayaraman 2013)). Nonetheless, here, I focus on the honeybee mushroom bodies.

The mushroom bodies themselves are located in the dorsal region of the brain, with a mushroom body near the central line of each hemisphere (Fig 1.1). Each of these is composed of a pair of calyces, cup shaped structures, which receive sensory input. These calyces merge at the bottom to form a stalk called the pedunculus (their name

indicating their resemblance to mushrooms). The calyces are subcategorised into three regions based on the differing sensory modalities that they receive; these are the lip, collar, and basal ring. The lip receives olfactory input from the ipsilateral antennal lobe, the collar receives visual information from each medulla and lobula, and the basal ring contains a mixture of sensory modalities, also including gustatory and mechanosensory inputs (Mobbs 1984, Gronenberg 2001, Ehmer and Gronenberg 2002). The collar, which receives the majority of the visual input, can be further differentiated into six specific layers. Layers 1, 3 and 5 receive input from the ventral region of the medulla. Inputs to layers 2 and 4 come from the dorsal medulla, and the sixth layer from lobula outputs. Within the layers there appears to be no separation by retinotopic origin (i.e. no distinctions to whether the neurons originated from the left or right side of the optic lobe, and ergo corresponding visual field regions) or the distribution of inputs from the left and right eyes (Ehmer and Gronenberg 2002). The mushroom body neuropile is formed from ~170,000 Kenyon cells (Withhöft 1967), whose cell bodies lie in the cup of the calyces, the dendritic fibres of these cells actually form the core structure of the calyces. The Kenyon cells appear in two general forms, Class I (often referred to as spiny) Kenyon cells that have large dendritic trees that spread out over a fan shaped areas of the calyx, and Class II (clawed) Kenyon cells which appear as a single main dendritic fibre with a small number of 5 - 15 boutons that appear as small blobs (or claws) a short distance from the main fibre (Strausfeld 2002). These boutons contain a bundle of post-synaptic synapses that connect to the sensory input projection neurons and also to GABAergic inhibitory interneurons (Mobbs 1984, Ganeshina and Menzel 2001). Within the calyx the octopaminergic VUMmx1 neuron also synapses with the Kenyon cells and sensory projection neurons (Hammer 1993, Hammer 1997). This VUMmx1 neuron generates a response when sucrose is detected at either the bees'

antennae or proboscis (tongue) and is thought to provide a pivotal role in associative learning (Szyzka, Galkin et al. 2008). After the pedunculus, the Kenyon cell fibres take on a more axonal like representation and then bifurcate to form the two mushroom body lobes (alpha lobe and beta lobe); here they create pre-synaptic connections to the mushroom body extrinsic neurons (Rybak and Menzel 1993). These extrinsic neurons in turn connect to the ipsilateral lateral horn, and the lobes of the contralateral mushroom body (Mobbs 1984, Rybak and Menzel 1993, Strausfeld 2002). It is the output of these extrinsic neurons that is then thought to help govern the honeybees' behaviour.

1.1.2 Neuronal minimalism and response specificity

The last section gave a brief summary of the flow of visual information through the neuropiles of the honeybee brain. It is important to remember that all this structure is confined within a volume of 1mm^3 , equivalent to just a tenth of a grain of rice! The miniature nature of the honeybee brain is in part aided by the invertebrate neurons themselves. Vertebrates "typically" have neurons composed of a central cell nucleus with a single axon that transmits an electric signal away from the cell body; in addition they have multiple dendrites that extend out-ward from the cell body that receive inputs from the axon termini of other neurons (Lodish 2000). In contrast, invertebrate brains are built from a number of distinct neuropiles, and as discussed above these are composed of dense arrangements of dendritic fibres (Ribi 1975, Ribi and Scheel 1981, Mobbs 1984, Galizia, McIlwraith et al. 1999). The cell bodies for these fibres are most often located on the surrounding edges of these structures (Withöft 1967, Ribi 1975, Strausfeld 2002). The dendritic fibres themselves contain both pre- and post-synaptic receptors blurring the distinction between the archetypal classification of dendritic

inputs and axonal outputs (Ribi 1975) (Kien and Menzel 1977). This arrangement does however allow a large number of synaptic connections to be configured within a very small area, and distinct layers within the neuropiles allow the required synaptic connections to be more easily established (Ribi and Scheel 1981, Ehmer and Gronenberg 2002). In addition to this elegant form of neuronal compression, insects also reduce the overall number of neurons they require through neuronal minimalism and response specificity. An extreme example of the former, neuronal minimalism, is the honeybees' reward response mechanism, here a **single neuron** the aforementioned VUMmx1 transmits a reward signal when sucrose is detected in either the honeybee's proboscis (tongue) or antennae to the rest of the brain's learning centres (mushroom bodies, central complex and lateral horn) (Hammer 1993). Although other neurons (Hammer 1997), as well as molecular and gene expression mechanisms (McNeill, Kapheim et al. 2016) have been implicated in the honeybee reward processing system, it is still remarkable that this one neuron has afferents in so many brain regions. Similarly, whereas the mammalian brain often uses highly imprecise responses - but from a large population of neurons - to transmit information around the brain (Pouget, Dayan et al. 2000), the insect optic ganglia extend only a very small number of distinct neuronal fibres to the higher brain regions (Strausfeld 2002), these transmit highly specific and precise types of responses depending on the presented stimuli; such as the bumblebee (*Bombus impatiens*) extrinsic medulla (2nd optic ganglion) neurons that respond in a phasic manner to one visual stimuli and produce tonic responses to another (Paulk, Dacks et al. 2009). In a similar way, honeybee (*Apis mellifera*) lobula large-field orientation-sensitive neurons (LOSNs) (Maddess and Yang 1997) have very precise but brief phasic responses that are maximally responsive to particular oriented edges within their receptive fields. Humans also have similar neurons that respond maximally to a

particular range of orientations (Yacoub, Harel et al. 2008); these neurons are organised into complex cortical maps with pinwheel configurations with at least six different regions maximally-sensitive to distinct orientations (Blasdel and Salama 1986). They also exhibit adaptive tuning curves (dependent on prior stimuli exposure) which can sharpen their responses to just a $\sim 50^\circ$ orientation range (Ringach, Hawken et al. 1997). In contrast, the honeybee neurons present a continuous firing rate response curve (above baseline firing rate) for the full 180° range of orientations with a consistent broad ca. 90° half-width tuning curves no matter where the moving stimulus is first presented, across the whole width of the eye. Interestingly, and in line with neuronal minimalism, to date only two such LOSN types, with two specific maximal sensitivities, have been discovered in honeybees (Maddess and Yang 1997).

These neuronal characteristics may allow a large breadth of sensory information to be compressed into a small number of neurons and subsequently passed without the necessity for substantial neuronal pathways throughout the rest of the insect brain. Indeed, one of the most striking examples of neuronal minimalism within the honeybee brain is the incredibly small number of neurons that extend from the optic lobes to the other brain regions. Considering that each of the bees' compound eyes contains approximately 5,500 individual lenses (Streinzer, Brockmann et al. 2013), and the three optic ganglia (lamina, medulla, lobula) contain $340,000 \pm 15\%$ neurons (Witthöft 1967), current estimates suggest that only ~ 340 and ~ 50 of these neurons extend from the medulla and lobula to the mushroom body calyces respectively (Ehmer and Gronenberg 2002).

Given that the whole honeybee brain contains only $\sim 960,000$ neurons and less than 400 of these neurons appear to extend from the optic lobes to the mushroom body learning centres, you might expect that the visual cognitive abilities of honeybees to be

only rudimentary at best, but as we will see throughout this thesis, this is most definitely not the case.

1.2 The study of honeybee visual cognition

As central-place foragers, worker bees may leave the nest and travel many kilometres on a single foraging bout, identifying and remembering useful landmarks for their return journeys (Chittka, Geiger et al. 1995, Chittka, Kunze et al. 1995). Once floral resources are found, foragers must learn the specific visual and olfactory cues of rewarding flowers and be able to correctly generalise those cues to the potential differences between conspecific flowers. Even here the bees must be adaptable, learning to prefer, for example, a specific flower colour in one location and a second different colour, in preference to the first, in another location (Collett and Kelber 1988). Similarly, bumblebees have been shown to rapidly transition from one rewarding colour cue to another in just a single foraging bout (Wolf and Chittka 2016), essential as flower species enter and exit bloom during the day. In addition, since not all flowers present themselves in the same way, with many radially symmetrical flowers facing upwards, whereas many others (often bilaterally symmetrical (zygomorphic) flowers) facing sideways, bees need to be flexible in what visual features they learn. Bees also need to learn to simultaneously avoid camouflaged predators, such as crab spiders (Thomisidae) (Morse 1981, Chittka 2001, Dukas and Morse 2005).

In my opinion, one of the most remarkable experimental examples of honeybee visual recognition is their ability to discriminate photos of one human face from other faces (Dyer, Neumeyer et al. 2005), a task that is completely outside of their normal environmental needs. They can even generalise to rotated versions of these learnt faces

(Dyer and Vuong 2008), an ability that has so far only been reported in very few species: humans: (Bulthoff and Edelman 1992), other primates: (Logothetis, Pauls et al. 1995) and pigeons: (Spetch and Friedman 2003). But, as remarkable as this is, it tells us little about *how* the bee brain is able to make the discriminations; do their brains build and store a photographic image of these faces, do they use particular features (e.g. the amount of black or white in the images), or do they identify particular unique landmarks on the pictures? To answer this, and the broader question of how the honeybees discriminate visual stimuli, scientists have broken the problem down into simpler and much more understandable pattern recognition tasks.

In the early 20th century, Karl von Frisch, as well as documenting the aforementioned honeybee waggle dance (v. Frisch 1927), began to conduct the first controlled experiments into the honeybees' visual cognitive abilities. These began with simple colour experiments where the bees were trained to visit a blue card placed on a table top in order to receive a sucrose solution reward; he would then test them with the same coloured card versus either different shades of grey, or different coloured cards (v. Frisch 1914). The bees' ability to consistently go to the correctly coloured blue card, even when no reward was presented (removing any secondary visual or odour cues), showed that bees had some form of colour vision. As described in the section above, we now know the bees in fact have three different types of photoreceptors in their compound eyes (maximally sensitive to blue, green and ultraviolet wavelengths) allowing full trichromatic vision and excellent colour acuity (see (Chittka, Faruq et al. 2014) for review of colour vision and colour constancy in insects). After confirming this colour discrimination ability, von Frisch then tested the honeybees' ability to discriminate different geometric shapes cut from coloured paper, again placed horizontally on a table. Once more the bees were able to discriminate between specific

types of patterns (i.e. radial spokes versus concentric circles) (v. Frisch 1914). However, it was only in later experiments where the patterns were presented vertically did the honeybees really start to show how remarkable their visual capabilities were.

1.2.1 Y-Maze flight arena

To extrapolate how honeybees can discriminate between flower species, or identify landmarks, experiments were designed that would expose the bees to specific types of visual cues. Subsequent control tests could then be performed to see how well the bees had learnt the particular cue types, and how adaptable they were to alterations in the presented stimuli. This format of experiments has shown that honeybees can be trained to discriminate an impressive range of vertically displayed visual cues; symmetry (Giurfa, Eichmann et al. 1996, Lehrer 1999, Rodriguez, Gumbert et al. 2004), arrangements of edges (Horridge and Zhang 1995, Horridge 2000, Horridge 2006), size (Srinivasan, Lehrer et al. 1989, Horridge, Zhang et al. 1992), pattern disruption (Horridge 1997) and edge orientation (van Hateren, Srinivasan et al. 1990, Srinivasan, Zhang et al. 1994, Giurfa, Hammer et al. 1999). These abilities are all the more impressive since the trained bees are then able to apply these same learnt cues to patterns which may have little or no resemblance to the original training patterns, so long as they fall into the same class of e.g. plane of symmetry, or edge orientation.

To aid in these investigations a new form of apparatus was developed, the now ubiquitous Y-Maze flight arena (van Hateren, Srinivasan et al. 1990). Figure 1.2 shows a top-down schematic view of the flight arena. In summary: a bee is allowed to enter the Y-Maze through the central entrance hole into a decision chamber; here it is presented with a choice of two arms. At a certain distance (offset distance) in each arm a stimulus

(pattern, photo, etc.) is displayed. One of these stimuli will have the chosen visual cue for the experiment and a feeder containing a sucrose solution reward. The remaining arm will have just a blank end plate, or present a distractor stimulus without the correct cue. In this arm the feeder will be either empty, contain just water, or contain a quinine or salt solution that the bees find unpalatable – depending on the particular type of experiment required. The stimuli (and associated feeders) are regularly swapped between the two arms to prevent the bees learning a rewarding location (van Hateren, Srinivasan et al. 1990), as well as the feeders being cleaned and stimuli swapped out for new versions to prevent the bees using odour cues to identify the correct feeders. This setup easily allows the angle that the stimuli subtend on the bee's eyes from the decision chamber to be controlled; by merely changing the stimuli offset distances. Correspondingly, this also allows a bee's choice to be recorded from a known, but adjustable, distance from the stimuli as it crosses an 'imaginary' choice line entering one of the Y-Maze arms (Fig 1.2). In some experiments it may also be beneficial to record the bee's 'final choice' when it either touches one of the stimuli or physically lands on a feeder.

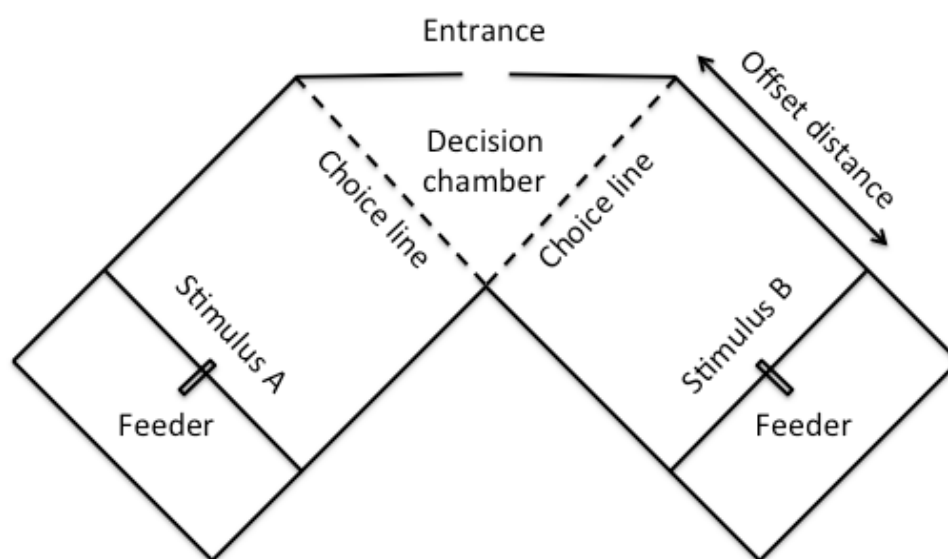


Figure 1.2 Top-down schematic view of the Y-Maze flight arena. One arm would contain the conditional stimulus (CS+) with the feeder providing a sucrose reward, and

the other arm housing a distractor stimulus (CS-) with the feeder providing either water or an unpalatable solution (quinine or salt).

This simple binary-choice flight arena has allowed hundreds of experiments to be conducted on honeybees; here I provide a brief description of two types of honeybee behaviour that have been regularly explored using this setup: free flight and fixation. The former, free flight, experiments would typically have consisted of large (diameter 15-20 cm) simple bar and grating patterns that were adjusted to different distances from the decision chamber. This allows particular visual acuities of the bees to be studied. For example, it allowed simple perpendicular grating patterns to be presented at different distances, then by recording the offset distances and the respective grating wavelengths where the bees were unable to discriminate the patterns the researchers were able to calculate that the minimum spatial frequency of gratings that the honeybee can discriminate is ~ 0.35 cycles per degree (Srinivasan and Lehrer 1988). Similarly, when discriminating vertical, horizontal or oblique bars made up of smaller squares, if the gap between the squares was greater than $\sim 3^\circ$ subtended on the eyes, the bees were unable to determine the overall orientation of the cue (Horridge 2003, Horridge 2003). These particular results also suggest the presence of small orientation edge detectors in the optic lobes that require a perceived edge to cover at least three adjacent ommatidia. Other experiments of this type have guided hypotheses that these small edge detectors must somehow be being combined to form larger visual feature responses in order to account for why the bees can discriminate certain forms of stimuli and pattern textures, but are prevented from discriminating others (Horridge 1997, Maddess, Davey et al. 1999, Horridge 2000). This apparatus configuration was also used to unequivocally prove that honeybees are able to generalise to particular edge orientations, even if the

novel test patterns didn't contain any direct photographic overlap with the training stimuli (van Hateren, Srinivasan et al. 1990).

The second category of experiments explores a phenomenon called fixation. This was first observed when the patterns were placed vertically during experiments, rather than the initial horizontal displays on a table. The bees would approach a stimulus, then hover a small distance (1-3 cm) in front of specific fixation points (see Fig 5.3 for an example of a fixation flight). Frame by frame analysis of motion pictures of bees approaching a feeder showed that head roll and pitch were stabilised during these manoeuvres, they also appeared to align their body axis into the same consistent positions, thereby producing a similar image on the retina on each fixation (Wehner and Flatt 1977). This gave rise to an early template-matching (or eidetic image memory) hypothesis of how bees discriminate patterns – still hotly debated (Giger and Srinivasan 1995, Stach and Giurfa 2001, Stach, Benard et al. 2004). Later Y-Maze experiments where the bees were allowed to fixate in front of more complicated stimuli (patterns made up of multiple gratings oriented at different angles) showed some intriguing behavioural responses. If bees were trained on just a single pattern and then tested with different versions of this pattern, they could only identify similarities in the lower half of the stimuli. Whereas if the bees were trained on two different patterns (one rewarding, one not) then during tests they could match either the top, or bottom, halves of the trained pattern in the doctored test patterns (Giurfa, Hammer et al. 1999). In addition, when the bees were trained for 21 visits using these same two training patterns they were unable to generalise to a novel pattern that presented the correct orientations in each part of the pattern but had bars instead of gratings. However, bees trained for 42 trials could make the generalisation, but peculiarly, they could no longer discriminate this simpler bar version from the original multiple grating pattern. These types of Y-

Maze experiments are particularly interesting as they allow us to examine how the bees perceive the patterns and how they subsequently learn to identify and generalise key visual features within the training stimuli. Potentially more enlightening however, is how this process may be being modulated by either selective attention in the optic lobes, memory formation, or behavioural fixation differences, depending on the experimental conditions employed.

1.2.2 PER, SER & virtual reality arenas

Over the past decades, understanding of honeybee olfactory learning has progressed at pace. This is in large part due to two behavioural conditioning techniques, Proboscis Extension Reflex (PER) (Bitterman, Menzel et al. 1983) and Sting Extension Reflex (SER) (Vergoz, Roussel et al. 2007). In both cases the honeybees are harnessed within a small tube to prevent movement, and then briefly exposed to a particular odorant. A few seconds later the bee is either conditioned to expect a reward, by tapping on its antennae with sucrose solution, causing its proboscis (tongue) to extend (PER), or anticipate a negative condition by applying a mild electric shock; in this situation the bee extends its sting (SER). In both cases, after a few conditioning trials the bee will either extend its proboscis, or sting, when the odour alone is presented (Bitterman, Menzel et al. 1983, Vergoz, Roussel et al. 2007). Because the honeybees are immobilised it means that electrophysiology on their brains can be conducted throughout the entire learning paradigm. This has allowed intracellular recordings (Sun, Fonta et al. 1993), extracellular and large field potential (LFP) recordings (Denker, Finke et al. 2010), as well as calcium imaging (Galizia, Sachse et al. 1999) of the bee antennal lobes (which receive sensory input from the bees' antennae). This combined with multi unit electrode

recordings (Brill, Reuter et al. 2014) and calcium imaging of the mushroom bodies during learning (Szyszka, Ditzen et al. 2005) has provided essential insights into how different concentrations and different mixes of odours are encoded in the bees' antennal lobes, and subsequently learnt by the higher brain regions (Cuevas Rivera, Bitzer et al. 2015).

Unfortunately, similar PER and SER approaches with harnessed bees using visual stimuli have had limited success (Hori, Takeuchi et al. 2006, Hori, Takeuchi et al. 2007) (Niggebrügge, Lebouille et al. 2009, Mota, Roussel et al. 2011). In these studies the bees are trained on simple colours, intensity differences, or moving grating discriminations, but results show much slower learning curves compared to those observed with free flying bees, and in the case of PER conditioning a very peculiar requirement is that of having to remove the bees' antennae in order to effectuate learning – overall this would make any attempt at neuronal analysis or modelling from these types of experiments, speculative at best. One new development that may hold future potential is that of closed-loop virtual reality arenas. Here, a tethered bee walks on a rotating ball, which in turn controls a LED visual display, thus allowing the bee to walk around a simple environment. This has already demonstrated one interesting phenomenon; LFP recordings from the bee optic lobes have shown signs of selective attention in the medulla and lobula neurons. They responded to only one specific stimulus in their field of view, while being unresponsive to other stimuli (Paulk, Stacey et al. 2014). The responses would also spontaneously switch to another available visual cue in their field of view, inhibiting responses of the former cue; this was followed by a behavioural trait with bee turning on its ball to face this new 'selected' cue. Although interesting, these current virtual reality systems work only for walking bees, and are therefore unable to explore one of the honeybees' most fascinating behaviours, that of

stimulus scanning and fixation during hovering manoeuvres. Indeed it might well be that experiments with tethered bees discriminating visual stimuli are unsuccessful for the simple reason that active scanning movements are an essential component of pattern recognition in the bee (Nityananda, Chittka et al. 2014).

To date, no closed-loop system is available for tethered flying bees, but, as with all things, technology is improving. A recent publication using tethered honeybees in a wind tunnel simulator has been able to provide high-speed videography and subsequent analysis of how the bees' posture changes as air speed and wind direction are manipulated (Taylor, Luu et al. 2013). It still remains to be seen if honeybees can be conditioned, either positively or negatively, to respond to particular stimuli in either of these environments; something that is routine using tethered flies in virtual flight simulators (e.g. flies learning to identify particular patterns to avoid unpleasant heat sources (Dill, Wolf et al. 1995)). Hopefully in the next few years, such developments will allow detailed electrophysiology of both the optic lobes and mushroom bodies during the learning of visual stimuli.

1.3 Structure of the thesis

Despite the current lack of detailed electrophysiology during visual learning, what is available is a vast behavioural catalogue of the visual stimuli that bees can, and cannot, discriminate, as well as the bees' relative performances at discriminating, and generalising to, different types of stimuli. This thesis therefore takes a cognitive modelling approach to understanding how the miniature brain of a honeybee is able to discriminate between different visual stimuli, how it can generalise between patterns containing common visual features. In addition, I will investigate what neuronal architectures are required to allow it to be invariant to the size of the stimuli, or

indifferent to the stimuli location within the visual field. Later chapters use these same methodologies to investigate how seemingly conceptual spatial relationship problems could be solved without needing the complexities of a large vertebrate brain, culminating in actual behavioural experiments on real honeybees to test these hypotheses.

Chapter 2: Theoretical models of how honeybees may discriminate and generalise simple bars and gratings

In this initial chapter I explore how neuronal minimalism and response specificity may support complex visual processing and cognition within the miniature brain of the honeybee. Utilising these principles, and the known anatomical structures and neuronal responses of the bee brain, I developed several theoretical bee brain models. Computer simulations using stimuli previously used in honeybee behavioural experiments, reveal that honeybees' precise grating pattern recognition and generalisation of oriented bars and gratings would be possible with just two types of optic lobe large-field orientation-sensitive neurons, not three - the previously theorised minimum. These neurons would also allow for both discrimination and generalisation of these patterns without the need for a photographic or eidetic image memory of an actual pattern.

Chapter 3: Theoretical models of how honeybees may discriminate and generalise complex patterns

In this chapter I investigated if combining visual information from both eyes onto single Kenyon cells, which receive sensory information, would have any functional benefits for my models. Similar anatomical pathways are seen in the honeybee, where the learning centres in each hemisphere of the brain receive sensory input from the optic

lobes of both eyes. These new models demonstrate that not only would this allow for discrimination of complex patterns with invariance to their location across the width of the visual field, but would also be tolerant to partial occlusion to the stimuli. This would undoubtedly be useful for a flying insect. One model also replicated surprising failures of bees to discriminate certain seemingly highly different patterns, providing clues to the neuronal processes that may also limit the utilisation of visual cues in honeybees.

Chapter 4: Theoretical models of how honeybees could solve the ‘above and below’ conceptualisation task

In recent decades we have seen a string of remarkable discoveries detailing the impressive cognitive abilities of bees (social learning, concept learning and even counting). In this chapter I challenged the existing models from the previous chapters to solve one of these conceptual learning tasks. The ‘above and below’ task requires the identification of a pattern where a variable (and potentially novel) target shape is either above or below a constant referent shape. Initially, the models failed in all but the simplest pattern discrimination tests. However, a simple adaption to how the models were allowed to perceive the test patterns produced simulation results almost identical to that of the empirical results of honeybees performing the same experiments. This work provided a set of hypotheses for how honeybees could solve the problem without needing to understand the underlying spatial relationship of the stimuli shapes.

Chapter 5: Behavioural experiments demonstrating how honeybees solve the ‘above and below’ conceptualisation task

Honeybees have already been shown able to solve the ‘above and below’ task. But, as is often the case, we still know little about *how* the bees actually approach such a problem.

Continuing from my work in previous chapter, I used high-speed videography to record honeybees actually learning to solve this task, and subsequently compared their flight paths to those predicted in the previous chapter. I find that honeybees do indeed appear to be solving the problem without needing to understand the fundamental spatial relationships of the stimuli. Surprisingly, they solved this task not by the exact means I hypothesised, but in an even simpler manner. The bees' technique was to fixate at the lowest available shape on a given stimulus and simply determine if this shape was the trained referent shape (a cross), or not. This approach allowed the bees to solve the task independent of whether the rewarding configuration was with the target shapes either above or below the referent shape.

Chapter 6: General discussion and conclusions

In the final chapter, I bring together my findings to summarise how the anatomy and known neuronal responses of the miniature bee brain appear to be perfectly configured to allow for complex visual discriminations, generalisations, and even solving seemingly complex conceptualisation tasks. I discuss how these models can be improved and how behaviour scientists can aid in capturing specific information that will be useful for computational modellers both now, and in the future. Finally, I conclude by highlighting how the study of honeybees may have very useful implications on how we should view animal cognition in general.

Chapter 2: Theoretical models of how honeybees may discriminate and generalise simple bars and gratings

The excitatory and inhibitory (EAI_AB) model design presented in this chapter is published in the following publication. However, none of the other models, nor any simulation results from this chapter, appear in the publication.

Roper, M. Fernando, C. & Chittka, L. 2017. Insect Bio-Inspired Neural Network Provides New Evidence on How Simple Feature Detectors Can Enable Complex Visual Generalization and Stimulus Location Invariance in the Miniature Brain of Honeybees. PLOS Computational Biology 13(2): e1005333.

2.1 Abstract

The honeybee brain contains less than one million neurons and yet, bees display remarkable visual recognition abilities allowing them to classify visual patterns by common features, use landmarks for navigation on extensive foraging routes, and they can even recognise particular human faces. But with such a miniature brain, does the honeybee use unique ways to encode visual information, thus reducing the neuron count and neuronal infrastructure required for complex recognition? Here, I build theoretical models using the known anatomical and electrophysiology of the bee brain to show that the neuronal responses of just two types of lobula (3rd optic ganglion) large-field orientation-sensitive neurons can be used for both generalisation and precise discrimination of achromatic bar and grating patterns. These abilities can be accomplished without the need for a previously assumed internal eidetic image (or photographic representation) of the patterns. My research highlights how having a small number of connections from the optic lobes to the higher brain learning centres, as seen in honeybees, may not hinder the insects, but facilitate cognitive abilities by allowing parallel processing of this information. Furthermore, bees would be able to use simple associative learning of these different simultaneously produced visual elements without

the need for unique or complex hierarchical architectures for each type of recognition task. I also discuss why honeybees may only need two orientation-sensitive neuron types whereas three types, the minimum theoretical requirement, were found in dragonflies.

2.2 Introduction

Behavioural experiments have shown that honeybees can be trained to discriminate and then generalise to a prodigious range of visual cues. Previous visual recognition experiments included colour (Schneirla 1951, Dyer and Neumeyer 2005), symmetry (Giurfa, Eichmann et al. 1996, Lehrer 1999, Rodriguez, Gumbert et al. 2004), radial, spokes, concentric bars and oriented gratings (van Hateren, Srinivasan et al. 1990, Srinivasan, Zhang et al. 1994, Horridge and Zhang 1995, Giurfa, Hammer et al. 1999, Horridge 2000, Horridge 2006) amongst other motifs. Honeybees also accomplish remarkable feats of social learning (Avargues-Weber, Dawson et al. 2013), using a complex communication system, the ‘dance language’ to indicate suitable foraging sites to nestmates (Su, Cai et al. 2008), and advanced cognitive abilities such as counting (Chittka and Geiger 1995) and forms of learning that could be classified as conceptual (Giurfa, Zhang et al. 2001, Avargues-Weber, Dyer et al. 2011).

Here I investigate the question, how can the miniature brain of honeybees facilitate such diverse cognitive abilities? In this chapter I explore the two phenomena of neuronal minimalism and response specificity (see Chapter 1.1.2), and how these may support the honeybees’ visual recognition abilities. The honeybee lobula (3rd optic ganglia) extends an astonishingly small number of just ~50 extrinsic neurons to the

mushroom bodies (higher learning centres) (Witthöft 1967), these neurons are typically very large-field responding to particular types of stimuli in large regions, if not the entirety, of a bee's eye. Among these extrinsic lobula neurons, two types of large-field orientation-sensitive neurons (LOSNs) have been discovered. These had maximal sensitivities to bars oriented at ca. 115° (type A) and ca. 250° (type B) moving anywhere across the width of the bee eye (Maddess and Yang 1997). Their responses were independent of the direction of the bar's movement, although did produce a higher firing rate when the number of bars presented was doubled (Maddess and Yang 1997). Given that these two types of large-field neurons do not encode any detailed retinotopic information (i.e. subsequent processing of these responses alone would not allow the location of the bar in the field of view to be determined), the question is, do they still provide useful feature detectors that could contribute to the bees' pattern discrimination abilities, and could they also be used for generalisation?

To investigate these questions, I produced four simple theoretical bee brain models. These limited the numbers of neurons connecting the optic lobes to the mushroom bodies to just these lobula large-field orientation-sensitive neurons (LOSNs). I explore if the response-specificity of these neurons is sufficient alone to allow honeybee equivalent performances on a disparate range of achromatic pattern recognition tasks. In addition, I examine what secondary processing may be required in the higher learning centres to correctly evaluate this limited visual input. I do not employ any form of learning in these models; this allows us to better comprehend how the LOSN responses alone may affect the bees' cognitive abilities and behavioural performance. As with original honeybee behaviour experiments, I begin with single bar and oriented grating pattern tasks. This allows us to study very simple visual inputs and corresponding neuronal outputs, but still scrutinise a large range of recognition tasks;

easy perpendicular edge discriminations, fine angle discriminations, exact template matching, and feature generalisation.

Here, I explore these core types of visual recognition tasks by simulating 164 previously conducted honeybee behavioural experiments using bar and grating patterns (experiments taken from four published papers (van Hateren, Srinivasan et al. 1990, Srinivasan, Zhang et al. 1994, Giger and Srinivasan 1995, Sathees chandra, Geetha et al. 1998), and directly compare the empirical results to each of my models' performances.

2.3 Methods

2.3.1 Pre-processing of patterns

Each achromatic pattern used in this study was taken from the pdf document of the published behavioural papers. These images were scaled and centred to fit within a 155 x 155 pixel PNG image. Where pattern image resolution was insufficient, I recreated the patterns in Microsoft PowerPoint using the stimuli instructions provided in the papers' method sections. For the scaled discrimination experiments, the 155 x 155 pixel patterns were enlarged by 125% and 300% creating new images 194 x 194 pixels and 465 x 465 pixels respectively.

All images were processed in Matlab (Mathworks) in the following way:

- Removal of excess pixel noise in the image
- Conversion to a binary black and white image using only the green channel
- Calculation of the orientation and gradient magnitude of each edge in the image using Canny edge detection and Sobel gradient analysis

- Removal of short edges with a gradient magnitude ≤ 1.7 . Equivalent to those edges subtending less than 3° on a honeybee eye, which have been shown to be undistinguishable by bees (Horridge 2003, Horridge 2003)
- Division of the image into four equal quadrants; for each quadrant I generated a histogram analysis of all oriented edge lengths in 1° increments (1° - 180°)
- Saving the histogram dataset for each quadrant into a unique file *per* image levels.

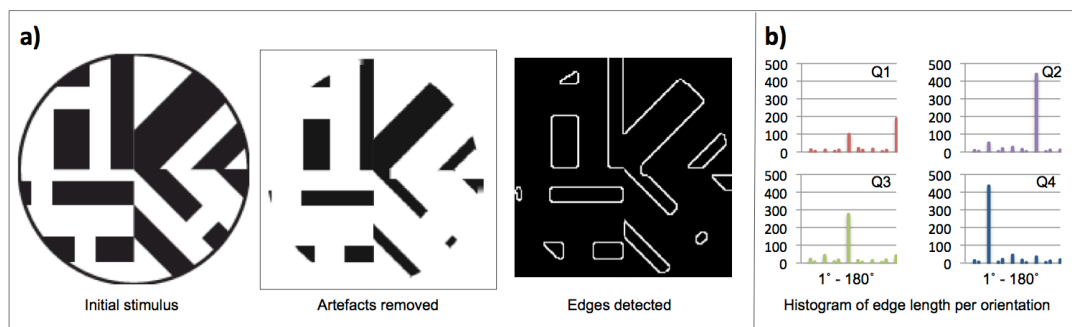


Figure 2.1 Schematic representation of the stimuli pre-processing (a) Left: pattern is loaded and converted to a black and white image (if not already). Middle: image artefacts are removed as well as any edges too small to be detected by bees. Right: remaining edges are detected and then the length and orientation of each edge calculated. (b) Histogram showing the orientation (1 - 180°) and the corresponding edge lengths for each quadrant (Q1 – Q4) of the pattern.

2.3.2 Calculating lobula neuronal responses

To date only two types of LOSNs have been discovered in honeybees (Maddess and Yang 1997). In these experiments, electrophysiological recordings were made from the lobula of tethered bees placed in front of CRT computer monitors; stimuli of oriented bars moving across one eye were presented at 30° angle intervals, in both the frontal and lateral eye regions. These neurons responded to the oriented bars moving anywhere across the whole width of the eye, and were maximally sensitive to orientations of 115° (LOSN type A) and 250° (LOSN type B) with angular half-widths of about 90° . In

previous electrophysiology experiments using dragonflies, three LOSN types were found (O'Carroll 1993). Two of these were similar to the LOSN type A and type B in honeybees and the third type had its maximal sensitivity offset from the other two by approximately 120°. Some researchers have suggested, on theoretical grounds, that a third type of LOSN must also be present in the honeybee (Srinivasan, Zhang et al. 1994, Sathees chandra, Geetha et al. 1998); and indeed because the total number of recordings of LOSNs in this species is so far relatively low, the lack of recordings from a third LOSN type is not evidence for absence. Therefore, here I produced two sets of models, those using only empirical evidence of type A and type B responses in honeybees (Maddess and Yang 1997) (suffixed `_AB`) and those with a third type, where maximal orientation sensitivities are offset by ~120° (Srinivasan, Zhang et al. 1994), similar to that seen in dragonflies (O'Carroll 1993) (suffixed `_ABC`). I modelled and subsequently simulated a single instance of the two, or three, LOSN types from the upper and lower half of the visual field of each eye (behavioural (Giurfa, Hammer et al. 1999), neuroanatomical (Ehmer and Gronenberg 2002) and neurophysiological (Paulk and Gronenberg 2008) evidence shows subdivision of visual information into such regions) producing for any given bar or grating pattern just eight or twelve theoretical LOSN responses for the `_AB` and `_ABC` models respectively (see Methods: Calculating LOSN type A, B & C responses).

Calculating lobula neuronal responses for the two LOSN type models

The virtual lobula (3rd optic ganglion) large-field orientation-sensitive neurons (LOSNs) used in my models were derived from the Yang & Maddess (1997) study on the honeybee (*Apis mellifera*). During electrophysiological recordings the honeybees were presented with a moving bar, the lobula neurons produced a fast phasic response only during the initial bar presentation and not as it continued across the eye. Behavioural

studies in bumblebees (Nityananda, Chittka et al. 2014) have also shown that bees are able to discriminate simple oriented bars on a computer monitor when presented for just 25ms, which would be brief enough to prevent the stimuli moving across the bee eye during free flight. Since the bees are able to do discriminate with just a quick ‘glance’ of the pattern, and to reduce the complexity of the model, here I assume that the models perceive just a single static ‘snapshot’ of the stimuli, and that this would be sufficient for the maximum LOSN firing rates to be produced for the particular edge orientations within each stimulus. I therefore produced best-fit curves to both the reported type A and type B responses so that I could provide a theoretical neuronal response to a fixed 280-pixel edge at any orientation (Fig 2.2a).

Bees presented with two identically oriented bars simultaneously in both the frontal and lateral regions of the eye generated LOSN responses that were higher than for a single bar in either eye region but less than the summed responses (Maddess and Yang 1997). A similar nonlinear response was seen in dragonflies (*Hemicordulia tau*) (O'Carroll 1993) where the response to an oriented moving bar would increase with the length of the presented bar. Assuming that the honeybee LOSN responses are due to a nonlinear summation of smaller orientation detectors in the lower lobula or medulla, I used this more detailed response curve recorded in the dragonfly to generate a best-fit scale factor curve (Fig 2.2c) for when the length of a presented edge increases. This allowed me to scale the LOSN responses for any oriented edge based on its length compared to the fixed length used for my LOSN tuning curves (Fig 2.2a, c).

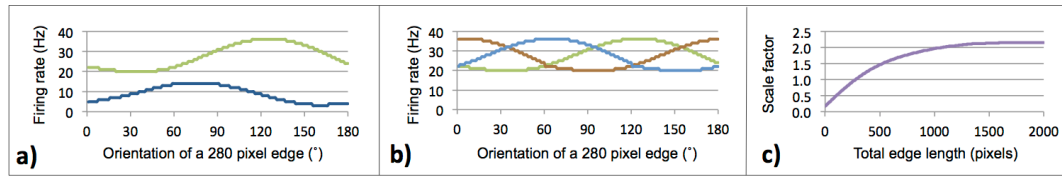


Figure 2.2 Schematic representation of the model neuron responses. **(a)** Firing rate responses of the theoretical LOSNs used for the *_AB* models (type A: green, type B: blue) to a 280 pixel edge at all orientations between 1° - 180° ; tuning curves adapted from honeybee electrophysiological recordings (Maddess and Yang 1997). **(b)** Firing rate responses of the three LOSNs used for the *_ABC* models (type A: green, type B: blue, brown: type C) to a 280 pixel edge at all orientations between 1° - 180° ; tuning curves adapted from honeybee electrophysiological recordings for the LOSN type A neurons (Maddess and Yang 1997) which are offset by $\pm 120^{\circ}$ to create the three LOSNs that were thought to be the minimum for orientation discrimination in bees (Srinivasan, Zhang et al. 1994). **(c)** Scale factor applied to the LOSN firing rates dependent on the total edge length in each quadrant of the visual field, derived from dragonfly neuronal responses to oriented bars with differing bar lengths (O'Carroll 1993).

To account for multiple edges at different orientations in any one image (see Fig 2.1), I again use the assumption that the overall LOSN response is composed from smaller subunits in the medulla or early lobula and will vary with both the total length and abundance of all oriented edges within the receptive field that that LOSN receives information from. To date we do not have recordings of lamina or medulla orientation-sensitive neurons from honeybees. However, such neurons are found in other insect medullas (McCann and Dill 1969, O'Carroll 1993, James and Osorio 1996, Maddess and Yang 1997, Okamura and Strausfeld 2007, Spalthoff, Gerdes et al. 2012). Using the data from these studies it would be conceivable to build and simulate an artificial neural network to process the pattern stimuli and produce theoretical LOSN responses. That said, the output of these networks would need to be tuned to produce the same neural response to oriented bars that were recorded from the honeybee LOSNs (Maddess and Yang 1997). So here, I remove this layer and directly use the known LOSN electrophysiological responses to particular orientations to mathematically calculate a theoretical response to novel stimuli.

I thus calculated the overall LOSN type A and type B responses for any given pattern using the edge length histogram datasets for all four quadrants of that pattern (see above). For each quadrant and each LOSN type, I summed the proportion (orientation edge length / total edge length) of each edge orientation (1°-180°) and multiplied it by the neural response for that orientation on my standard 280 pixel edge curve (Fig 2.2a). This total value was then corrected by the scaling factor derived from the total edge length within that quadrant (Fig 2.2c). This produced a type A and type B LOSN response (Equation 2.1) for each quadrant of the visual field, and therefore eight LOSN responses in total for a given pattern (see Fig 2.3). These image specific responses were saved with the pattern's unique identification number (UID) and subsequently used as the sensory inputs to the Kenyon cells of my two LOSN type mushroom body models (suffixed _AB).

$$LOS_{N_AB}(x, q) = \left(\sum_{i=1}^{180} \left(\frac{hist(q, i)}{\sum hist(q)} * curve_AB(x, i) \right) \right) * scale \left(\sum hist(q) \right)$$

(2.1)

Where q: visual field quadrant 1:4; x: LOSN type a or b; hist: matrix of edge lengths for each orientation (1° increments) in each quadrant; curve_AB: response of AB model LOSN type x to a 280 pixel edge at orientation i (Fig 2.2a); scale: scale factor for given total edge length (Fig 2.2c).

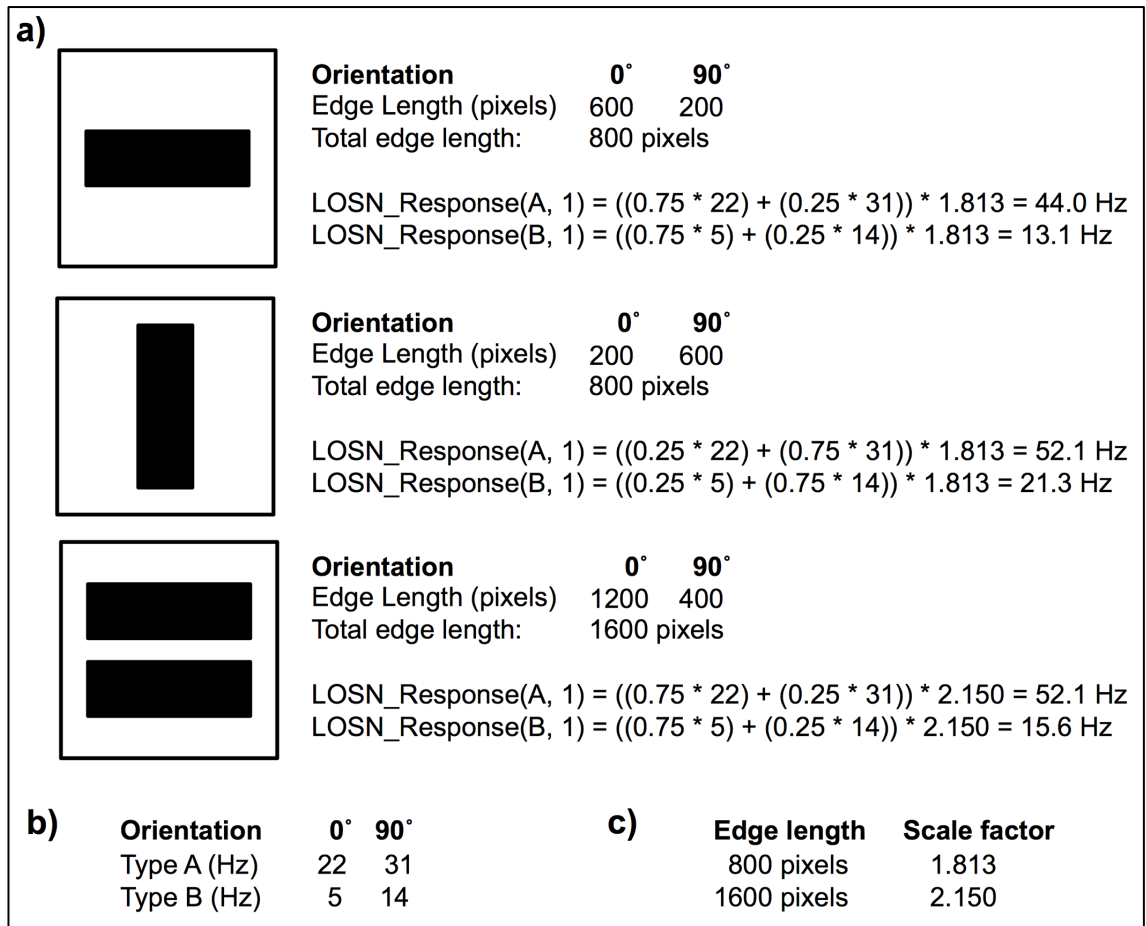


Figure 2.3 Simplified example of the lobula orientation-sensitive neuron (LOS_N) type A and type B firing rate response calculations. **(a)** Here I calculate values for just the left dorsal eye (quadrant I) with only horizontal (0° / 180°) and vertical (90°) edges presented. In the single horizontal bar example (top) 75% of the overall edge length is at a 0° orientation (600 pixels out of total edge length of 800 pixels) and 25% of the edges at 90° orientations, thus the LOS_N responses are influenced more by the response curve values at 0° than 90°. Conversely, the vertical bar is influenced more by the response curve values at 90°, resulting in overall higher LOS_N firing rates. The two horizontal bars example (bottom) has the same proportion of orientations as the single horizontal bar (top). Although the total edge length is doubled, the LOS_N firing rates are not twice as high; instead they are scaled using the non-linear scaling factor derived from dragonflies (see Fig. 2.2c and Equation 2.1). Note that the LOS_N type A firing rate is the same for a single vertical bar as it is for two horizontal bars (52 Hz). **(b)** LOS_N type A and type B response curve values for 0° and 90° (see Fig. 2.2a). **(c)** LOS_N scale factors for 800 and 1600 pixel edges (See Fig. 2.2c). Image replicated from my publication (Roper, Fernando et al. 2017).

Calculating lobula neuronal responses for the three LOSN type models

To compare the performance of just the two LOSN types known in honeybees honeybees (Maddess and Yang 1997) with that of the proposed theoretical minimum of three types (Srinivasan, Zhang et al. 1994, Sathees chandra, Geetha et al. 1998), I created a second set of models (suffixed: *_ABC*). For these models, I took the LOSN type A responses and offset the values by $\pm 120^\circ$ to create the new type B and type C LOSN responses with the required maximal sensitivity values (Fig 2.2b). The generation of the LOSN responses for a given pattern for these models was exactly the same as above except that three LOSN type response curves to a 280 pixel edge were provided (Fig 2.2b, Equation 2.2) therefore in each visual field quadrant a LOSN type A, B & C response was generated providing in total twelve LOSN responses for that pattern. These responses were again saved and passed to the appropriate models' Kenyon cells (see below).

$$LOSN_ABC(y, q) = \left(\sum_{i=1}^{180} \left(\frac{hist(q, i)}{\sum hist(q)} * curve_ABC(y, i) \right) \right) * scale \left(\sum hist(q) \right) \quad (2.2)$$

Where q: visual field quadrant 1:4; x: LOSN type a, b or c; hist: matrix of edge lengths for each orientation (1° increments) in each quadrant; curve_ABC: response of _ABC model LOSN type y to a 280 pixel edge at orientation i (Fig 2.2b); scale: scale factor for given total edge length (Fig 2.2c).

2.3.3 Calculating mushroom body Kenyon cell responses

The honeybee mushroom bodies contain approximately 340,000 Kenyon cells (Withöft 1967) that receive input from the olfactory, gustatory, mechanosensory and visual systems (Gronenberg 2001, Ehmer and Gronenberg 2002). Within the mushroom bodies

there are two classes of Kenyon cells; class I ‘spiny’ Kenyon cells each receive input from large numbers of sensory neurons and class II ‘clawed’ Kenyon cells that only synaptically connect to approximately five to fifteen input projection neurons (Strausfeld 2002). My model LOSNs make presynaptic connections to just these class II ‘clawed’ Kenyon cells (hereafter simply referred to as Kenyon cells) since this allowed me to limit the model size to simple, yet plausible, LOSN to Kenyon cell connection configurations.

For this study I produced four simple theoretical models. For the two ‘single excitation only’ models (SEO_AB, SEO_ABC), I assume that an individual Kenyon cell would exclusively receive excitatory synaptic input from LOSNs. For these very simple models each of the ~8,000 individual Kenyon cells in the respective models were configured to receive input from just one of the eight or twelve LOSNs, dependent on whether two (suffix _AB) or three (suffix _ABC) types of orientation detectors were modelled (Fig 2.4 purple neurons). The two ‘excitatory and inhibitory’ models (EAI_AB, EAI_ABC) were created using the same eight or twelve LOSNs as above, but the LOSN to Kenyon cell connection configurations were slightly more complex. Here each individual Kenyon cell could establish one or more excitatory synapses with a single LOSN type in either the dorsal or ventral region of one eye, and one or more inhibitory synapses from one of the other LOSN types from the same eye region (Fig 2.4 red neurons).

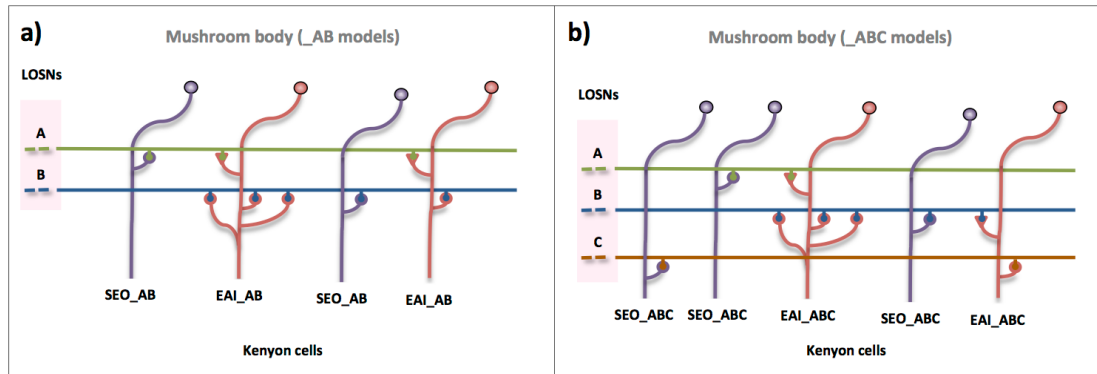


Figure 2.4 Schematic representation of SEO and EAI models. Representation of how the lobula orientation-sensitive neurons (LOSN) connect to each models' Kenyon cells. Here I show connections from the left-dorsal eye, distinct connections would be established from the other three eye regions. **(a)** 'Single Excitatory Only' SEO_AB model, these Kenyon cells (purple) only receive input from a single LOSN type. 'Excitatory And Inhibitory' EAI_AB Kenyon cells (red) receive either excitatory input from the LOSN type A and inhibitory input from the LOSN type B, or vice-versa. **(b)** The SEO_ABC Kenyon cells (purple) make single excitatory connections with either a LOSN type A, B or C. The EAI_AB Kenyon cells (red) establish different connections with just two of the three LOSN types, one type always being excitatory and the other inhibitory.

Calculating Single excitatory only (SEO) Kenyon cell responses

In the first single excitatory only model (SEO_AB) each of the eight LOSN inputs were connected to 1,032 Kenyon cells, producing in total 8,256 Kenyon cells. Here, a Kenyon cell received input from either a type A or type B LOSN from a single quadrant of the visual field. The SEO_ABC used the twelve LOSNs, three LOSN type inputs per quadrant; each was connected to the single excitatory synapse on one of 688 Kenyon cells forming the same 8,256 Kenyon cell population. For a given pattern, I loaded the correct LOSN responses (from above) then for each Kenyon cell synapse set the synaptic value to the firing rate value of the LOSN connected to it, to this a small synaptic signal to noise distortions was applied. The latter was to account for natural variation in both the LOSN responses when presented with the same pattern, and in pre- and post- synaptic neurotransmitter signals. Matlab's (Matworks) AWGN (Add White

Gaussian Noise) function was used with a signal to noise ratio value of 30. This setting produced approximately 2-5Hz variations on the 36Hz response of the type A LOSN at its maximal sensitivity and an edge length of 280 pixels. This would be similar to the response variation reported in the honeybee LOSNs after the deduction of the neuronal background firing rates (Maddess and Yang 1997) (see Chapter 6.2: for further discussion on applying noise to the LOSN responses). The input firing rate values of each synapse were rounded to the nearest integer value and stored in a single array. This array was again saved and cross-referenced with the presented pattern's UID.

Excitatory and inhibitory (EAI) Kenyon cell connections

The first of the excitatory and inhibitory models (EAI_AB) uses just the known honeybee type A and type B LOSNs (Fig 2.2a). I established a set of simple excitatory and inhibitory synaptic configurations, with each configuration having a different number of type A and type B LOSNs connecting to the Kenyon cells (with that Kenyon cell's LOSNs all originating from the same quadrant of the visual field, see Fig 2.4a red neuron), in total 86 different LOSN to Kenyon cell connection types were produced (see Table 2.1). I replicated 24 copies of each of these 86 types per quadrant; resulting in a total of 8,256 Kenyon cells. Although, it must be noted that for these EAI models it could have been configured that, for example, rather than a Kenyon cell receiving three excitatory LOSN type B inputs instead it received just one such input with a synaptic weight of +3, which would have produced the exact same result. However, to reinforce the importance that there is no learning in my models, and to focus the investigation into the LOSN responses, here I restrict the models to the most basic synaptic configuration, with all synaptic weights equal to ± 1 .

001: 1A+, 1B-	010: 2A+, 5B-	019: 3A+, 13B-	028: 7A+, 3B-	037: 11A+, 13B-
002: 1A+, 2B-	011: 2A+, 7B-	020: 5A+, 1B-	029: 7A+, 5B-	038: 13A+, 1B-
003: 1A+, 3B-	012: 2A+, 11B-	021: 5A+, 2B-	030: 7A+, 11B-	039: 13A+, 2B-
004: 1A+, 5B-	013: 2A+, 13B-	022: 5A+, 3B-	031: 7A+, 13B-	040: 13A+, 3B-
005: 1A+, 7B-	014: 3A+, 1B-	023: 5A+, 7B-	032: 11A+, 1B-	041: 13A+, 5B-
006: 1A+, 11B-	015: 3A+, 2B-	024: 5A+, 11B-	033: 11A+, 2B-	042: 13A+, 7B-
007: 1A+, 13B-	016: 3A+, 5B-	025: 5A+, 13B-	034: 11A+, 3B-	043: 13A+, 11B-
008: 2A+, 1B-	017: 3A+, 7B-	026: 7A+, 1B-	035: 11A+, 5B-	
009: 2A+, 3B-	018: 3A+, 11B-	027: 7A+, 2B-	036: 11A+, 7B-	
044: 1A-, 1B+	053: 2A-, 5B+	062: 3A-, 13B+	071: 7A-, 3B+	080: 11A-, 13B+
045: 1A-, 2B+	054: 2A-, 7B+	063: 5A-, 1B+	072: 7A-, 5B+	081: 13A-, 1B+
046: 1A-, 3B+	055: 2A-, 11B+	064: 5A-, 2B+	073: 7A-, 11B+	082: 13A-, 2B+
047: 1A-, 5B+	056: 2A-, 13B+	065: 5A-, 3B+	074: 7A-, 13B+	083: 13A-, 3B+
048: 1A-, 7B+	057: 3A-, 1B+	066: 5A-, 7B+	075: 11A-, 1B+	083: 13A-, 5B+
049: 1A-, 11B+	058: 3A-, 2B+	067: 5A-, 11B+	076: 11A-, 2B+	085: 13A-, 7B+
050: 1A-, 13B+	059: 3A-, 5B+	068: 5A-, 13B+	077: 11A-, 3B+	086: 13A-, 11B+
051: 2A-, 1B+	060: 3A-, 7B+	069: 7A-, 1B+	078: 11A-, 5B+	
052: 2A-, 3B+	061: 3A-, 11B+	070: 7A-, 2B+	079: 11A-, 7B+	

Table 2.1 *EAI_{AB} LOSN to Kenyon cell configuration types. List of all 86 lobula large-field orientation-sensitive neurons (LOSNs) to mushroom body Kenyon cell configurations. Format [configuration number]: [number of LOSN type A synapses]A[+/- = excitatory/inhibitory synapses], [number of LOSN type B synapses]B[+/- = excitatory/inhibitory synapses]. The first 43 configurations each had one or more LOSN type A excitatory connection and one or more LOSN type B inhibitory connection. The second 43 configurations were the reciprocal of these with type A inputs being inhibitory and type B excitatory. The use of prime numbers provided a simple way to exclude duplicate responses i.e. 2A+, 5B- would generate the same Kenyon cell response as 4A, 10B-. All synaptic weights were set to 1 or -1 for the individual excitatory and inhibitory connections respectively.*

The theoretical Kenyon cells defined above will each fire for a large number of perceived edge orientations and edge lengths. However, the combinatorial firing code of these 86 types allows small ranges of orientations to be uniquely identified by my models, and furthermore these edge orientations can be recognised invariant of the presented edge lengths, since an almost identical combinatorial code of the fired Kenyon cells is produced if the same edge orientations are presented (see Chapter 2.4.1). Adding additional LOSN combinations would not increase the models ability to discriminate more specific angles, as the acuity is fundamentally constrained by the

particular LOSN response curves, which often have the same firing rate for several adjacent orientations (Fig 2.2a). It is most likely that within the honeybee mushroom bodies a large variety of random LOSN to Kenyon cell synaptic connections are initially established. Equally these synapses are most certainly plastic, adapting the synaptic strengths, and even adding and removing LOSN synapses, during a bee's foraging life (Durst, Eichmüller et al. 1994). In this way these Kenyon cells could become highly selective and fire only for particular rewarding visual inputs. In addition, the honeybee brain may be capable of adapting the Kenyon cell synapses to better account for noise in the LOSN responses and produce more effective combinatorial codes for identifying particular orientations than my models (see Chapter 3.5), however, since this chapter is primarily concerned with the LOSNs effectiveness as feature detectors, and not on learning or other 'fine-tuning' neuronal mechanisms, this additional model complexity of random connectivity and weight adaption was omitted.

The second EAI model (EAI_ABC) used the theoretical responses of three LOSN types (Fig 2.2b). In this case, each Kenyon cell formed synapses with a number of LOSNs, each connection originating from just two of the three LOSN types from a single quadrant of the visual field; all of the synapses of one type would be excitatory and the other type all inhibitory. The EAI_ABC model required 24 different LOSN to Kenyon cell configurations to subdivide the 360° of orientations into distinct regions (see Table 2.2). I created 86 of each Kenyon cell configuration type, per quadrant, to produce the same 8,256 Kenyon cells as the other models.

001: 1A+, 1B-	009: 1B+, 1A-	017: 1C+, 1A-
002: 2A+, 3B-	010: 2B+, 3A-	018: 2C+, 3A-
003: 3A+, 4B-	011: 3B+, 4A-	019: 3C+, 4A-
004: 4A+, 5B-	012: 4B+, 5A-	020: 4C+, 5A-
005: 1A+, 1C-	013: 1B+, 1B-	021: 1C+, 1B-
006: 2A+, 3C-	014: 2B+, 3B-	022: 2C+, 3B-
007: 3A+, 4C-	015: 3B+, 4B-	023: 3C+, 4B-
008: 4A+, 5C-	016: 4B+, 5B-	024: 4C+, 5B-

Table 2.2 EAI_ABC LOSN to Kenyon cell configuration types. List of all 24 lobula large-field orientation-sensitive neurons (LOSNs) to mushroom body Kenyon cell configurations. Format [configuration number]: [number of LOSN type A/B/C excitatory synapses][A/B/C]+, [number of LOSN type A/B/C inhibitory synapses][A/B/C]-. The first 8 configurations each had one or more LOSN type A excitatory connections and one or more LOSN type B/C inhibitory connections. The second 8 configurations were the reciprocal of these with type B inputs being excitatory and type A/C inhibitory. The final 8 configurations had the type C LOSN synapses excitatory and A/B inhibitory. All synaptic weights were set to 1 or -1 for the individual excitatory and inhibitory connections respectively.

Calculating EAI Kenyon cell responses

Each EAI models' Kenyon cell response, to a given pattern, was calculated by first summing the value of all its synapses (number and type of synapses dependent on that Kenyon cells particular configuration type). If this total summed synaptic input was greater than zero the output of the Kenyon cell was set to 1 (fired). Otherwise the response was set to 0 (completely inhibited). The individual Kenyon cell synaptic values were calculated by taking the firing rate of the connected LOSN, applying the same small synaptic signal to noise distortion as the SEO models, and multiplying this by +1 for excitatory synapses and -1 for inhibitory ones. In this way the binary values of all 8,256 Kenyon cell responses were calculated; these values were stored in an array and saved cross-referenced to the pattern's UID.

2.3.4 Calculating Kenyon cell similarity ratios and experiment performances

Each experiment simulated in this study was composed of three patterns, the rewarding pattern used during the honeybee training (CS+) and two novel test patterns used in the experimental evaluation trial. The test stimuli patterns that honeybees preferred during their trials were designated as TS^{COR} patterns and the TS^{INC} patterns were accordingly the patterns the bees least preferred. To simulate the experiments from published behavioural work, I first pre-processed the LOSN responses for all the used patterns and compiled them in an experiment-specific unique Matlab (Mathworks) file (hereafter referred to as “study file”). For each individual experiment within a study file, I defined the CS+, TS^{COR} and TS^{INC} pattern UIDs as well as recoding the behavioural results of the honeybees. For each model I loaded the study file, extracted the unique pattern image UIDs for each experiment and the corresponding eight, or twelve, LOSN firing rate values and from these calculated the model’s Kenyon cell responses to all three patterns. This provided separate arrays of Kenyon cell responses for the CS+, TS^{COR} & TS^{INC} patterns, which I used to calculate the Euclidian distance from the CS+ array to the TS^{COR} array and CS+ array to the TS^{INC} array. The Euclidian distance provided a consistent mechanism when comparing the models that produced a binary output (EAI_AB, EAI_ABC) with the other models (SEO_AB, SEO_ABC) that directly used the Kenyon cell synaptic input firing rates. The ratio of these CS+ to TS^{COR} , CS+ to TS^{INC} Euclidian distances provided the simulation’s Kenyon cell similarity ratio (KCSR) for that experiment for a single trial (Equation 2.3). Each experimental simulation was repeated one thousand times and the average, standard deviation, minimum and maximum KCSR results of each experiment were recorded. For the original honeybee generalisation experiments, bees were trained on multiple CS+ and CS- pattern pairs selected from relevant pools (Fig 2.11b) (van Hateren, Srinivasan et al. 1990). For these

experiments I followed the same procedure as above but created individual simulations for each possible pattern triplet combination. Simulations were again performed one thousand times for all pattern triplet combinations. The KCSR results for all combinations were then averaged to create an overall KCSR value for that simulated experiment.

$$KCSR = 1 - \frac{E(CS+,TSCOR)}{E(CS+,TSCOR) + E(CS+,TSINC)} \quad (2.3)$$

Where KCSR: Kenyon cell similarity ratio, $E(x, y)$: Euclidian distance between x and y , CS+, TSCOR, TSINC: array of Kenyon cell response values for the respective patterns.

2.3.5 Evaluating honeybee and model experimental performances

Due to the difficulties attaining electrophysiological recordings from honeybees during visual learning tasks (see Chapter 1.2.2) we know almost nothing about how a bee's final behavioural decision is made given its Kenyon cell responses to a particular visual stimulus. However, we can assume that if the Kenyon cell responses to a presented test stimulus (TS^{COR}) is very similar to the previously learnt CS+ stimulus (i.e. the same pattern is presented) and the distractor pattern is very different to the CS+ pattern, then the honeybee KCSR would be almost 1.0, and we would expect the bee to almost always visit the TS^{COR} pattern, with an experimental correct choice performance close to 100%. Similarly, if the TS^{COR} and TS^{INC} patterns are different from each other and also different to the CS+ pattern, but both produced Kenyon cell responses equally similar/dissimilar to that of the CS+ pattern (i.e. $KCSR = 0.5$) then we would expect the honeybee to visit each pattern equally likely, and therefore over multiple trials (and multiple bees) have an experimental 'correct' choice performance of ~50%. If the honeybees were trained on a particular CS+ pattern and then tested with a TS^{COR} pattern

similar to this CS+ stimulus and a very different TS^{INC} pattern, and then a second test conducted with the same TS^{COR} pattern and a very similar TS^{INC} pattern, we would again assume the honeybees correct choice accuracy for the first test would be far higher than the second test. Similarly, the KCSR of the first experiment would undoubtedly be much higher than that of the KCSR of the second experiment.

Therefore, to allow me to directly compare my model simulation results against the empirical honeybee experimental results I make the following declaration: the average KCSR of all simulations for a given experiment is directly correlated to my virtual bees' experimental performance. In this way if a model's average KCSR for a given experiment were 0.72 then its overall experimental performance for selecting the correct TS^{COR} pattern would be 72%. It would have been possible to implement a probabilistic 'Monte Carlo' style binary response for the virtual bee to choose either the TS^{COR} or TS^{INC} pattern per trial (based on that simulation trial's KCSR result) and then average these choices, but given the large number of simulations executed per experiment, the added probabilistic variability, and in order to keep the calculations as simple as possible, this was judged an unnecessary complication. The above declaration does have some limitations when assuming a direct comparable mechanism within the honeybee brain (discussed in more detail in Chapter 3.5) but nonetheless provides an effective method for assessing the models' performances over a wide range of pattern experiments. This mechanism also benefits from not needing to train and test an artificial neural network on each pattern experiment, and the inherent parameter tuning and subsequent performance evaluations that this approach would require.

It would have been desirable to assess how my models correlated with the honeybees' relative performances over all of the tested experiments. Each set of the

original honeybee experiments (van Hateren, Srinivasan et al. 1990, Srinivasan, Zhang et al. 1994, Giger and Srinivasan 1995, Sathees chandra, Geetha et al. 1998) only provided a number of mean data points for comparison. In each study, the bees were tested on patterns that typically varied in one particular aspect (e.g. number and orientation of bars in each pattern), but were similar otherwise. Moreover, the used publications addressed similar issues and used similar patterns. While this is a good approach when probing the limits of the learning abilities of bees, it also means that the data points are not independent. A correlation coefficient involving data from multiple different experiments would, therefore, be misleading. Instead, we displayed our models' experimental performance results (equivalent to the KCSR averages) side-by-side with the empirical data, similar to that done in the original studies, so that the relative performance of the different simulated experiments could be assessed, and compared to that of the real honeybees' relative performances on the same sets of pattern pairs.

2.4 Results

2.4.1 Experiment set 1: simple bar and grating pattern discrimination

Honeybees are able to learn, and subsequently discriminate, simple bar and grating patterns when presented vertically (Wehner 1967, Srinivasan and Lehrer 1988, van Hateren, Srinivasan et al. 1990). In these experiments the honeybees were trained to associate a particular orientation of a bar or grating pattern (CS+) with a reward (a sucrose solution) and then tasked to discriminate this same pattern (TS^{COR}) from a non-rewarding distractor pattern (TS^{INC}); the experimenter would record a bee's choice

selection as it flew into one of the Y-mazes arms 17cm from the pattern (see (Srinivasan and Lehrer 1988) for apparatus).

Simple bar and grating simulations

To see if the two or three LOSN types alone would be sufficient to underpin discrimination of these types of patterns, I simulated the experiments of Srinivasan et al. (Srinivasan, Zhang et al. 1994). Figure 2.5 displays the pattern experiments simulated and clearly shows that for both perpendicular pattern discriminations (Fig. 2.5a) and patterns with orientations offset by 45° (Fig. 2.5b) both the two and three LOSN type model simulations are able to make the discriminations using either the SEO (single excitatory only) or EAI (excitatory and inhibitory) LOSN-to-Kenyon-cell connection configurations. Remarkably, given the small number of LOSN inputs, the simulation discrimination performances were similar, and often better, than those of the actual honeybee behavioural results (Fig. 2.5). The two LOSN type EAI_AB model produced the worst individual experiment performance (55%) when discriminating a single vertical bar from that of a 45° bar. However, this was also the pattern pair that real honeybees performed worst at with a correct choice accuracy of just 60% in a dual choice test. The simulation results of both single excitatory-only models (SEO_AB, SEO_ABC) outperformed those of the excitatory and inhibitory models (EAI_AB, EAI_ABC) in all experiments (achieving no less than 87% during simulations). They also consistently outperformed the real bees that only achieved a maximum correct choice accuracy of 86% for the horizontal vs. vertical bar experiment. These SEO model simulations also substantially outperformed the actual honeybee choice accuracy on the more difficult 45° offset pattern discriminations.

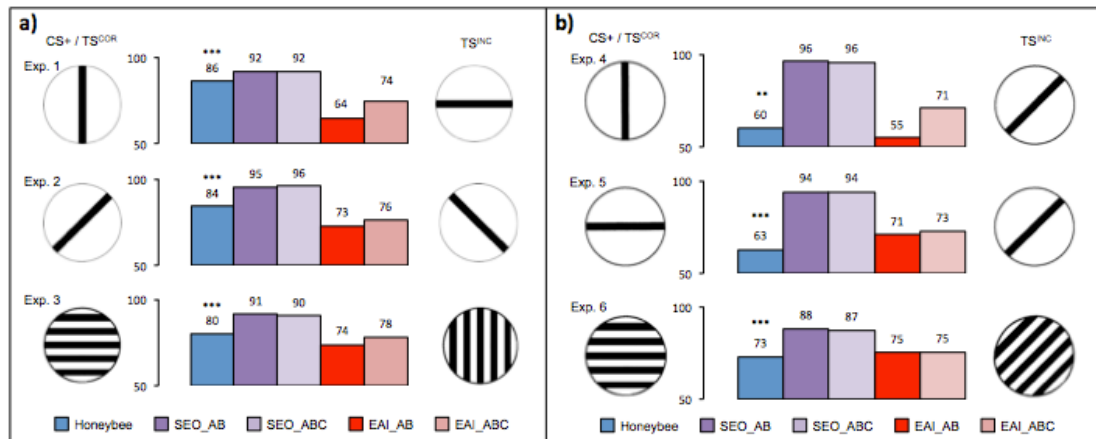


Figure 2.5 Summary of honeybee empirical results and model performances for discrimination tasks of simple bars and gratings. Blue bars: honeybee performance (value above bar is percentage of correct rewarding pattern selections of bees after training, ***: $P < 0.001$, **: $P < 0.005$ see (Srinivasan, Zhang et al. 1994) for statistical tests), Model results, value above bar is average discrimination result of 1,000 simulation trials. **(a)** Results for discrimination of perpendicular bars and gratings. **(b)** Results for discrimination of bars and gratings with 45° angle differences.

Variable distances from patterns (scale simulations)

For the above simulations I assumed that the honeybee would learn the CS+ pattern at the same distance (17cm) as it chose a test (TS^{COR} / TS^{INC}) pattern during trials. It is however possible that the bees would instead learn the pattern while much nearer to the pattern and closer in time to when they would receive the reward. In this situation the CS+ and TS^{COR} would appear as differently scaled versions of each other, with the learnt CS+ pattern being much larger than the patterns at the entrance to the apparatus decision chamber, this may therefore have an affect how well a bee can learn a particular stimuli.

Figure 2.6 shows a replication of the above simulations but this time with zero, 25% or 200% larger versions of the CS+ pattern compared to the TS^{COR} and TS^{INC} patterns (*i.e.* CS+ scaled 100%, 125%, 300% respectively). In this new scenario, I saw that a slight increase of 25% in the size of the CS+ pattern resulted in both SEO models performing approximately 5-20% lower than with no scaling. Both EAI models showed almost identical performances ($\pm 1-4\%$) between the zero and 125% scaling simulations,

the only exception again being on the vertical versus 45° bars, with 125% scaling of the CS+ pattern the EAI_AB model now failed to make the discrimination. With a trebling in size of the CS+ pattern, there was a substantial reduction in the SEO performances. Only two out of the six experiments using the SEO_AB model achieved simulation results greater than 55% accuracy, and interestingly, for the SEO_ABC model using three LOSN types only one of the experiments attained this 55% simulated performance. Conversely EAI_AB only failed to discriminate two of the experiment pattern pairs, with all other results above 55% accuracy in dual choice tests. These results were however always lower than the no scaling and 125% scaling simulation performances.

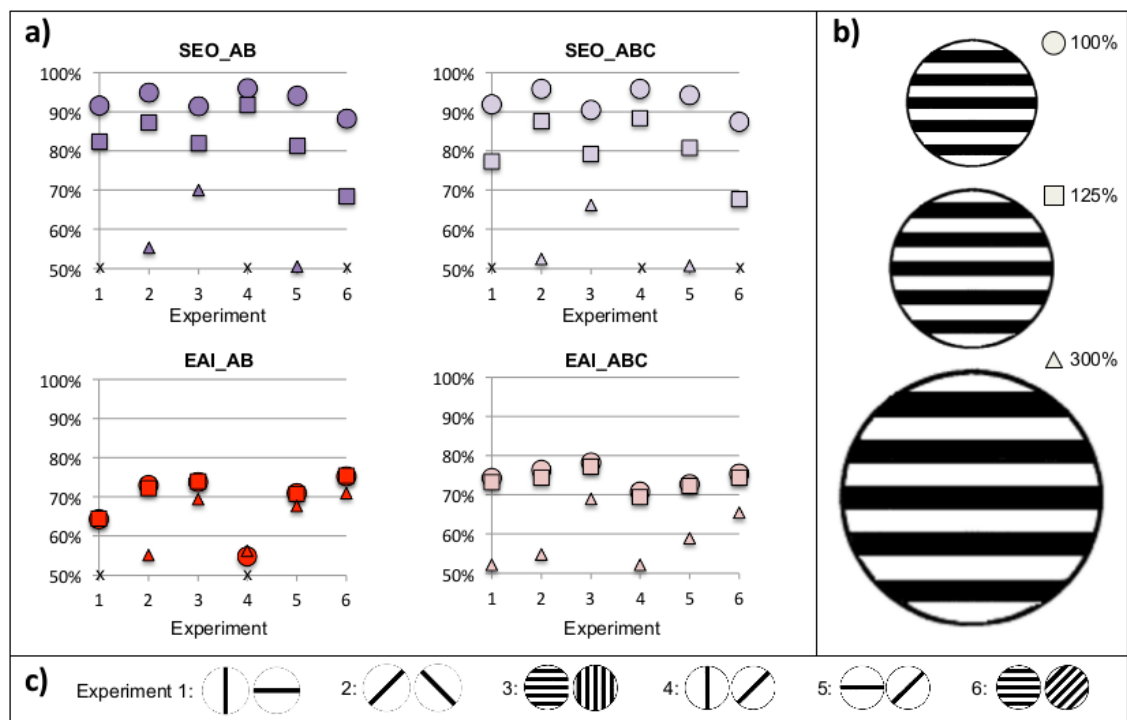


Figure 2.6 Summary of model performances for discrimination tasks of simple bars and gratings when scaled. **(a)** Repetition of simple bar and grating pattern simulations for each model with either no scaling: dots, 125% scaling: squares, or 300% scaling: triangles, of the CS+ pattern compared to TS^{COR} and TS^{INC} patterns, a cross 'x' on x-axis indicates an average result of $\leq 50\%$. **(b)** Examples of a CS+ scaled image *Images not displayed to actual scale. **(c)** Experiments simulated showing CS+/ TS^{COR} and TS^{INC} patterns.

Simulation analysis

The reason for the SEO models failure to correctly identify the correct scaled pattern can be clearly seen in the SEO_AB example in Table 2.3. The larger CS+ pattern presents longer edges, and thus higher firing rates in the LOSNs compared the test stimuli. In this example two of the TS^{INC} pattern quadrants have higher LOSN type A responses (due to their greater sensitivity to 45° than horizontal oriented edges) than the TS^{COR} pattern, and are therefore more similar to the responses of the larger horizontal bar than the smaller horizontal bar. The other two quadrants of the TS^{INC} pattern have almost no edges in them; this produces minimal firing rate responses, and much lower responses than the TS^{COR} pattern. This makes the TS^{INC} pattern to more dissimilar to CS+ in these quadrants. The overall effect of these two competing quadrant pairs means that the SEO_AB model cannot easily differentiate which test pattern is most similar to the CS+ pattern. The described simulation achieved a Kenyon cell similarity ratio (KCSR) of just 0.505.

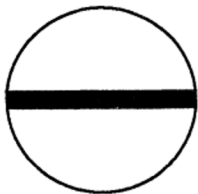
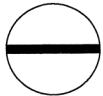

Pattern	LOS N type A	LOS N type B
CS+ (300%) 	58, 56, 56, 58	21, 23, 23, 22
TS ^{COR} (100%) 	21, 21, 20, 21	9, 9, 9, 9
TS ^{INC} (100%) 	9, 45, 45, 9	2, 8, 9, 2

Table 2.3 LOSN type A, B (using _AB model) responses in each quadrant to scaled single bar patterns. *Images not displayed to scale.

In contrast the EAI model performances are not dependent on the actual firing rates of the LOSNs, but the correlation of the responses between the respective type A and type B neurons from each quadrant. Figure 2.7 shows the EAI_AB model Kenyon cell responses to the same patterns as above (Table 2.3) and the difference in the Kenyon cell activations between the CS+ pattern and the TS^{COR} and TS^{INC} patterns. Despite the large difference in LOSN firing rates there were only 221 inaccurate Kenyon cell activations (either incorrectly fired or didn't fire when should have) between the CS+ and TS^{COR} simulations, compared to 1,233 for the CS+ / TS^{INC} pattern pair. This allows the EAI_AB model to easily identify the horizontal bar independent of its edge length.

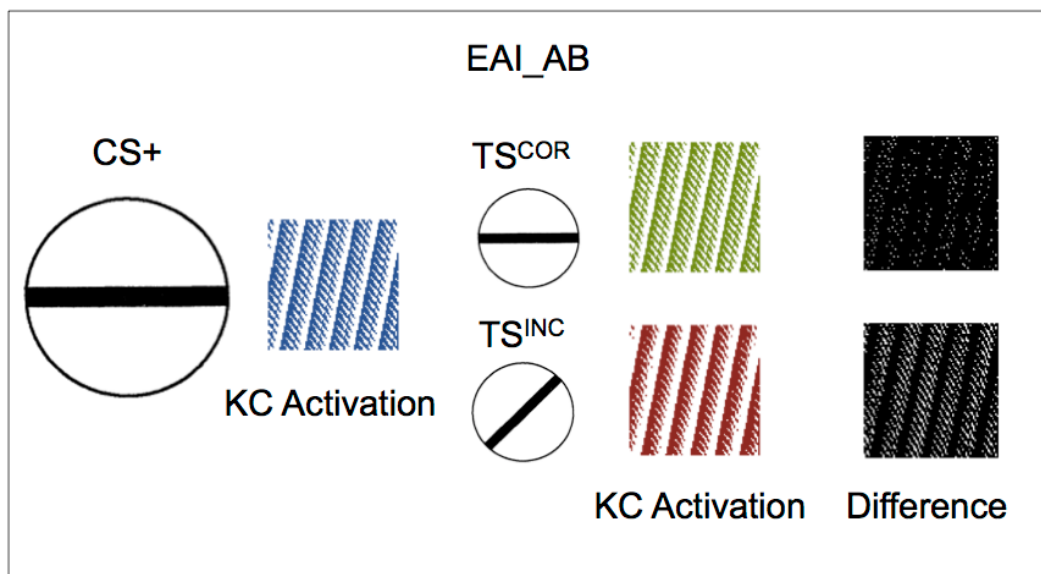


Figure 2.7 Model Kenyon cell activation for scaled bar patterns. Blue: Kenyon cell activation when EAI_AB model is presented with the 300% scaled CS+ pattern. Green: Kenyon cell activation to the TS^{COR} pattern, Red: Kenyon cell activation to the TS^{INC} pattern. White dots on black square: shows the Kenyon cell activation differences between a test stimulus (TS^{COR} or TS^{INC}) and the CS+ pattern.

Summary of experiment set 1

Remarkably, LOSN optic neurons appear able to facilitate performances equivalent, and often better, than the empirical honeybee results, even where the two LOSN type models (SEO_AB, EAI_AB) extend just four neuronal outputs from each eye to the mushroom bodies. Overall the SEO models outperformed the EAI models in all experiments apart from those where the TS^{COR} and TS^{INC} patterns were half the size of the CS+ patterns.

2.4.2 Experiment set 2: fine angle discrimination

In the above simulations, I found very little performance difference between the respective two and three LOSN type models; the only exception being the discrimination of the vertical and 45° inclined bars where the EAI_ABC model simulations attained 71% outperforming EAI_AB (55%) and real honeybees correct choice selection of 60%.

Srinivasan et al (Srinivasan, Zhang et al. 1994) and Chandra et al (Sathees chandra, Geetha et al. 1998) hypothesised that honeybees would require at least three orientation sensitive neuron types in order to discriminate an oriented bar independently of its orientation. To test if honeybees could in fact discriminate bars at any orientation, Chandra et al (Sathees chandra, Geetha et al. 1998) trained honeybees to one of twelve rewarding orientations (-90° to +75° in 15° increments). Subjects were then tested to see if they could correctly identify the learnt orientation when presented with either a single distractor pattern with an orientation offset between $\pm 90^\circ$ to $\pm 15^\circ$, in 15° increments (dual-choice), or with all twelve orientations presented simultaneously (multiple choice).

Honeybees were able to discriminate a 30° difference in orientations for dual-choice scenarios and 15° in the multi-choice experiments.

Fine angle discrimination simulations

To replicate the above procedure I simulated the fine angle discrimination experiments by presenting a single 100 pixel oriented edge in each image quadrant. Each experiment was composed of one of the twelve rewarding orientations used for both the CS+ and TS^{COR}, and then each of the twelve 15° increment angle differences as TS^{INC}.

The SEO_AB model achieved over 70% for all rewarding orientations with a 30° or greater angle difference to the distractor patterns. For an angle difference of ±15°, the lowest performances were for 45° and 60° (from horizontal) rewarding orientations both achieving 59% (Fig. 2.8a). SEO_ABC produced a minimum performance of 64% for an angle difference of 15° with similar results for all orientations (overall average 69%); the lowest simulation result for ≥30° difference was 79%. EAI_ABC achieved ≥62% for 15° differences and 73% or more for ≥30° differences. EAI_AB was the only model where a striking difference was seen dependent upon the rewarding orientation presented. Fewer than half of the orientations tested had simulation performances better than 60% for ±15° differences (average 59%(±10%)). Figure 2.8b shows a contour map of the EAI_AB model simulation performance against angle difference (x-axis) and rewarding orientation (y-axis). Even at angle differences of up to ±45° between the test patterns this model still produced simulation results of less than 60% accuracy in dual choice tests for specific rewarding and distractor pattern orientations.

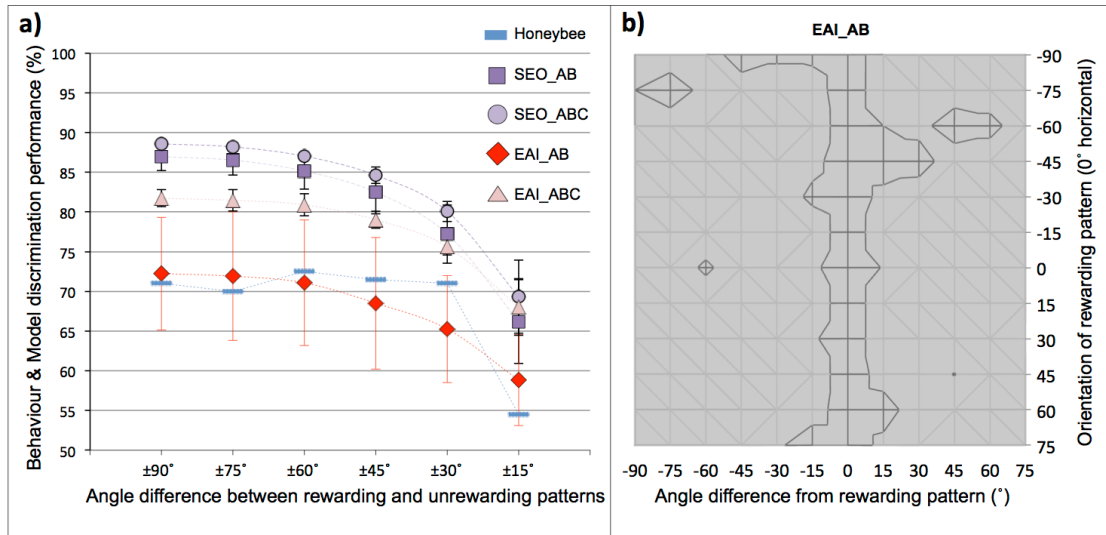


Figure 2.8 Summary model performances for discrimination of fine angle differences. **(a)** Average model performance when discriminating an angle difference between $\pm 90^\circ$ and $\pm 15^\circ$ for twelve rewarding orientations (-90° to $+75^\circ$ in 15° increments). Blue bars: Honeybee result for bees trained on a horizontal bar as rewarding and then tested with the same rewarding pattern and patterns differing in angle between $\pm 15^\circ$ to $\pm 90^\circ$ (Sathes chandra, Geetha et al. 1998). Error bars show standard deviation between different orientation of rewarding pattern results for same \pm angle difference ($n=24,000$ simulations, 1,000 simulations of each 12 rewarding orientations with plus and minus angle difference), these were not available for the honeybee results. Only EAI_AB showed a large variance in simulated results dependent upon the rewarding orientation with performances of less than 60% accuracy for an angle variance of $\pm 15^\circ$. **(b)** Contour map showing EAI_AB performance for each rewarding orientation. y-axis: rewarding orientation, x-axis difference of the unrewarding orientation. Region enclosed within the dark grey lines achieved less than 60% for that orientation / angle difference combination. This model achieved poor discrimination performance ($<60\%$) even for -45° angle differences at the -90° (horizontal) rewarding orientation.

Analysis of EAI_AB model performance dependency on LOSN firing rates

Given the large variance in results by the EAI_AB model I performed additional analysis on these results. Of particular interest is the markedly different firing rates recorded between the LOSN types (Maddess and Yang 1997). The LOSN type B responses were confined between 3Hz to 14Hz for all orientations, with these always greater than the spontaneous background firing rate of less than 1Hz (recorded between the stimuli presentations). In contrast the LOSN type A recordings produced higher

firing rates (20Hz-36Hz, background: ~10-13Hz). To first test if the very low firing rates of the LOSN type B might be affecting the discrimination performance I repeated the simulation but first doubled, then quadrupled, the edge lengths presented in each quadrant of the pattern. Figure 2.9a shows that increasing the length of the edges, and thus the firing rates of the type A and type B neurons, did indeed increase the performance of the EAI_AB model. This would seem to be corroborated in the behavioural experiments (Srinivasan, Zhang et al. 1994) (see Fig 2.5b) where the honeybees performed better at discriminating the 45° angle difference with gratings rather than with single bars. However, even with the quadrupled edge lengths the EAI_AB model was still unable to discriminate some particular rewarding orientations and angle differences of $\geq \pm 15^\circ$ (Fig 2.9b).

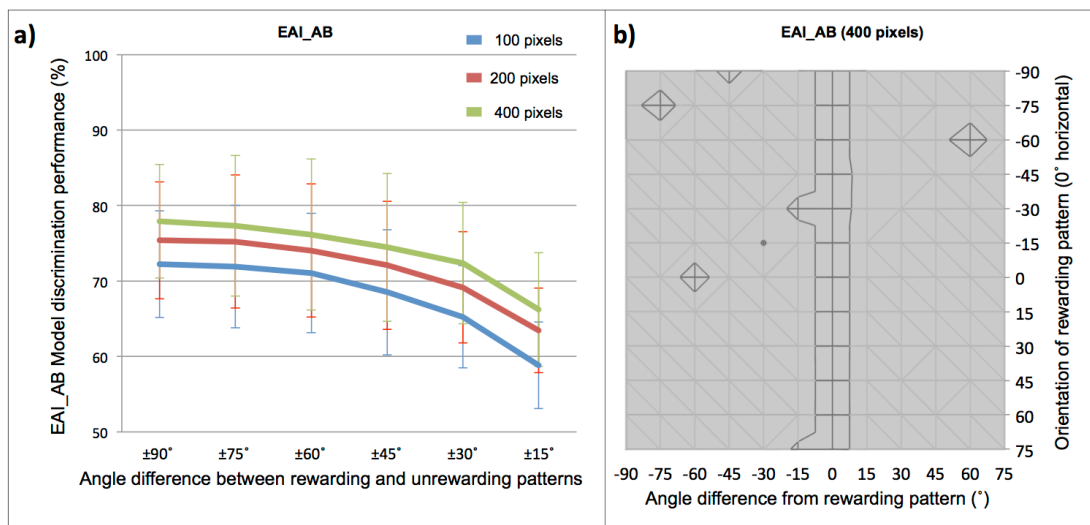


Figure 2.9 Performance of EAI_AB with differing edge lengths. **(a)** EAI_AB model performance at angle discrimination using a 100 pixel (blue), 200 pixel (red,) or 400 pixels (green) length edges in each quadrant of the CS+, TS^{COR} and TS^{INC} patterns. **(b)** Contour map showing EAI_AB performance with 400 pixel edges for each rewarding orientation. Y-axis: rewarding orientation, X-axis difference of the unrewarding orientation. Region enclosed within the dark grey lines achieved less than 60% for that orientation / angle difference combination.

Summary of experiment set 2

These very basic models have once again shown that with just two types of orientation-sensitive neurons, honeybees would be able to use these non-retinotopic neurons for discriminations of at least 30° angle difference discriminations, directly inline with the dual-choice empirical honeybee results (Sathes chandra, Geetha et al. 1998). In these original honeybee experiments Chandra et al (Sathes chandra, Geetha et al. 1998) also performed tests where the honeybees were simultaneously given the option of all twelve possible angles (15° increments). Here the bees mostly ignored any patterns with an angle difference of $\pm 30^\circ$ or more from the trained pattern, but the percentage of visits to the -15° , 0° and $+15^\circ$ angle difference stimuli did differ dependent on the originally trained orientation. Additional experiments would be required to see if gratings (which would present a longer total edge length) could affect the 15° angle discrimination ability of the honeybees, in particular at those orientations that my EAI_AB model consistently failed at.

2.4.3 Experiment set 3: eidetic imagery and orientation discrimination

To explore if honeybees exclusively rely on pattern features or on some form of image template, Giger & Srinivasan (Giger and Srinivasan 1995) performed experiments designed to evaluate honeybees' ability to discriminate two slightly different horizontal gratings; this therefore presented the same orientation features in both patterns but displayed unique retinotopic images. Bees successfully trained on a rewarding horizontal grating (CS+) and unrewarding vertical grating (CS-) subsequently struggled to discriminate the learnt pattern (TS^{COR}) from a second different horizontal pattern

(TS^{INC}), but could discriminate the rewarding pattern when initially trained with this second horizontal pattern being unrewarding.

Model simulation results

When tasked with discriminating horizontal and vertical gratings (Fig. 2.10a: Test a) all my model simulations achieved over 70% accuracy. In contrast, when discriminating the two horizontal gratings (Fig. 2.10a: Test b, Fig. 2b: Test a) or the two horizontal bar patterns (Fig. 2.10c: Test a), both the EAI_AB and EAI_ABC model simulations failed to solve the tasks with performances of ~50% accuracy. This was not unexpected; as seen above, these models' Kenyon cells generate similar responses invariant to the length of the oriented edges presented. However, most surprisingly given the extreme similarity of these pairs of horizontal bar and grating test patterns, I found that the excitatory model simulations actually achieved performance averages of over 70%. All the models showed a preference for the offset horizontal grating to that of a vertical grating (Fig. 2.10b: Test b); which was a peculiar result during honeybee trials as the bees also preferred this pattern, despite it being identical to the trained CS- unrewarding pattern.

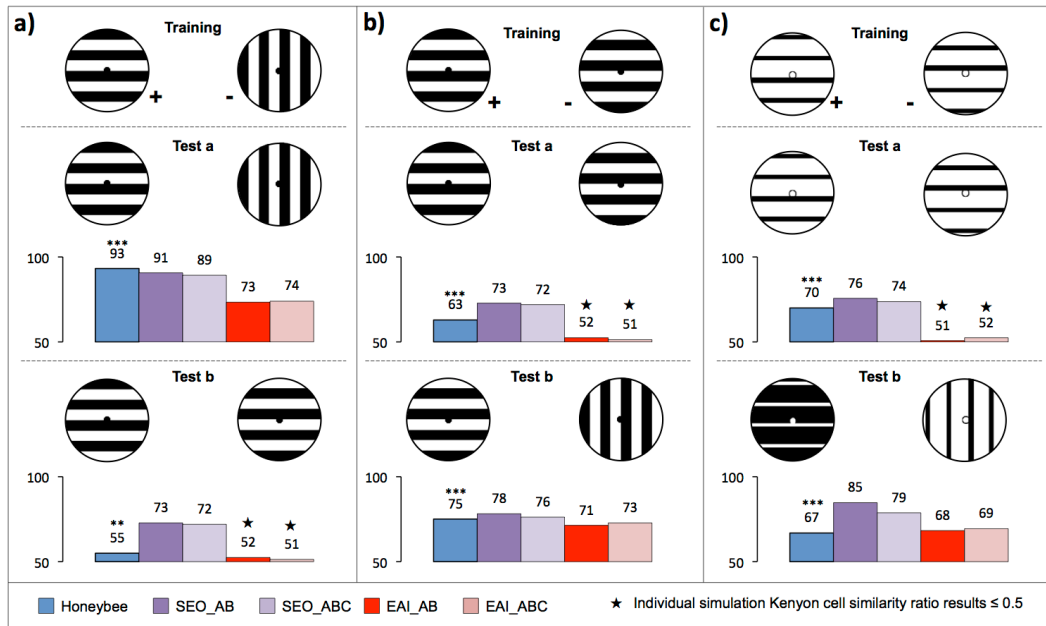


Figure 2.10 Summary of honeybee behaviour and model performance for discrimination of two horizontal gratings. Blue bars: honeybee performance (value above bar is percentage of correct rewarding pattern selections of bees after training, n : number of recorded choices, ***: $P < 0.001$, **: $P < 0.005$, p = significance level for percentage being different from random choice (50%) see (Giger and Srinivasan 1995) for statistical methodology). Model results, value above bar is average discrimination result for 1,000 individual simulations, star: individual KCSR of ≤ 0.5 . Both excitatory only models can correctly discriminate the two offset horizontal gratings (a-b) and bar patterns (c), whereas both opponent ratio models failed.

Simulation analysis

Since my models do not utilize the CS- pattern used during the original honeybee experiments, from the models' perspective, there was no difference between (Fig 2.10a: Test b and Fig 2.10b: Test a). The models only compare the neural responses of the CS+ to the TS^{COR} and TS^{INC} stimuli. In contrast, the honeybee results are very different for these experiments showing the bees must also utilize the CS- patterns, further analysis of this is provided in this discussion section below (see also Chapter 3.5 on how a non-rewarding stimuli, as in these experiments, can affect behavioural results).

As with honeybees, all four of my models preferred the incorrect horizontal grating to that of vertically oriented gratings. Table 2.4 shows that the LOSN responses

to the TS^{COR} horizontal grating (Table 2.4 row: 3) pattern are more similar to the CS+ than TS^{INC} responses (Table 2.4, rows 1 and 2 respectively). Similarly, all models showed a preference for the colour-inverted horizontal bars pattern to that of vertical bars (Fig. 2.10c: Test b, Table 2.4 rows: 4-6), as did the real honeybees.

My model results therefore support the proposition that during the honeybees' training phase with two horizontal bars, the highly specific LOSN firing rate responses provide a useful 'feature' that a honeybee can learn to solve these discrimination tasks. This is contrary to previous hypotheses which simply assumed that bees would always learn the orientation (i.e. my EAI model Kenyon cell activations) even when there was no difference in pattern orientation and it provided no useful feature for the pattern task (Giger and Srinivasan 1995).








Pattern	_AB models		_ABC models		
	LOSN type A	LOSN type B	LOSN type A	LOSN type B	LOSN type C
	45, 41, 47, 49	18, 19, 21, 21	45, 41, 47, 49	44, 46, 51, 50	31, 31, 34, 33
	29, 28, 26, 31	6, 7, 7, 6	29, 28, 26, 31	25, 28, 28, 27	35, 38, 36, 38
	49, 47, 42, 44	21, 21, 19, 18	49, 47, 42, 44	50, 51, 47, 44	34, 34, 31, 30
	42, 41, 48, 47	19, 18, 22, 21	42, 41, 48, 47	45, 44, 51, 49	28, 28, 31, 30
	48, 47, 42, 41	22, 21, 19, 19	48, 47, 42, 41	51, 49, 45, 44	31, 30, 28, 28
	47, 42, 50, 53	18, 19, 22, 21	47, 42, 50, 53	45, 48, 56, 52	34, 34, 38, 37
	22, 24, 22, 25	5, 5, 5, 5	22, 24, 22, 25	21, 23, 21, 23	31, 35, 31, 36

Table 2.4 LOSN type A, B and C responses in each quadrant to grating patterns.

Summary of experiment set 3

Overall the EAI models were able to discriminate the horizontal and vertical oriented gratings, as we saw earlier, but failed to differentiate either of the pairs of horizontal gratings or bars. Remarkably though, both SEO models were able to discriminate all patterns, achieving discrimination performances on the horizontal pattern pairs marginally higher than those of the empirical honeybee results.

2.4.4 Experiment set 4: oriented grating generalisation

Van Hateren et al. (van Hateren, Srinivasan et al. 1990) tested the honeybee's ability to learn the correct orientation when trained on a pair of patterns randomly selected from ten rewarding grating patterns all at the same orientation and another set of ten unrewarding perpendicular 'distractor' grating patterns. After training, they subsequently tested the bees to see if they could generalise to a completely novel pattern with edges in the correctly oriented direction. In these experiments, the authors (van Hateren, Srinivasan et al. 1990) point out that it is conceivable that honeybees could initially learn all ten rewarding grating patterns, but if the bees are using only a pure template matching approach, they should then fail to generalise to the novel control tests.

Discrimination of training patterns

Initial simulations could discriminate any one of the ten rewarding gratings (CS^+ / TS^{COR}) from each of the ten potential perpendicular distractor patterns (TS^{INC}). Both SEO model simulations achieved performance levels of ~90% on the discrimination test for horizontal, vertical and 45° oriented gratings being rewarding, with very similar

results to that of the real honeybees correct choice performances. The EAI models also managed to discriminate the patterns, albeit with slightly lower performances in the range of ~70-80% (Fig. 2.11)

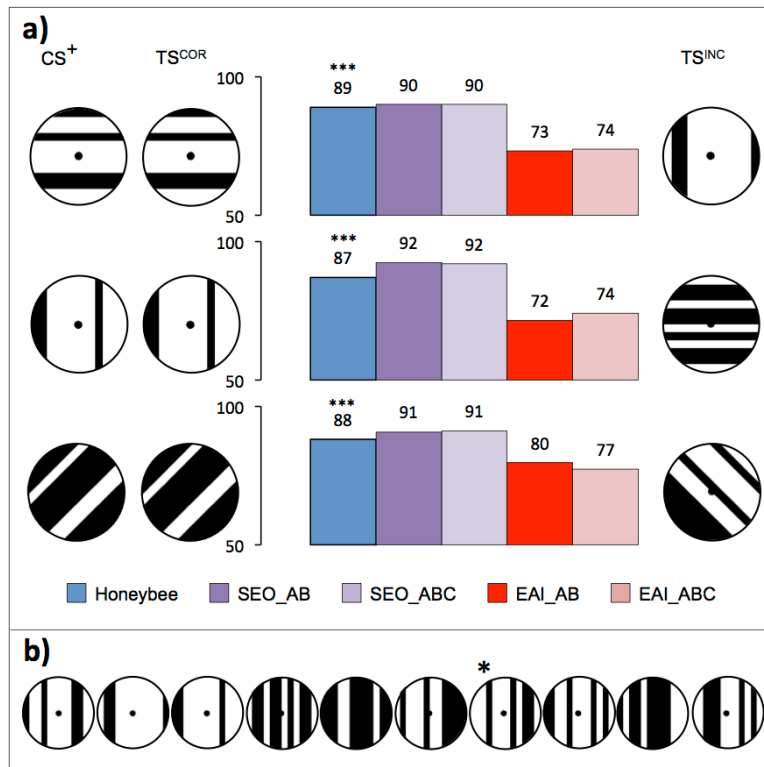


Figure 2.11 Summary of honeybee behaviour and model performance for discrimination of training grating patterns. **(a)** Discrimination task of identifying each of the ten CS⁺ patterns (see b) from each of the ten perpendicular distractor patterns. Blue bars: honeybee performance, value above bar is percentage of correct rewarding pattern selections of bees after training ***: $P < 0.001$, **: $P < 0.005$ see (van Hateren, Srinivasan et al. 1990) for statistical analysis. Model results, value above bar is average discrimination result for 10,000 individual simulations, star: individual simulation $KCSR \leq 0.5$. **(b)** Vertical grating training patterns, these patterns are rotated through 90°, 45° and 135° for the other pattern sets. * Indicates an additional bar added to training pattern 7 (see (van Hateren, Srinivasan et al. 1990) for original pattern).

Generalisation between training patterns

To see if the models could generalise between each of the ten rewarding gratings, I calculated the model simulation preferences (smallest difference in Kenyon cell

responses) from one of the rewarding gratings to one of the other nine rewarding gratings and one of the ten perpendicular gratings; repeated for all possible combinations (Fig. 2.12). The EAI model simulations averaged over 60% correct preference for each of the three rewarding oriented gratings (0° , 90° , 45°). However, careful analysis of all the individual experiments reveals that a single grating pattern accounted for all the lowest performances (49% and 51% for EAI_AB, EAI_ABC respectively). This grating was the single example from the set of ten random gratings per orientation that was composed of black bars in only one half of the pattern, the remaining half being all white (see (van Hateren, Srinivasan et al. 1990) Fig. 1 P7). Replacing this pattern with a new grating consisting of bars in both halves (Fig. 2.11b star; all subsequent experiments reported used this pattern) increased the previously lowest values of EAI_AB (vertical rewarding) to 58%, and EAI_ABC (horizontal rewarding) to 58%.

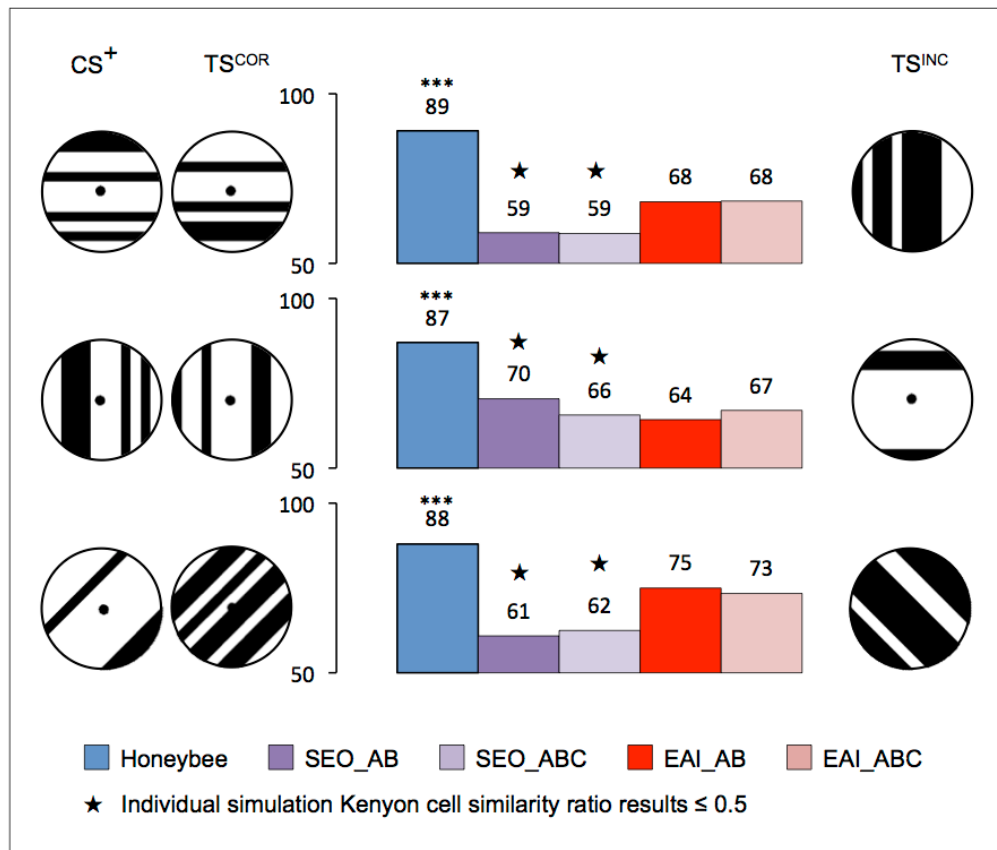


Figure 2.12 Summary of honeybee behaviour and model performance for generalisation between training patterns. Generalisation task of identifying the correct orientation of each of the ten CS⁺ patterns in each of the other nine different TS^{COR} patterns against each of the ten possible TS^{INC} patterns. Blue bars: honeybee performance, value above bar is percentage of correct rewarding pattern selections of bees after training ***: $P < 0.001$, **: $P < 0.005$ see (van Hateren, Srinivasan et al. 1990) for statistical analysis. Model performance, value above bar is average discrimination result for 900,000 individual simulations, star: individual simulation KCSR ≤ 0.5 .

SEO_AB individual simulation trial KCSRs ranged from 0.23 (indicating a very strong similarity between the Kenyon cell responses to the TS^{INC} and CS⁺ patterns) to 0.91 (which had a greater similarity between TS^{COR} and CS⁺ responses) with SEO_ABC performing marginally better with a range of 29% to 81%. In these cases, any particular simulation trial (with a single CS⁺, TS^{COR} and TS^{INC} grating pattern) produced simulation results with a large variation in the degree of preference for either

of the two test gratings presented. This generated performance accuracies for each experiment ranging from 59-70%, but overall the model showed very little trial-by-trial similarity to the real honeybee results.

Generalisation between training patterns and novel stimuli

Following the original behavioural experiment procedure, I tested the models' abilities to generalise to a novel pattern with the correct orientation (Fig. 2.13). I again found that neither SEO model was able to correctly generalise, with performances of no more than 53% (individual simulation trial KCSRs ranging from 0.29 to 0.63). In contrast the EAI model simulations were all able to generalise to the correct novel patterns, always achieving performances $> 62\%$ accuracy with every individual trial simulation KCSRs ≥ 0.58 (Fig 2.13).

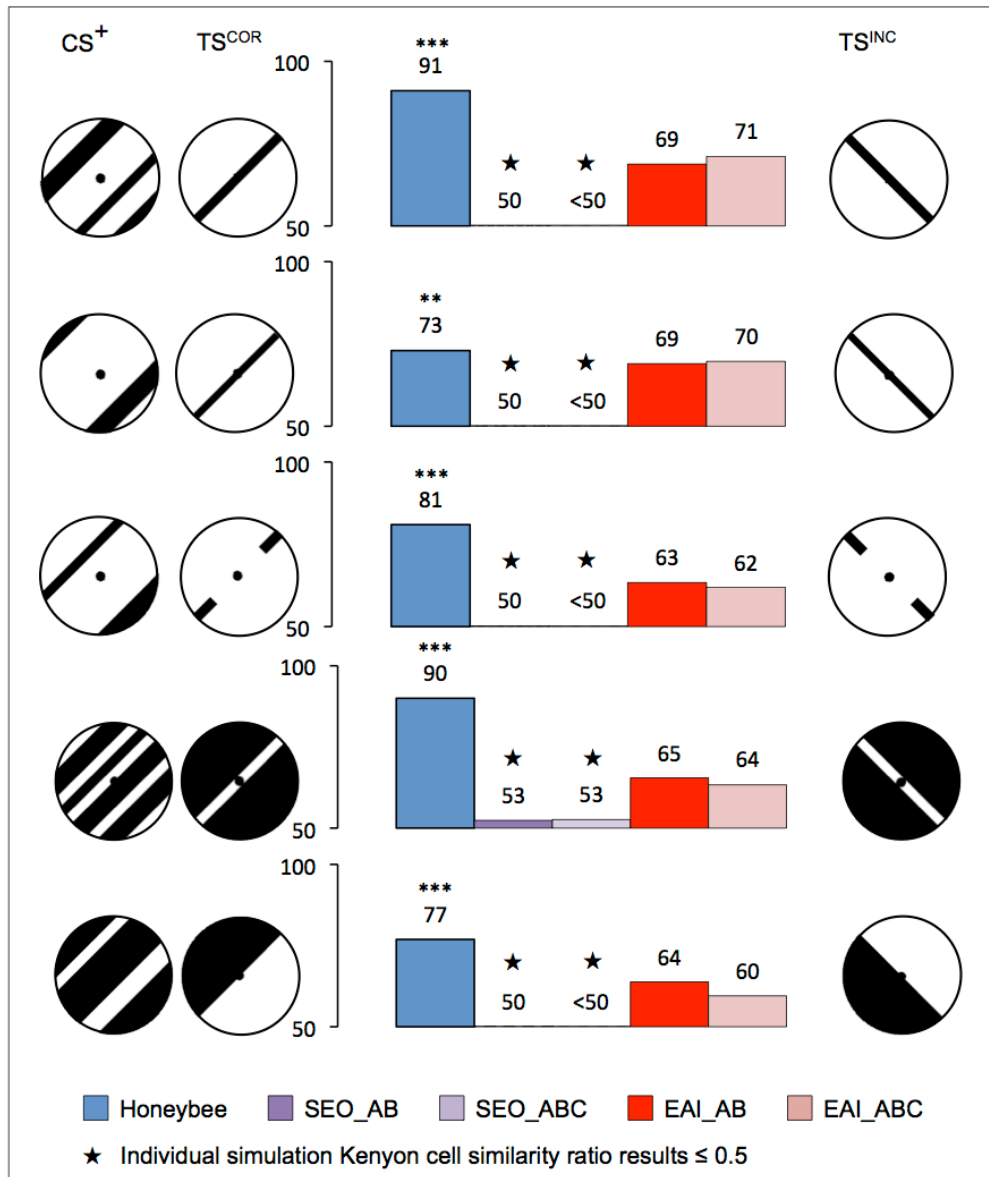


Figure 2.13 Summary of honeybee behaviour and model performance for generalisation to novel stimuli tasks. Generalisation task of identifying the correct orientation of each of the ten CS⁺ patterns in each of the five novel TS^{COR} patterns against a 90° rotation of the novel pattern (TS^{INC}). Blue bars: honeybee performance, value above bar is percentage of correct rewarding pattern selections of bees after training ***: $P < 0.001$, **: $P < 0.005$ see (van Hateren, Srinivasan et al. 1990) for statistical analysis. Model performance, value above bar is average discrimination result for 1,000 individual simulations, star: individual simulation KCSR ≤ 0.5 .

Simulation analysis

The ability of the EAI models to generalise between common orientations, and equally the SEO models' inability, is due to similar reasons for the scale / size invariance results

in experiment set 1. Figure 2.14 shows an example of the SEO_AB and EAI_AB models' generalisation results for a single CS+ vertical grating pattern and a single TS^{INC} horizontal grating, to each of the other nine possible TS^{COR} horizontal gratings. Each pattern produced specific LOSN type A and B responses (only dorsal LOSNs from each eye shown) dependent on the edge length within the particular pattern quadrants. The SEO_AB performances on each TS^{COR} pattern (average of 1,000 simulations) range between 40-70% (i.e. occasionally preferring the TS^{INC} pattern). These differences are purely down to the similarity of the edge lengths between the CS+ pattern and each TS^{COR} pattern. The EAI_AB model consistently achieved over 60% accuracy, once again showing that it is not the LOSN firing rates themselves that is important, but the correlation of the response between the respective type A and type B neurons in each eye region.

Summary of experiment set 4

The results for this final set of experiments show that the SEO models are unable to generalise to a common orientation 'feature'. In contrast, the EAI models show extremely good generalisation ability from one oriented grating to another completely novel but similarly oriented pattern.

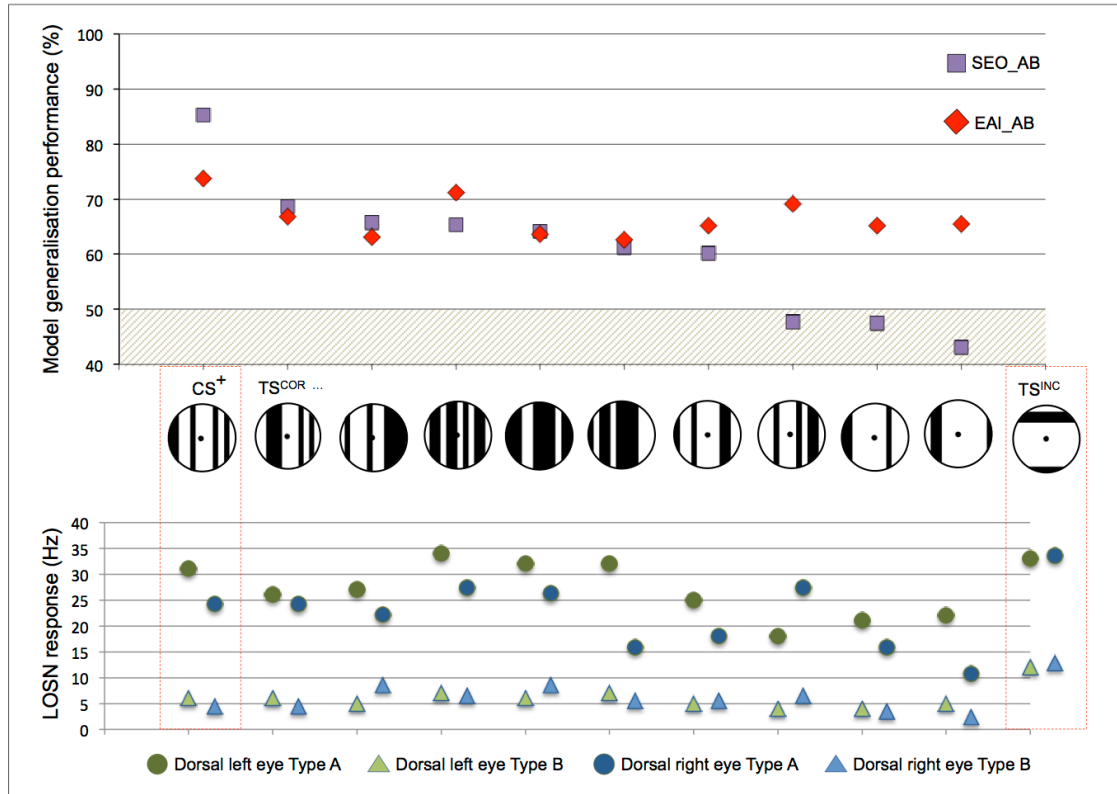


Figure 2.14 Analysis of SEO_AB and EAI_AB model performance for generalisation between vertical gratings. **(Top)** model generalisation performances with a fixed CS^+ and TS^{INC} pattern (red boxes) to the nine possible TS^{COR} patterns (also shown the CS^+/TS^{COR} discrimination performance). Hatched area: x-axis extends to 40% (i.e. where incorrect pattern was chosen). **(Bottom)** LOSN type A and type B responses in the upper left (left eye – dorsal) and upper right (right eye – dorsal) image quadrants for each pattern. Ventral LOSN responses for CS^+ / TS^{COR} were very similar given the vertical symmetry of the patterns.

2.5 Discussion

In this chapter I investigated how neuronal minimalism and response specificity could aid in compressing complex cognition into a miniature brain. Using simple theoretical models with minimal connections from the lobula (third optic ganglion) to the mushroom bodies (higher learning centres), I simulated a range of discrimination and generalisation tasks previously conducted on honeybees (van Hateren, Srinivasan et al. 1990, Srinivasan, Zhang et al. 1994, Giger and Srinivasan 1995, Sathees chandra,

Geetha et al. 1998). The extraordinary finding here is that despite each model's simplicity, as well as none of the model parameters being adjusted to mimic any behavioural capacity and the models being based only on empirical neuroscientific information, they nonetheless capture, with surprising precision, a variety of visual cognitive affordances that are typically regarded as computationally highly demanding or requiring complex visual representations.

2.5.1 Minimising connections between neuropiles

It may seem peculiar to us that the honeybee brain extends so few axonal like fibres from the optic lobes to the higher brain regions, especially given the highly complex and 'accurate' photographic representation that our own brains create in order for us to interact with our environment. My models, nonetheless, show that for orientation pattern discriminations, often used during honeybee behavioural experiments, very few optic neuron outputs are required. The LOSNs themselves provide a very coarse representation of the visual field, providing no detailed retinotopic representation but instead responding maximally to particular orientations anywhere across the width of the bee eye, maintaining a consistent $\sim 90^\circ$ tuning curve response to orientations independent to where the stimuli are presented (Maddess and Yang 1997). In previous theoretical models (Srinivasan, Zhang et al. 1994, Sathees chandra, Geetha et al. 1998) it was suggested that just two types of these orientation-sensitive neurons would be insufficient for discrimination of a 45° -oriented bar from a bar at 135° . However, in their models, the authors assumed that the tuning curves of the two orientation-sensitive neuron types would be offset by 90° (maximally sensitive to horizontal and vertical orientations) perhaps similar to that seen in the octopus (Sutherland 1957). Octopi can

indeed differentiate vertical from horizontal patterns but not 45° and 135° orientations (Sutherland 1957). In contrast, here I based my two LOSN type models (SEO_AB, EAI_AB) on orientation sensitive neurons maximally sensitive at ca. 115° and ca. 250° as recorded in the honeybee (Maddess and Yang 1997). These “non-symmetric” tuning curves return different firing rates for any two orientations differentiated by at least 15°, resulting in fair (>60%) discrimination results for the two LOSN type SEO_AB model simulations. Although, as seen in experiment set 1, this model’s performances may be degraded if the rewarding and test patterns are perceived as different sizes (*i.e.* the bee learns the pattern closer than the distance that it must make a choice during tests). The EAI models are less susceptible to this effect and the EAI_AB model was able to discriminate 30° differences in presented edge orientations (similar to honeybees during dual-trial evaluations (Sathes chandra, Geetha et al. 1998)) in all but a few distinct orientations and angle differences. The worst simulation performances were most notable around vertical orientations and $\pm 30^\circ$ angle differences (Fig 2.8b). It must be reiterated that my models implemented just the LOSNs from the optic lobes to the mushroom bodies, no other sensory inputs, and although these two LOSN type models produced poor results at certain orientations, this does not necessarily mean three LOSN type are required. Dragonflies, which have all three orientation-sensitive LOSN types at the required $\sim 120^\circ$ maximal sensitivity offsets (O’Carroll 1993), display impressive aerobic flight manoeuvres during flight and prey catching, and therefore their heads are capable of being in almost any rotation and position (Olberg, Seaman et al. 2007). Although the dragonfly LOSNs are not used directly in prey detection or tracking, as they were shown to be unresponsive to small moving stimuli (O’Carroll 1993), they may help in orienting the insect within its environment during capture flights. In addition, perching species of dragonflies (*e.g. Libellulidae, Perithemis tenera*) have preferred

perches where they wait for passing prey or potential mates (Switzer and Walters 1999, Olberg, Seaman et al. 2007); the combination of these three LOSN types and interneurons that respond to head rotation (even in the dark) (Olberg 1981) would allow specific perches or other landmark cues to be discriminated independent of the rotation of the head. In contrast, honeybee heads typically counter-rotate to the roll of the thorax during flight using optic flow stabilisation to keep the head in a relatively fixed position (Berry and Ibbotson 2010, Boeddeker, Dittmar et al. 2010, Boeddeker and Hemmi 2010). These flight stabilising mechanisms as well as visual altitude detectors (roll, pitch and yaw) mediated through the ocelli (three small lens eyes on the top of the bees head) (Ribi, Warrant et al. 2011) may be used to augment the two LOSN types for the experimental discrimination experiments near vertical. If honeybees do indeed have three LOSN types, then from our simulated results we might expect honeybees to perform substantially better than the 60% accuracy displayed for vertical and 45° oriented bar discriminations (Srinivasan, Zhang et al. 1994). Only additional electrophysiological recordings will be able to confirm the existence of a third LOSN type in honeybees, but it may simply be that if this third LOSN type adds little to the recognition abilities of honeybees, as my models suggest, then the exclusion of this neuron type may allow more useful synaptic connections to occupy the same limited neuronal substrate.

2.5.2 Neuronal response specificity

Giger & Srinivasan (Giger and Srinivasan 1995) proposed that their behavioural results showing the honeybees' ability to discriminate two horizontal grating patterns demonstrated that the bees must be using some form of photographic template for

discriminations when orientation (or other feature) cues were not a useful predictor of reward. Although, surprisingly, the bees still learnt the orientation of the gratings even though this was of no use for discrimination of the consistently horizontal training patterns. During their experiments, the bees were allowed to approach either pattern and fixate (slow scanning movements 1-3 cm in front of a target) and, if they desired, fly to the other pattern. The final choice selection was therefore not recorded until a bee physically touched one of the two stimuli. The SEO simulation results demonstrate that if the bees were to fixate at the height of the centrally located feeding hole (or any consistent height above the ground during fixation hovering), then utilizing just the eight (SEO_AB) or twelve (SEO_ABC) LOSN responses from the optic lobes and establishing excitatory-only synapses onto the mushroom body Kenyon cells these highly similar patterns could be easily discriminated without the need for a more complex retinotopic or template matching approach. This is possible due to the specificity of the LOSN responses. The induced firing rates of these neurons are not only affected by the orientation of presented pattern edges but also the total edge length they perceive (O'Carroll 1993, Maddess and Yang 1997). Although during the horizontal offset pattern simulations there were predominantly horizontal edges in both the dorsal and ventral regions of both patterns, the small LOSN response differences in all of the LOSNs caused by the slightly different edge lengths in each pattern region (distinct LOSNs with receptive fields confined to either the dorsal and ventral half of one eye) were sufficient to allow discrimination (see Table 2.4). This also provides a better account for why honeybees, during one of the evaluation trials, preferred a pattern identical to the training unrewarding CS- pattern to that of a novel vertically oriented one (Fig. 2.10b Test b) as here the LOSN responses to this TS^{COR} / CS- pattern are still more similar to the CS+ than the novel TS^{INC} pattern (Table 2.4).

Honeybees trained on the horizontal and vertical gratings subsequently failed to discriminate the very similar horizontal bar pattern. This is not unusual, even with much simpler stimuli Stach and Giurfa found that after 42 training trials the honeybees could not discriminate the training patterns from novel stimuli that shared the same edge orientations (Stach and Giurfa 2005). Assuming that the honeybee mushroom body contains LOSN to Kenyon cell configurations akin to both our SEO and EAI models, the initial experiment (horizontal versus vertical) suggests that the honeybees are either learning the Kenyon cell activations associated with both models and then learning that the SEO responses are unnecessary, or are only learning the EAI Kenyon cell activations. The former is more likely, as again in the aforementioned simpler experiment the authors found that if the honeybees were trained for just 21 trials before testing, then the bees could still identify the correct pattern versus the novel patterns (Stach and Giurfa 2005).

It is unclear precisely why the bees lose the ability to identify the original stimulus during training, but in the horizontal and vertical grating experiment, it may simply be that the EAI type Kenyon cells will consistently fire for the CS+ pattern independent of distance, or indeed height. So the association of these Kenyon cells with reward may eventually become sufficient for the bee to make a decision from a distance, thereon if the bee did not fixate at the correct position in front of the CS+ pattern then the SEO Kenyon cells would fire inconsistently, and thus their correlation to receiving reward reduced (meaning the synaptic weight of these Kenyon cells to the mushroom body extrinsic neurons, which are thought to mediate behavioural decisions, would be negatively adapted). When trained initially on the two horizontal patterns the honeybees are able to make the discrimination, here the EAI type Kenyon cells would fire consistently for both the CS+ and CS- pattern (both being horizontal), and hence be of

no use for the discrimination task. This would make the SEO activations the more reliable indicator of reward, and hence the connections of these Kenyon cells to the mushroom body extrinsic neurons should be positively adapted in synaptic strength, allowing them to have greater influence upon the honeybee's decision during the task.

It is easy to assume that orientation-sensitive neurons such as the LOSNs only encode orientation. However, here we see that these same neurons can also represent much finer details that may be useful for very precise discrimination tasks such as the bee finding the correct nest hole, to accurate landmark detection during navigation. In insects, limiting the number of neuronal fibres required between neuropiles has an evolutionary advantage in reducing the overall size of the required brain; by transmitting highly precise, albeit coarse, information within a single neurons firing rate responses allows such a reduction, but without sacrificing behavioural competence.

2.5.3 Parallel processing

In this study, I am aimed to investigate how the use of a few neurons as possible to transmit information throughout the brain, and neuronal specificity (ability to encode detailed information into a single neuron's responses) may aid in the miniature nature of the honeybee brain, while still allowing for their diverse range of visual recognition abilities. The most remarkable discovery in this study, which may have a significantly greater influence on reducing the neural substrate requirements of the bee brain, is that the same high precision neuronal responses seen in honeybee LOSNs can be used simultaneously for both discrimination and generalisation using the very same mushroom body architecture. The initial SEO models, had only excitatory synaptic connections from the LOSNs to the Kenyon cells, to aid understanding of the Kenyon cell activations in these models we further reduced the complexity by only allowing one

connection from an LOSN to each Kenyon cell. Even with this limited connectivity, it is clear that the LOSNs allow for very fine discrimination (differentiation of two horizontal gratings) and for discrimination of oriented edges with just 15° differences. That being said, none of my models were able to replicate the empirical results in every experimental condition perfectly. The SEO models failed to solve any of the generalisation tasks and discrimination simulation performances were strongly affected when the relative sizes of the CS+ and TS^{COR} / TS^{INC} tests patterns was altered. Subsequent models with more biological equivalent numbers of between 5 to 15 synapses per Kenyon cell (Strausfeld 2002) produced equivalent discrimination performances, but showed no improvement in generalisation. Analysis of the individual LOSN and Kenyon cell activation reveals the reason for this ineffectiveness (see Fig 2.14). The LOSNs firing rates are dependent on the orientation of the perceived edges but also directly affected by the length of those edges. It is therefore possible for a horizontal grating with only a small total edge length to generate the same LOSN type response as a vertical grating with a large number of edges. Therefore, with all ten grating pattern variations (van Hateren, Srinivasan et al. 1990) used in the generalisation simulations any particular CS+ pattern may have LOSN firing rates more similar to either of the perpendicular test grating stimuli dependent on their relative orientations and edge lengths, resulting in poor experiment averages but also a uncharacteristic variance of the individual simulation performances of each CS+, TS^{COR} , TS^{INC} pattern triplet when compared to the honeybee performances.

The EAI models provided a solution to the size invariance deficiency of the SEO models. With these EAI models a Kenyon cell received a variety of synaptic connections from both (EAI_AB), or any two of the three (EAI_ABC) LOSN types in a particular quadrant of the visual field, all synapses were set to be either excitatory or

inhibitory for a particular type. During simulations the Kenyon cell firing was dependent on the total summation of the excitatory LOSN type connections being greater than the inhibitory inputs, producing a binary activation (0 / 1) output. For example, a short horizontal bar may produce activation of specific Kenyon cell, increasing the total edge length of the bar will induce an increase in the firing rates of both the type A and type B LOSNs or all three LOSN types in the respective _AB, _ABC models, thus the respective excitatory and inhibitory synaptic inputs to this Kenyon cell will increase in unison, causing the cell to still fire, as the excitatory input remains greater than the inhibitory effect (see Fig 2.7). Equally, Kenyon cells which do not fire for a particularly oriented bar will not fire irrespective of the edge of that bar as the inhibitory input from that LOSN type will always be less than the excitatory input of the other connected LOSN type. The establishment of different numbers of excitatory and inhibitory LOSN synapses to the Kenyon cells within the population allowed for discrimination of oriented bars and gratings at $\geq 30^\circ$ angle difference albeit with some shortcomings in the EAI_AB two LOSN type model (described above).

The most remarkable finding of this study therefore lies in the mechanism discovered for solving generalisation tasks, an ability that is usually assumed to require higher computational processing and hierarchical image processing, it is actually possible to use the very same Kenyon cell and LOSNs required for discrimination. Furthermore, these could be easily established within the same mushroom body structures by having a large variety of synaptic connections to the LOSNs with both excitatory only, and excitatory and inhibitory LOSN synaptic configurations. This configuration would allow the bees to simultaneously produce fine discrimination features and generalisation features, and learn which Kenyon cell responses were the best indicators of reward dependent on the environmental needs (similar to that described above for the two

horizontal bar discriminations). The mushroom bodies contain around 340,000 Kenyon cells (Witthöft 1967) that receive sensory input from almost all sensory modalities (Gronenberg 2001, Ehmer and Gronenberg 2002); although this is a large proportion of the total bee brain neuron count, almost 40%, having this single structure able to learn visual cues relevant for both discrimination and generalisation within the same neuronal mechanisms not only reduces the overall brain size and complexity, but as generalisation here is no more complex, or different, to discrimination they can both be learnt through simple associative learning.

Chapter 3: Theoretical models of how honeybees may discriminate and generalise multi-oriented bar and grating patterns

The modelling research and data from this chapter is published, in the following publication.

Roper, M. Fernando, C. & Chittka, L. 2017. Insect Bio-Inspired Neural Network Provides New Evidence on How Simple Feature Detectors Can Enable Complex Visual Generalization and Stimulus Location Invariance in the Miniature Brain of Honeybees. PLOS Computational Biology 13(2): e1005333.

3.1 Abstract

The ability to generalise over naturally occurring variation in cues indicating food or predation risk is highly useful for efficient decision-making in many animals. Honeybees have remarkable visual cognitive abilities, allowing them to classify visual patterns by common features despite having a relatively miniature brain. Here I ask the question of whether generalisation of more complex achromatic patterns requires more sophisticated visual recognition than required for the simple patterns seen in the previous chapter. I employed the excitatory and inhibitory model from the last chapter, as well as an enhanced model inspired by the known anatomical structures and neuronal responses within the bee brain, and subsequently compared their abilities to generalise achromatic patterns to the observed behavioural performance of honeybees on these more variable cues. Neural networks with just eight large-field orientation-sensitive input neurons from the optic ganglia and a single layer of simple neuronal connectivity within the mushroom bodies (learning centres) show performances remarkably similar to the empirical results without requiring any form of fine-tuning of neuronal

parameters to replicate these results. Indeed, the new model simply combining sensory input from both eyes onto single mushroom body neurons returned correct discriminations even with partial occlusion of the patterns and an impressive horizontal invariance to the location of the test patterns on the eyes. This model also replicated surprising failures of bees to discriminate certain seemingly highly different patterns, providing novel and useful insights into the inner workings facilitating and limiting the utilisation of visual cues in honeybees. The results reveal that reliable generalisation of visual information can be achieved through simple neuronal circuitry that is biologically plausible and can easily be accommodated in a honeybee brain.

3.2 Introduction

Behavioural experiments using simple bar and grating patterns have allowed scientists to explore how the physical constraints imposed by the honeybees' compound eyes (Seidl and Kaiser 1981) directly correlate to the bees' behavioural performances (Srinivasan and Lehrer 1988, Srinivasan, Lehrer et al. 1989, Srinivasan, Zhang et al. 1993, Sathees chandra, Geetha et al. 1998, Horridge 2003, Horridge 2003). Similarly, in the previous chapter I used these same pattern types to understand how the miniature brain of the bees may utilise just a few large-field optic neuronal responses for discrimination and generalisation tasks. These initial, somewhat simple, experiments provided a core understanding of honeybee vision and form the foundation from which more complex visual capabilities can be understood. In subsequent behavioural experiments, researchers began to look at what features, other than edge orientation, bees might use to help discriminate visual targets (symmetry (Giurfa, Eichmann et al. 1996, Lehrer 1999, Rodriguez, Gumbert et al. 2004), size (Srinivasan, Lehrer et al. 1989, Horridge, Zhang et al. 1992), pattern disruption (Horridge 1997)) as well as whether

bees are able to identify patterns composed of more complex arrangements of shapes and edges (Horridge and Zhang 1995, Horridge 2000, Horridge 2006). The bees, with only a few notable exceptions, had no difficulty discriminating these types of patterns. More impressive though, was the fact that these trained bees were then able to apply these same learnt cues to patterns that may have had little or no resemblance to the original training patterns. Here, I investigate if the discrimination and generalisation of more complicated oriented edge patterns would necessitate a larger number of optic neuron outputs and/or more sophisticated neuronal architectures in the higher brain learning centres, than previously shown to be required for the simpler bar and grating examples.

Extending upon the work in the previous chapter, using the published intracellular recordings of large-field optic ganglia neurons to achromatic stimuli (O'Carroll 1993, Maddess and Yang 1997) and the known anatomical morphologies of mushroom body (learning centres) class II 'clawed' Kenyon cells (Strausfeld 2002), I investigated two simple, but biologically inspired models. These models were not created, or indeed in any way 'tweaked' to replicate performances on the particular visual patterns, nor did they implement any form of learning within the models. Instead they attempt to explore how well, or poorly, the known neuronal types within the bee brain could solve the presented problems and how much neuronal complexity would be required to do so. The models described here were again kept very basic, with limited neuronal pathways and very simple synaptic connections from the optic lobes to the mushroom bodies. Since two of the optic ganglia (medulla and lobula) of bees extend a variety of axonal fibres to both the ipsilateral and the contralateral mushroom bodies (see Fig 1.1) and, as apposed to axons from different regions of the optic lobes that are distinctly layered within the mushroom bodies, there is no apparent segregation within

these layers of the visual afferents from the individual corresponding left and right eye regions (Ehmer and Gronenberg 2002, Paulk and Gronenberg 2008), I tested the discrimination and generalisation performance difference between retaining independent inputs from each eye and combining the neuronal input from both eyes within my simulated mushroom body models. This allowed me to compare the results of my two distinctly different bee-brain models to the performance of actual honeybees in specific experiments.

In this chapter I drew on twenty-four experiments from three published honeybee behaviour papers (Zhang and Horridge 1992, Stach and Giurfa 2001, Stach, Benard et al. 2004) providing results on both the discrimination abilities of free flying bees perceiving complex bar and spiral patterns from a distance, and the bees generalisation abilities while fixating, slow hovering scans 1-3 cm in front of presented patterns. These particular experiments were selected primarily because of the complexity of the patterns used, having variation in both the orientation and length of the edges within small regions of the patterns (in Chapter 2 patterns always presented a single predominant orientation). In addition, the chosen experiments provided a broad range of behavioural results, including tasks bees found difficult or impossible to solve, and tasks with over 80% correct pattern selections. This allowed me to additionally analyse model performance in respect of the bees' relative ability during different experiments.

3.3 Methods

Sensory input for my models was generated in the same way as the previous chapter (see Chapter 2.3) using the known neuronal responses of lobula (3rd optic ganglion) large-field orientation-sensitive neurons (LOSNs) discovered in insects (O'Carroll 1993,

Maddess and Yang 1997). These intracellular tuning curve recordings allowed me to calculate the theoretical responses of eight LOSNs (a type A and a type B LOSN from the upper and lower region of each eye) for each of the required experiment patterns. The firing rate responses of these neurons to the presented patterns were subsequently passed as inputs to the appropriate mushroom body models' Kenyon cells.

Each achromatic pattern used within this chapter was taken directly from the pdf document of the published behavioural papers (Zhang and Horridge 1992, Stach and Giurfa 2001, Stach, Benard et al. 2004), or, where necessary, reproduced in Microsoft PowerPoint using the stimuli instructions provided in the papers' method sections. These images were scaled and centred to fit within a 150 x 150 pixel PNG image. To produce images for offset discrimination experiments, the 150 x 150 pixel patterns were placed centrally within a larger white 300 x 150 pixel image and horizontally offset left and right between 0 and 200 pixels in 25 pixel increments to create a set of 17 test images per original pattern. For offsets greater than 75 pixels the original images were cropped accordingly (see Fig 3.3c). All images were then pre-processed in Matlab (Mathworks) using the same process as described in Chapter 2.3.1.

The first model studied in this chapter was based on the EAI_AB model described in Chapter 2 (for simplicity hereon referred to as the DISTINCT model). It assumed that each Kenyon cell would receive distinctly segregated LOSN inputs originating from **either** the left or the right eye, and from either the dorsal or ventral half of that visual field (Fig 3.1 red neurons). This DISTINCT model used the same 86 different types of simple excitatory and inhibitory synaptic configurations of the LOSNs to Kenyon cells as the EAI_AB model (see Table 2.1 for Kenyon cell synapse configurations). This configuration achieves the 30° orientation acuity (Chapter 2.4.2) that was reported for honeybees during dual trial discrimination tasks (Sathes chandra,

Geetha et al. 1998). The model had 30 copies of each of these Kenyon cell configuration types per quadrant of the visual field; resulting in a total of 10,320 Kenyon cells, which is still a small proportion of the 340,000 Kenyon cells (Withhöft 1967) in the honeybee mushroom bodies. I set a particular Kenyon cell's response to 1 (fired) if its summed synaptic input total was greater than zero. Otherwise the response was set to 0 (inhibited). In this way the binary values of all 10,320 Kenyon cell responses were calculated for a particular presented pattern (see Chapter 2.3.3 for Kenyon cell calculation details).

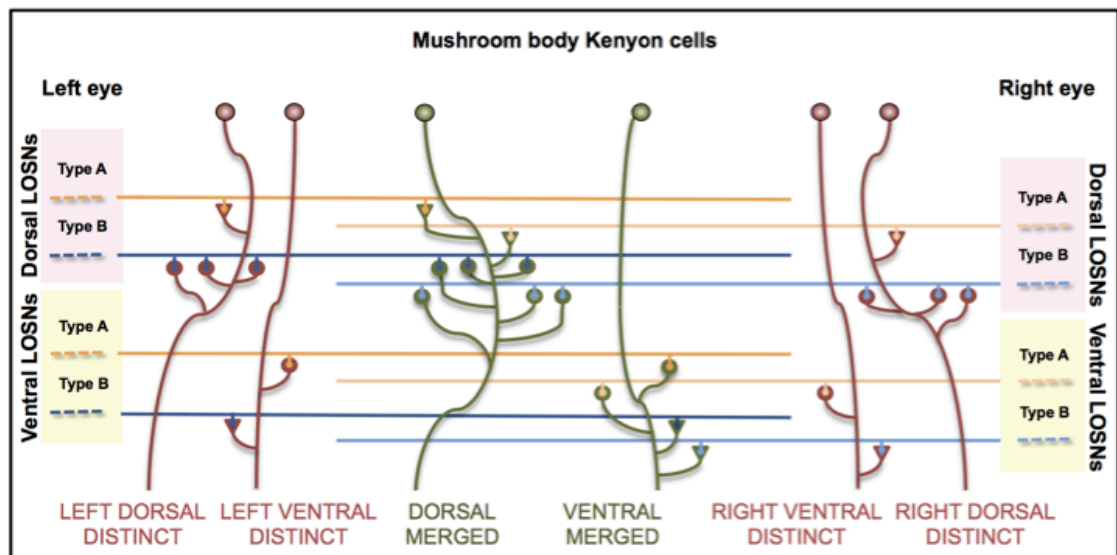


Figure 3.1 Schematic representation of *DISTINCT* and *MERGED* models. Representation of how the lobula orientation-sensitive neurons (LOSNe) connect to each model's Kenyon cells. The *DISTINCT* model's Kenyon cells (red neurons) receive LOSNe inputs from just one quadrant of the visual field, either the dorsal or ventral half of the left or right eye. In this example the dorsal Kenyon cells each have an inhibitory (triangle) LOSNe type A synapse and three LOSNe type B excitatory (circle) synapses (see Table 2.1 type 046). The dorsal *DISTINCT* Kenyon cells in this example each have one excitatory type A and one inhibitory type B synapse (see Table 2.2 type 001). The *MERGED* model Kenyon cells (green neurons) have the same configuration types as the respective dorsal and ventral *DISTINCT* neurons, but this model combines visual input originating from either the dorsal or ventral regions of both eyes; in the example the ventral *MERGED* neuron has one inhibitory connection from a type A LOSNe and three excitatory LOSNe type B synapses from the dorsal left eye and therefore must have the respective three excitatory type B and one inhibitory type A synapses from the ventral right eye. Figure replicated from my publication (Roper, Fernando et al. 2017).

Given the apparent non-retinotopic distribution of visual inputs from the corresponding left and right eye regions in the bee mushroom bodies (Ehmer and Gronenberg 2002) the second model “MERGED” was created to explore the effect of merging LOSN synaptic connections from both eyes onto the Kenyon cells. To keep my theoretical model simple and comparable to the DISTINCT model, I again relied on the 86 LOSN-to-Kenyon cell configuration types. However, in this model, rather than the previous model’s segregation of Kenyon cells into different groups per quadrant, here just two distinct groups of Kenyon cells were formed; an upper group receiving LOSN type A and type B inputs from both of the top two visual field quadrants (i.e. dorsal regions of both left and right eyes), and a similar group of Kenyon cells in the lower ventral region receiving the bottom quadrant inputs. This created in total 5,160 Kenyon cells for the model. The simulation of these Kenyon cell responses was performed as described above, except that each Kenyon cell in a given top or bottom group would summate synaptic inputs derived from **respective pairs** of LOSN type A and type B inputs. This was done in such a way that, if a Kenyon cell in the upper group received an excitatory input from a type A LOSN from the dorsal-left eye, it would also have an excitatory synapse from the type A LOSN originating from the dorsal-right eye (see Fig 3.1 green neurons), and the same duplication for all the other excitatory and inhibitory synapses.

For the simulations performed in this chapter, as in Chapter 2, I again assumed that honeybee decision-making is correlated to the neuronal similarity of their Kenyon cell responses to perceived stimuli, just as olfactory learning in the mushroom bodies is thought to rely on the coincidence detection of Kenyon cell responses (Heisenberg 2003). For this reason I used the simulated Kenyon cell similarity ratios (KCSR) (see Chapter 2.3.4) to different test patterns as a measure of my models’ performance

accuracy. The overall model performance for a given experiment is therefore directly correlated to average KCSR of 1,000 simulation trials of a presented rewarding pattern (CS+) and a pair of test stimuli patterns (see Chapter 2.3.4 and Equation 2.3). The test pattern pair consisted of a pattern that was preferred by honeybees in behavioural experiments (TS^{COR}), and therefore *should* be “preferred” by my model also. The other test stimulus (TS^{INC}) was therefore the pattern that the bees visited least often during their trials. A model performance of ~50%, with individual trial KCSRs of <0.5, meant that there was an equal or greater similarity from the CS+ pattern to the TS^{INC} than TS^{COR} patterns, and therefore assumed to be my models’ equivalent of the bees’ inability to discriminate or generalise to the test patterns.

These simulated results were then compared with the empirical honeybee experimental results to assess the DISTINCT and MERGED models’ performance. In addition, I wished to assess how my models correlated with the honeybees’ relative performances over all of the tested experiments. However, as in the previous chapters, each set of the original honeybee generalisation experiments (Stach and Giurfa 2001, Stach, Benard et al. 2004) only provided a number of mean data points for comparison. In each study, the bees were tested on patterns that typically varied in number and orientation of bars in each pattern quadrant, but were similar otherwise. Moreover, the used publications addressed similar issues and used similar patterns. While this is a good approach when probing the limits of the learning abilities of bees, it also means that the data points are not independent. A correlation coefficient involving data from multiple different experiments would, therefore, be misleading. Instead, I grouped the experiments into five batches of related generalisation tasks, similar to that done in the original studies, so that the relative performance of the different simulated experiments

could be assessed, and compared to that of the real honeybees' relative performances on the same sets of pattern pairs.

3.4 Results

3.4.1 Experiment set 1: discrimination of multi-oriented bar patterns

The ability to discriminate between visual patterns is essential for honeybees allowing them to identify familiar flowers and landmarks while navigating on foraging trips and locating the correct hive entrance upon their return. Nonetheless even for these types of precisely defined visual stimuli, some form of location invariance of a stimulus on the retinae would undoubtedly be required as it is unlikely bees would instantaneously and perfectly align the stimulus against their eyes on every single flight in order to make a discrimination decision. Indeed it would be an undesirable necessity that they should have to do so.

To test my two models (DISTINCT, MERGED) for the effect of location of the stimuli within the visual field, I simulated the experiments of Zhang and Horridge (Zhang and Horridge 1992) who explored the ability of freely flying honeybees to discriminate two large (24cm diameter) vertically displayed patterns composed of multiple oriented bars. For these experiments a bee's pattern choice was recorded when it approached within 27cm of either pattern (see (Zhang and Horridge 1992) for apparatus description). Presuming that honeybees would learn the correct pattern features when feeding at, or being close to, the centre of a rewarding pattern, I first calculated the Kenyon cell responses to these same CS+ patterns. I next determined each of my models' performance accuracies when any of the two given test stimuli

patterns (TS^{COR} identical to the CS+ pattern, TS^{INC} a rotated or mirrored version of the CS+ pattern) were offset horizontally between -200 pixels and +200 pixels in 25 pixel increments. Here a ± 200 pixel offset would almost entirely obscure the pattern and a zero pixel offset would align the pattern perfectly in the centre of the field of view (see Fig 3.3c).

Zero horizontal offset simulations

With zero offsets of the TS^{COR} and TS^{INC} patterns, I found that the DISTINCT model was able to discriminate all of the presented pattern pairs. Indeed, despite its simplicity, the model outperformed real honeybees, whose best result was 67%, compared to DISTINCT model's 78% accuracy for the same pattern pair (Fig 3.2 vii). The model also discriminated the two pattern pairs that bees failed to discriminate (Fig 3.2, i: spiral patterns – bee: 53.7% $p > 0.7$ $n = 54$ (Zhang and Horridge 1992) – DISTINCT: 67%, ii: octagonal patterns – bee: 56.4% $p > 0.2$ $n = 140$ (Zhang and Horridge 1992) – DISTINCT: 74%). The MERGED model results were far lower than the DISTINCT model's discrimination accuracies but compared better to that of the empirical results. As with real honeybees' behaviour, the MERGED model did not reliably discriminate the spiral and octagonal pattern, achieving simulation results below 60%. Out of the seven tested pattern pairs the only notable difference from the behavioural results was the MERGED model's inability to discriminate the two left / right reversed pattern pairs (Fig 3.2: iv, vi).

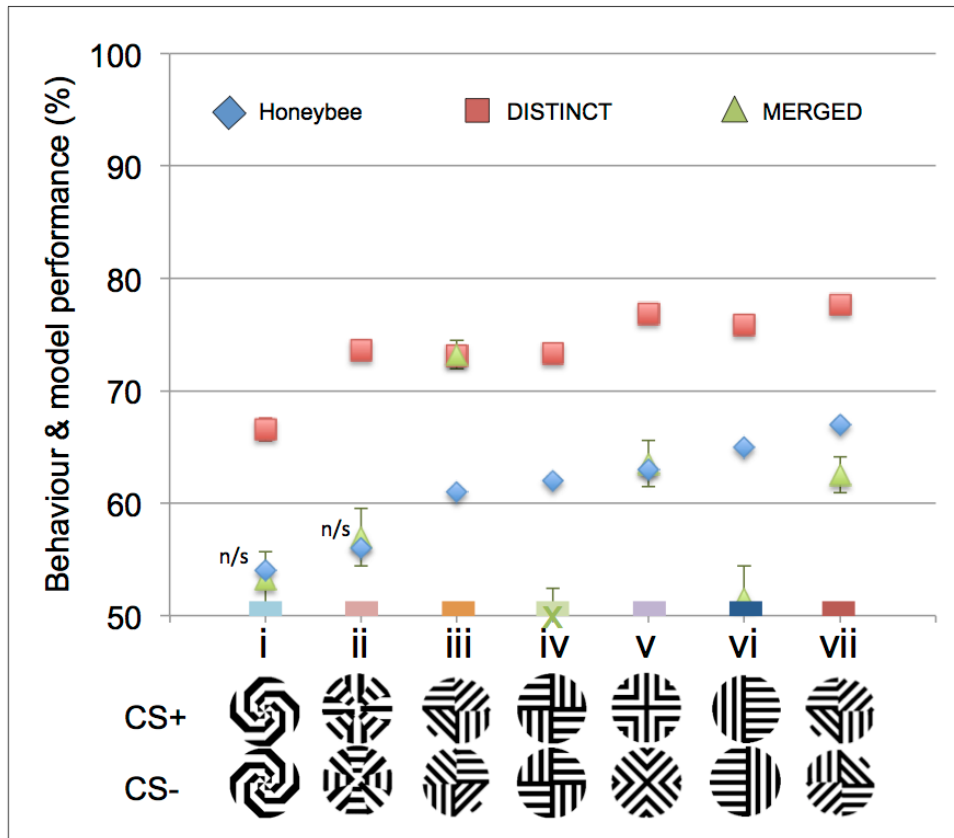


Figure 3.2 Exemplary summary of honeybee behaviour and model performance for discrimination of multi-oriented patterns. In the behavioural experiments (Zhang and Horridge 1992) different groups of honeybees were differentially trained on a particular pattern pair, one rewarding (CS+) and one unrewarding (CS-). Blue diamonds: honeybee result, percentage of correct CS+ pattern selections after training. Red squares: performance accuracy of the DISTINCT model when test stimuli were presented in the centre of the field of view. Green triangles: performance accuracy of the MERGED model for the centralised stimuli. Cross on x-axis: model performance < 50%. Error bars show standard deviation (these were not available for the behaviour results). Figure adapted from my publication (Roper, Fernando et al. 2017).

Clearly the simpler model (DISTINCT) returned more accurate discrimination results and outperformed both the more derived model (MERGED) and the real honeybees' behavioural performance. These results raise the interesting question why the honeybees performed so poorly on some of the patterns, when a very simple model (DISTINCT) was easily able to discriminate the patterns while using just eight large-field orientation-sensitive neuronal inputs.

Horizontal offset simulations

Progressively offsetting the test patterns from the centre of the field of view revealed the lack of robustness of the DISTINCT model to cue variation. Here the simulation performances dropped much faster than that of the MERGED model. In fact with as little as ± 75 pixel offset (where the whole pattern was still visible, see Fig 3.3c) the performance of the DISTINCT model fell below 52% for all pattern pairs (Fig 3.3a).

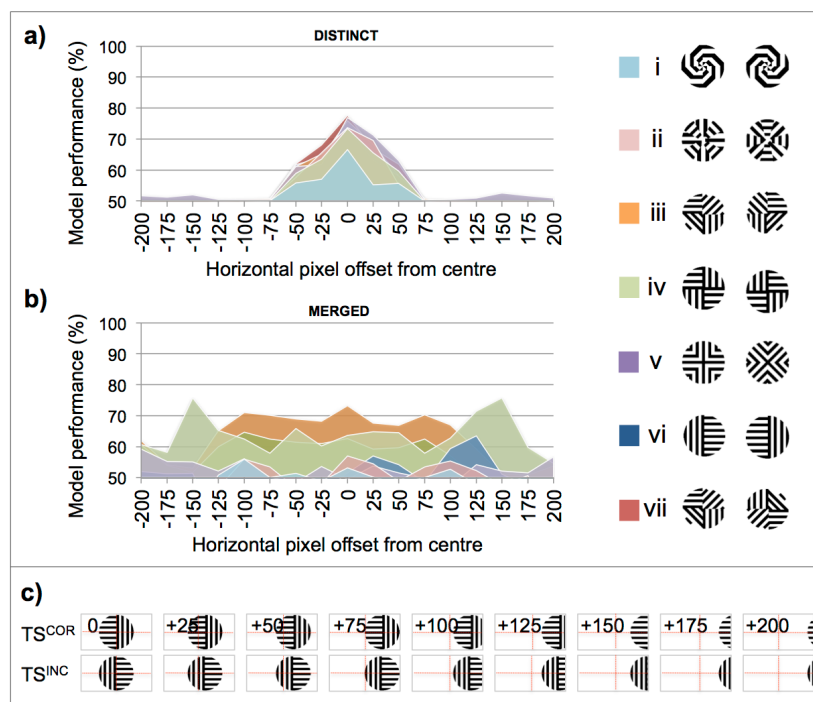


Figure 3.3 Model performance for discrimination of multi-oriented patterns when horizontally offset. Performance accuracy of models when comparing the CS+ patterns with the corresponding TS^{COR} and TS^{INC} pattern pairs when these patterns were horizontally offset between 0 and ± 200 pixels in 25 pixel increments (see c) the (a) DISTINCT, (b) MERGED. Colour of region indicates the corresponding experiment on right (also in Fig. 3.2) (c) Example of the TS^{COR} and TS^{INC} pattern images when horizontally offset by 0 pixels to +200 pixels, similar images were created for -25 pixels to -200 pixels. Experiment images were 300 x 150 pixels in size; patterns occupied a 150 x 150 pixel box cropped as necessary. Number in top right of each image indicates number of pixels it was offset by; these were not displayed in actual images. Red dotted line shows the subdivision of the image into the four visual field regions. The DISTINCT model performs much better than the MERGED model and honeybee results when there is no offset in the patterns, but with only a small offset (± 75 pixels) the DISTINCT model is unable to discriminate the patterns (a) whereas the MERGED model is able to discriminate most of the patterns over a large range of offsets (b). Figure adapted from my publication (Roper, Fernando et al. 2017).

Simulation analysis

The reason why the MERGED model is unable to discriminate the spiral and cross patterns (Fig 3.2 i, ii), but can easily discriminate the quadrant grating patterns (Fig 3.2 iii), can be seen from the LOSN responses to these patterns (Table 3.1). In the DISTINCT model each image quadrant produces very different LOSN responses for all pattern pairs, whereas the summation of LOSN responses from both eyes in the MERGED model produces very similar combined results in the dorsal and ventral regions on both the spiral and cross pattern pairs; these combined dorsal and ventral responses for the grating patterns are sufficiently different to allow discrimination.







Pattern	DISTINCT		MERGED	
	LOSN type A	LOSN type B	COMBINED LOSN type A	COMBINED LOSN type B
	51, 44, 44, 50	11, 21, 20, 10	95, 94	32, 30
	57, 37, 37, 56	17, 15, 15, 16	94, 93	32, 31
	56, 44, 46, 58	13, 19, 20, 14	100, 104	32, 34
	45, 57, 56, 45	20, 15, 16, 18	102, 101	35, 34
	57, 68, 41, 34	24, 13, 21, 8	125, 75	37, 29
	41, 55, 40, 67	21, 24, 10, 13	96, 107	45, 23

Table 3.1 LOSN type A & type B responses in each quadrant of spiral, cross and grating patterns. Numbers correspond to LOSN responses for image quadrants 1-4 (top-left, top-right, bottom-left, bottom-right). Combined results are the summation of the quadrant 1 + quadrant 2 (dorsal), and quadrant 3 + quadrant 4 (ventral) responses for the type A and type B LOSNs. The DISTINCT model cannot discriminate the spiral and cross patterns as the respective combined LOSN responses (see red and burgundy text on dorsal responses) are very similar but the grating patterns' dorsal ventral responses are discriminable (see green text on dorsal responses).

When the patterns are offset the DISTINCT model failed to discriminate the correct pattern with only minor horizontal offsets, whereas the MERGED model could still discriminate some of the patterns even with partial occlusion of the images (Fig 3.3). This is not solely down to the similarity of the combined LOSN firing rates (see Table 3.2). Here the respective DISTINCT quadrant LOSN responses are all different between the three patterns (CS+, TS^{COR}, TS^{INC}), but unlike the previous spiral and cross pattern examples so are the MERGED model's respective values, preventing generalisation on just the LOSN responses.




Pattern	DISTINCT		MERGED	
	LOSN type A	LOSN type B	COMBINED LOSN type A	COMBINED LOSN type B
 CS+	57, 68, 41, 34	24, 13, 21, 8	125, 75	37, 29
 TS ^{COR}	21, 72, 15, 47	9, 20, 8, 19	93, 62	29, 66
 TS ^{INC}	16, 55, 13, 68	8, 26, 4, 14	71, 81	34, 18

Table 3.2 LOSN type A & type B responses in each image quadrant of the quadrant grating patterns offset horizontally. Numbers correspond to LOSN responses for image quadrants 1-4 (top-left, top-right, bottom-left, bottom-right). Combined results are the summation of the quadrant 1 + quadrant 2 (dorsal), and quadrant 3 + quadrant 4 (ventral) responses for the type A and type B LOSNs. TS^{COR} and TS^{INC} are from experiment 3 (Fig 3.3 iii) offset by +50 pixels. Red dotted lines shows how the images are subdivided into the four image quadrants.

Figure 3.4 shows the respective Kenyon cell activations (for a single simulation) of the CS+, TS^{COR} and TS^{INC} patterns for both the DISTINCT and MERGED models. Similar to the generalisation experiments in Chapter 2 the pattern offset invariance is due to a combination of the MERGED model's LOSN responses, and the excitatory and inhibitory connections established by the LOSNs onto the Kenyon cells within the

model's mushroom body. Despite the MERGED model's LOSNs having different firing rates when presented with the offset TS^{COR} pattern compared to the CS+ pattern, the correlation of the firing rates within the dorsal and ventral regions activate many of the same Kenyon cells for both patterns enabling the successful discrimination.

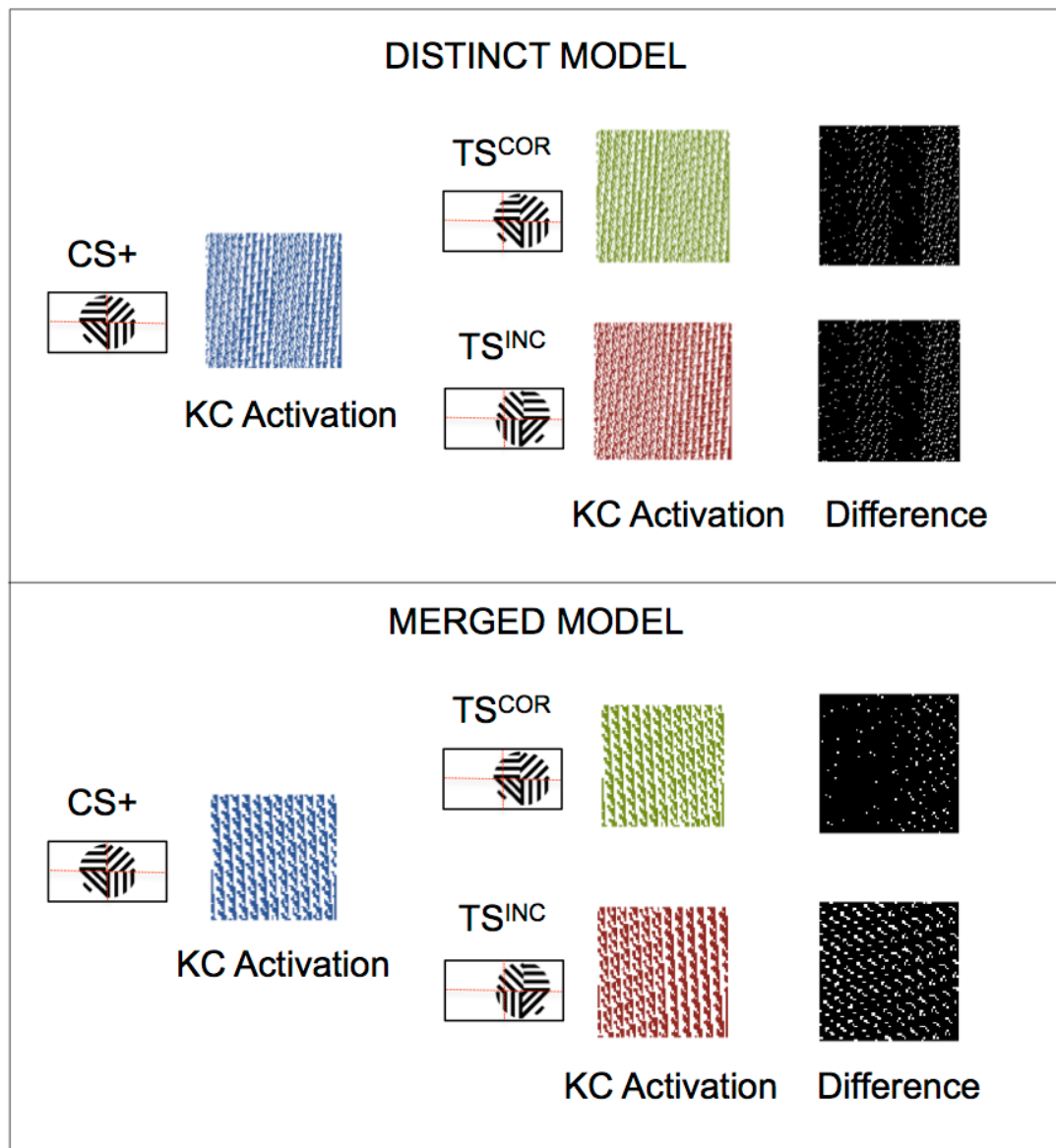


Figure 3.4 Model Kenyon cell activation for offset grating quadrant pattern. Blue: Kenyon cell activation when each model is presented with the zero offset CS+ pattern. Green: Kenyon cell activation to the offset TS^{COR} pattern, Red: Kenyon cell activation to the offset TS^{INC} pattern. White dots on black square: shows the Kenyon cell activation differences between the test stimulus (TS^{COR} or TS^{INC}) and the CS+ pattern. **(a)** *DISTINCT* model activations. **(b)** *MERGED* model activations. *MERGED* model shows

fewer activation differences on the TS^{COR} pattern during offsets. Red dotted lines shows how the images are subdivided into the four image quadrants.

Summary of experiment set 1

My results show that by simply combining inputs from both the left and right eyes onto mushroom body Kenyon cells, discrimination abilities are effectively freed of requiring perfect horizontal cue alignment on the retinae. Although this reduces the maximal discrimination accuracy, it allows for a much more robust and versatile employment of this cognitive tool in most realistic free flight navigation and resource locating scenarios.

3.4.2 Experiment set 2: generalisation of multi-oriented bar and grating patterns

Experienced honeybee foragers may identify rewarding flowers based on those features that most reliably predict reward amongst the available flower species. Honeybees able to generalise to this limited feature set would reduce the need to learn all the exact features (or indeed photographic templates) of each individual flower type visited and subsequently having to best-match these numerous complex templates when foraging on novel or less frequented floral resources (van Hateren, Srinivasan et al. 1990, Giger and Srinivasan 1995, Stach and Giurfa 2001).

To explore these generalisation abilities, Stach et al. (Stach and Giurfa 2001, Stach, Benard et al. 2004) trained honeybees on two sets of six patterns where within each set there were similarly oriented bars in each quadrant of the patterns (Fig 3.5a). They then tested the bees' ability to generalise from these training patterns to novel variations of the patterns. Unlike the previous experiments, these bees were able to

fixate a small distance from the pattern before their final choice selection was recorded when they actually touched either of the two test patterns. For my simulations I therefore presented all the patterns in the centre of the field of view with zero horizontal, or vertical, offset applied, assuming this would be where a honeybee would make its final decision. Here I followed the approach of the original studies (Stach and Giurfa 2001, Stach, Benard et al. 2004) and compared the model results against the experimental performances within smaller batches of similar generalisation type tasks.

Batch 1: Identical orientations in each pattern quadrant

Using data from Stach et al 2004 (Stach, Benard et al. 2004), I tested simple generalisation from the training sets of six patterns to three novel pattern pairs. The experimentally preferred test stimulus (TS^{COR}) patterns had bars oriented in the same direction as the corresponding quadrants of the CS+ patterns, versus the incorrect distractor (TS^{INC}) patterns with a similar visual style to the matching TS^{COR} pattern but with bars oriented in different directions to those of the CS+ pattern in each quadrant. I found that simulations of both the DISTINCT and MERGED models had average results almost identical to the honeybee behavioural results. Both the percentage of honeybee choice selections for TS^{COR} patterns and my model performances were all between 67% and 72% (Fig 3.5).

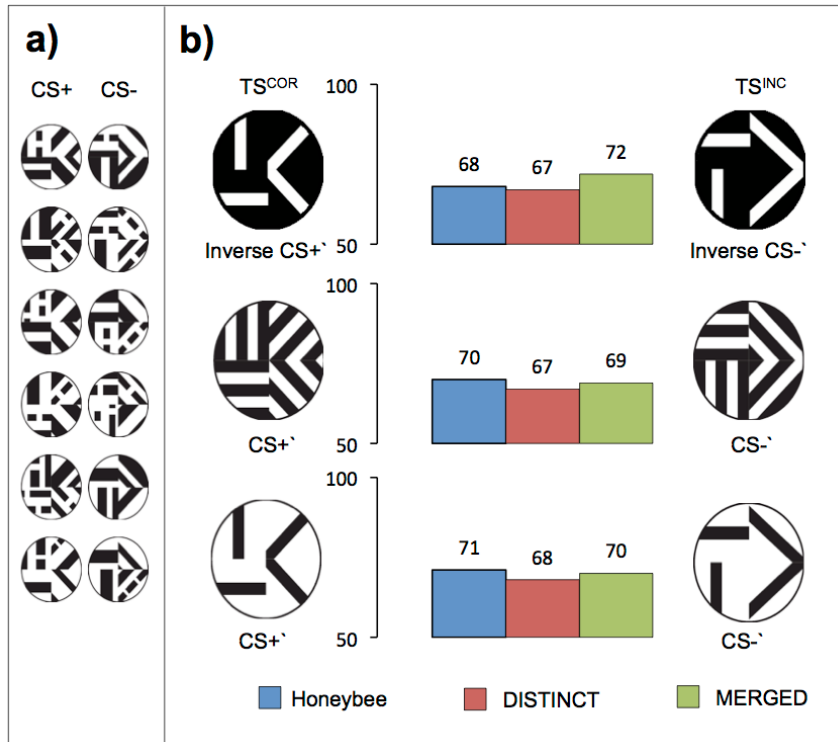


Figure 3.5 Honeybee behaviour and model performance for simple generalisation of quadrant multi-oriented bar patterns. **(a)** The two sets of quadrant patterns (each set having similarly oriented bars in each quadrant of the pattern) that were used during the behavioural experiments (Stach and Giurfa 2001, Stach, Benard et al. 2004). Honeybees were trained on random pairs of a CS+ pattern and CS- pattern selected from the two pattern sets, different groups of bees were tested on the reversal such that the CS- pattern would become the CS+ and vice-versa. **(b)** Blue bar: honeybee result, percentage of correct choice selections when tested with novel patterns (here TS^{COR} and correct choice is the pattern the bees visited most often). Models results, value above bar is average for 12,000 simulations.

Batch 2: Identical orientations in all but one CS+ pattern quadrant

This batch of experiments again followed the pattern experiments of Stach et al (Stach, Benard et al. 2004), here the TS^{COR} patterns had three quadrants with correctly oriented bars and the final quadrant did not, TS^{INC} patterns had incorrectly oriented bars in all four quadrants. The DISTINCT model achieved $\geq 58\%$ throughout, but performed typically 5-10% below the honeybees (Fig 3.6). The MERGED model outperformed the

DISTINCT model on all test pattern pairs, with results once again extremely similar to that of the honeybee behavioural performances.

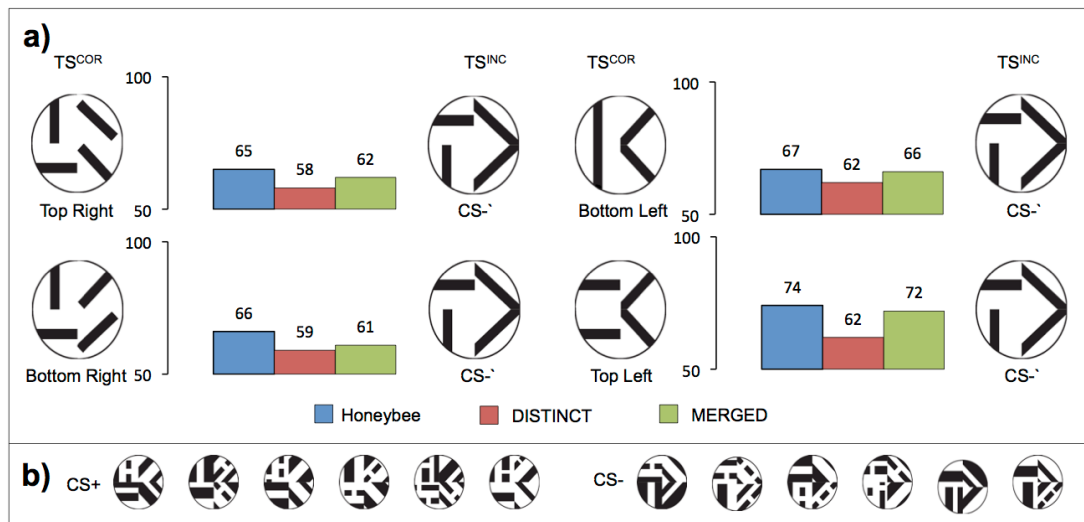


Figure 3.6 Honeybee behaviour and model performance when generalising to a modified CS+ quadrant pattern. **(a)** Blue: honeybee result, percentage of correct choice selections when tested with novel patterns of varying degrees of difference from the training CS+ / CS- patterns (here TS^{COR} and correct choice is the pattern the bees visited most often). Red: DISTINCT model performance when comparing each of the six CS+ patterns in a pattern set (b) against a novel TS^{COR} and TS^{INC} pattern pair. Green: MERGED model results for the CS+ pattern sets compared against each TS^{COR} and TS^{INC} pattern pair. **(b)** The two sets of quadrant patterns (each set having similarly oriented bars in each quadrant of the pattern) that were used during the behavioural experiments (Stach and Giurfa 2001, Stach, Benard et al. 2004). Honeybees were trained on random pairs of a CS+ pattern and CS- pattern selected from the two pattern sets, different groups of bees were tested on the reversal such that the CS- pattern would become the CS+ and vice-versa.

Batch 3: TS^{INC} differs from CS+ / TS^{COR} in just one pattern quadrant

In the third batch of experiments utilising the same Stach et al dataset (Stach, Benard et al. 2004), the TS^{COR} and TS^{INC} were very similar, the TS^{COR} patterns having correctly oriented bars in all four quadrants and the TS^{INC} pattern had just one quadrant with incorrectly oriented bars. Simulations of the MERGED model failed to generalise to the correct pattern in three out of four experiments with individual simulation trials failing to achieve a KCSR of more than 0.5 (Fig 3.7). The DISTINCT model managed to

correctly generalise all of these patterns but with lower accuracy than the corresponding honeybee results (Fig. 3.7).

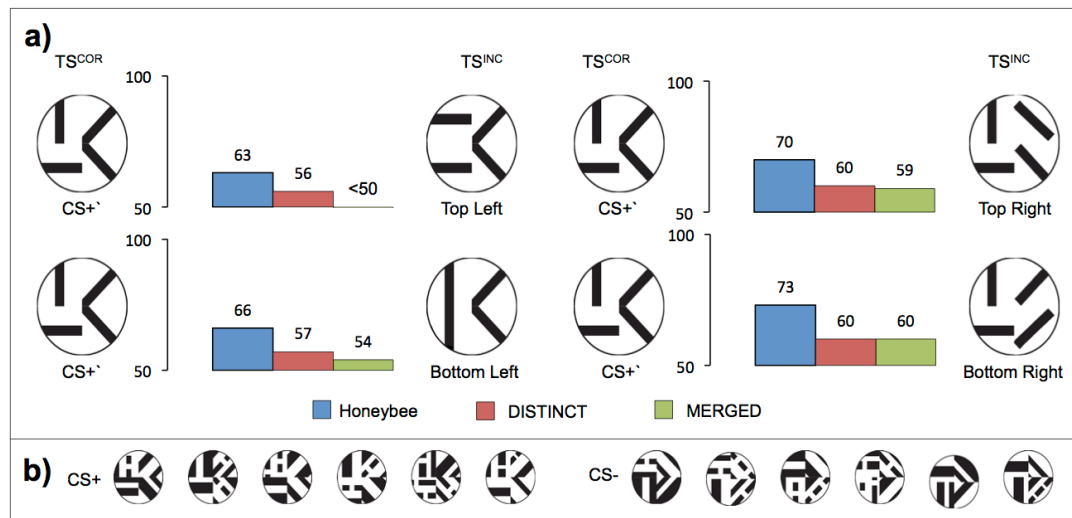


Figure 3.7 Honeybee behaviour and model performance when generalising to patterns when there is only a single quadrant different between $CS+ / TS^{COR}$ and TS^{INC} . **(a)** Blue: honeybee result, percentage of correct choice selections when tested with novel patterns of varying degrees of difference from the training $CS+ / CS-$ patterns (here TS^{COR} and correct choice is the pattern the bees visited most often). Red: DISTINCT model performance when comparing each of the six $CS+$ patterns in a pattern set (b) against a novel TS^{COR} and TS^{INC} pattern pair. Green: MERGED model results for the $CS+$ pattern sets compared against each TS^{COR} and TS^{INC} pattern pair. **(b)** The two sets of quadrant patterns (each set having similarly oriented bars in each quadrant of the pattern) that were used during the behavioural experiments (Stach and Giurfa 2001, Stach, Benard et al. 2004). Honeybees were trained on random pairs of a $CS+$ pattern and $CS-$ pattern selected from the two pattern sets, different groups of bees were tested on the reversal such that the $CS-$ pattern would become the $CS+$ and vice-versa.

Batch 4: Mirror image and left / right reversal generalisations

This experiment set was compiled by taking test pattern pairs from the earlier work of Stach and Giurfa (2001) (Stach and Giurfa 2001). In this study, honeybees were presented with different combinations of either the original $CS+$ pattern configuration, or the mirror image, or the left / right reversal of this layout. The DISTINCT model was once again able to generalise correctly to all the experimental patterns (Fig 3.8). Each individual experimental result varied from between 4-20% less than that of the

corresponding empirical result, but, as with honeybees, the model showed lower generalisation performances on the mirror image versus left-right patterns compared to that of the original CS+ versus the mirror image patterns (Fig 3.8). The MERGED simulations typically resulted in higher accuracies and were more similar to the honeybee results than that of the DISTINCT model, correct generalisation performances ranged from +1% to -12% different to the empirical result. Of note, the bees achieved a surprising 82% correct choice accuracy on one of these test pattern pairs, almost 10% higher than any other task. My models achieved simulation results $\geq 60\%$ on this experiment. Only two of the eight test pattern pairs (TS^{COR}: original configuration, TS^{INC}: left / right reversal) failed to generalise correctly with a performance of just 51% (individual trial KCSRs ranging from 0.39 to 0.62 dependent on the particular pattern triplets presented) compared to the honeybee correct choice selection of 69%. During simulations both the DISTINCT and MERGED models showed a preference for the left / right reversal configuration compared to the mirror image pattern, they also preferred the correct configuration to the mirror image layouts, as did real honeybees (Fig 3.8).

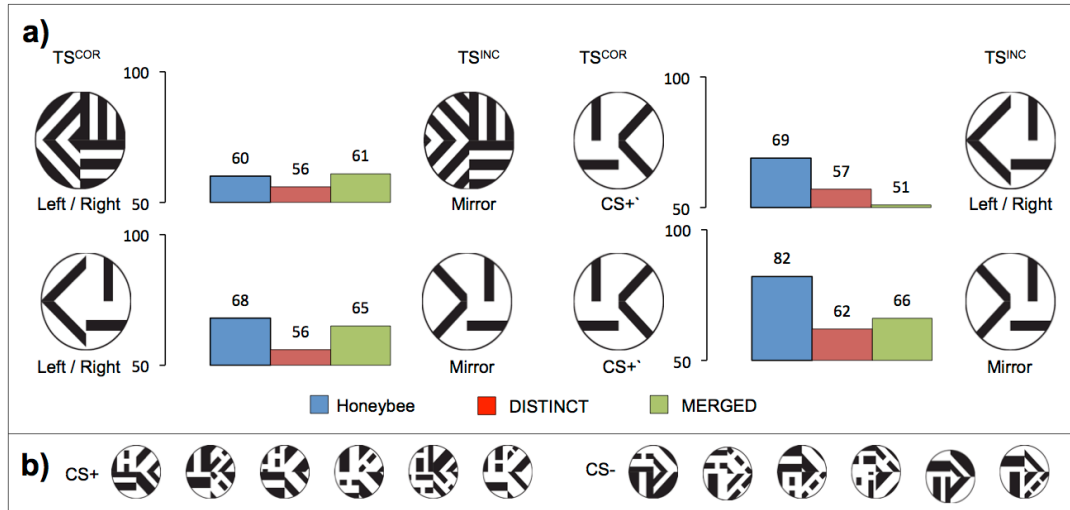


Figure 3.8 Honeybee behaviour and model performance when generalising to a mirror image or left right reversed quadrant patterns. **(a)** Blue: honeybee result, percentage of correct choice selections when tested with novel patterns of varying degrees of difference from the training CS+ / CS- patterns (here TS^{COR} and correct choice is the pattern the bees visited most often). Red: DISTINCT model performance when comparing each of the six CS+ patterns in a pattern set (b) against a novel TS^{COR} and TS^{INC} pattern pair. Green: MERGED model results for the CS+ pattern sets compared against each TS^{COR} and TS^{INC} pattern pair. **(b)** The two sets of quadrant patterns (each set having similarly oriented bars in each quadrant of the pattern) that were used during the behavioural experiments (Stach and Giurfa 2001, Stach, Benard et al. 2004). Honeybees were trained on random pairs of a CS+ pattern and CS- pattern selected from the two pattern sets, different groups of bees were tested on the reversal such that the CS- pattern would become the CS+ and vice-versa.

Batch 5: Chequerboard generalisations

The last of my experiment sets again used patterns from Stach and Giurfa (2001) (Stach and Giurfa 2001). Figure 3.9 shows that both models were unable to generalise correctly when presented with a chequerboard distractor pattern, with individual trial KCSRs as low as 0.4. Conversely, honeybees always preferred left / right or mirror image versions of the CS+ pattern configuration to that of the chequerboard option.

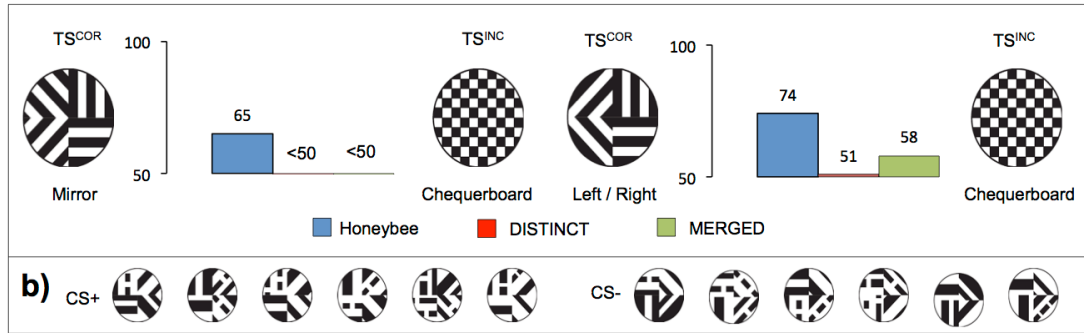


Figure 3.9 Honeybee behaviour and model performance when generalising to a chequerboard pattern. Blue: honeybee result, percentage of correct choice selections when tested with novel patterns of either the mirror image or left / right reversal of the training CS+ patterns (here TS^{COR} and correct choice is the pattern the bees visited most often). Red: DISTINCT model performance when comparing each of the six CS+ patterns in a pattern set (b) against a novel TS^{COR} and TS^{INC} pattern pair. Green: MERGED model results for the CS+ pattern sets compared against each TS^{COR} and TS^{INC} pattern pair.

Simulation analysis

The MERGED model's failure to discriminate the left / right reversal patterns (Fig 3.8 top-right) was no surprise as both the TS^{COR} and TS^{INC} patterns presented the exact same orientations only in the reverse eyes, and hence produced the same summed input to the Kenyon cells (see Table 3.1 for similar examples).

The inability of either model to discriminate the checkerboard pattern (TS^{INC}) versus the mirror pattern (TS^{COR}) from the CS+ patterns was due to the Kenyon cell similarity to an orthogonal orientation (as is the case with two of the four mirror quadrants) being less than that of the orientations of the square edges. During a single simulation using the first CS+ pattern (Fig 3.9b) the DISTINCT model had 1168 Kenyon cells incorrectly activate (or not activate) when viewing the mirror image TS^{COR} pattern, but just 833 differences for the checkerboard pattern (MERGED model TS^{COR} : 539, TS^{INC} : 409). The DISTINCT model performed marginally better on the left / right pattern test (58%, still low compared to honeybees' 74% accuracy). For this

pattern the model at least perceived the correct orientations in each dorsal / ventral region (TS^{COR} : 70, TS^{INC} : 424 incorrect activations); however the DISTINCT model still received the wrong orientation information for each quadrant, and thus only marginally preferred the left / right pattern (TS^{COR} : 544, TS^{INC} : 841 incorrect activations). It is most likely that in these experiments and while observing other similar stimuli the honeybees could use other visual features (optic flow, symmetry, etc.) to identify the checkerboard as very different to the training patterns and reject it.

The Batch 3 experiments (where the TS^{COR} and TS^{INC} patterns were very similar) showed that the DISTINCT model consistently outperformed the MERGED model, but neither model achieving more than 60% accuracy. The potential reasons for this poor performance are discussed in length in the discussion section below.

Apposed to those experiments mentioned above, the MERGED model always outperformed the DISTINCT model (see Fig 3.11), as with the pattern-offset experiments, by combining LOSN inputs from both eyes the MERGED model was less affected by minor variances in edge orientations and lengths, or indeed incorrectly oriented bars, in the TS^{COR} patterns. For example in the Batch 2 experiments the TS^{COR} patterns had the orientation in one quadrant rotated through 90° meaning that a large proportion of DISTINCT model's Kenyon cells receiving LOSN input from that quadrant would activate incorrectly, whereas within the MERGED model a smaller subset would be incorrect for the whole dorsal or ventral region. Figure 3.10 displays the DISTINCT and MERGED models' Kenyon cell activations to the CS+ and test stimuli, and differences in activation.

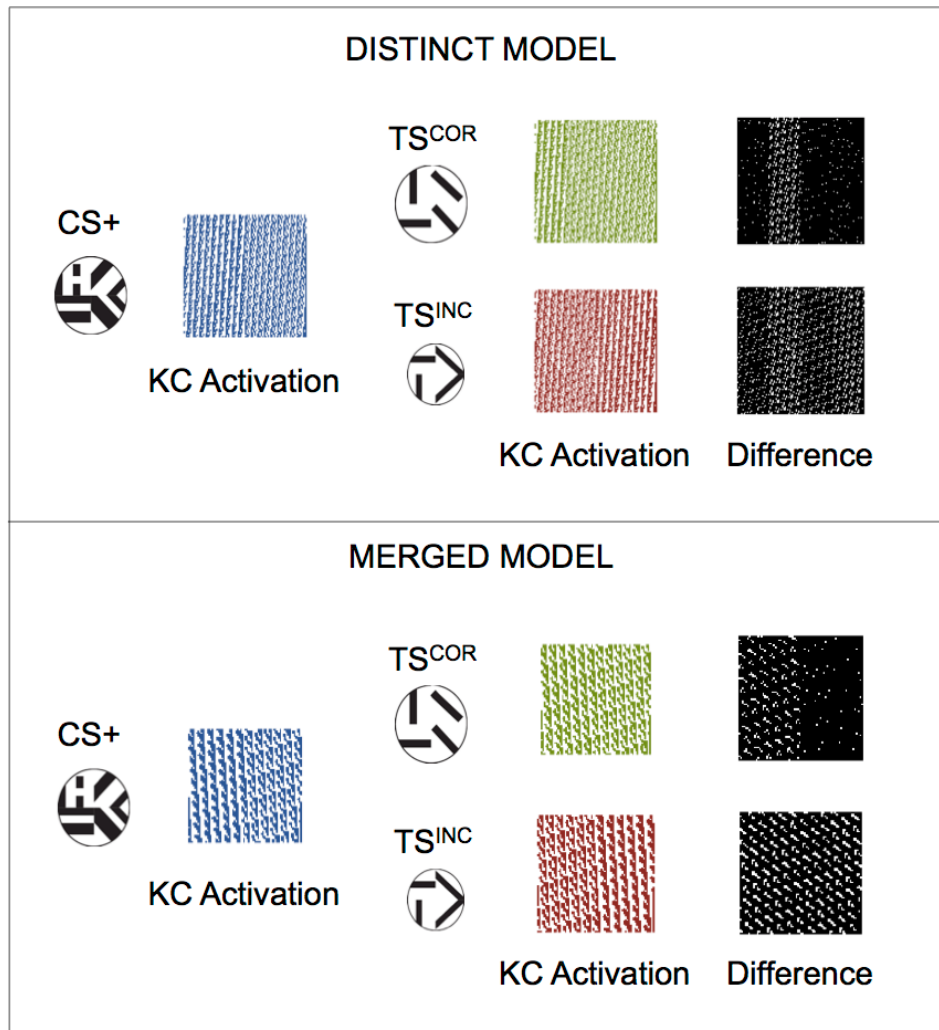


Figure 3.10 Model Kenyon cell activation for generalization experiments Batch 2. Blue: Kenyon cell activation when each model is presented with the first of the six CS+ patterns (Fig 3.6b). Green: Kenyon cell activation to the TS^{COR} pattern with the top-right quadrant having an incorrectly oriented bar, Red: Kenyon cell activation to the TS^{INC} pattern, with all quadrants incorrectly oriented. White dots on black square: shows the Kenyon cell activation differences between the test stimulus (TS^{COR} or TS^{INC}) and the CS+ pattern. *MERGED* model produced slightly fewer activation differences between the CS+ and TS^{COR} patterns, relative to the CS+ / TS^{INC} differences, compared to the *DISTINCT* model. Thus producing a marginally better performance (KCSR *MERGED*: 0.62, *DISTINCT*: 0.58).

Summary of experiment set 2

Figure 3.11 shows a summary of the experiments I simulated and the corresponding honeybee experimental results (Stach and Giurfa 2001, Stach, Benard et al. 2004).

Despite my models' extreme simplicity, they largely predicted the honeybees' generalisation performances accurately for a majority of the tested pattern pairs where the TS^{COR} and TS^{INC} patterns had identical, or mostly similar, orientations to the respective CS+ and CS- training patterns, even though they were novel variants. The models only consistently failed when the TS^{COR} and TS^{INC} were very similar, and also when viewing chequerboard patterns. This shows that seemingly 'complex' pattern generalisation tasks do not require advanced cognition. Instead, my DISTINCT and MERGED models provide evidence that visual pattern recognition and classification may in fact be the emergent properties of connecting just a small number of large-field visual inputs and require no more neuronal complexity to that of generalising simple bars and gratings.

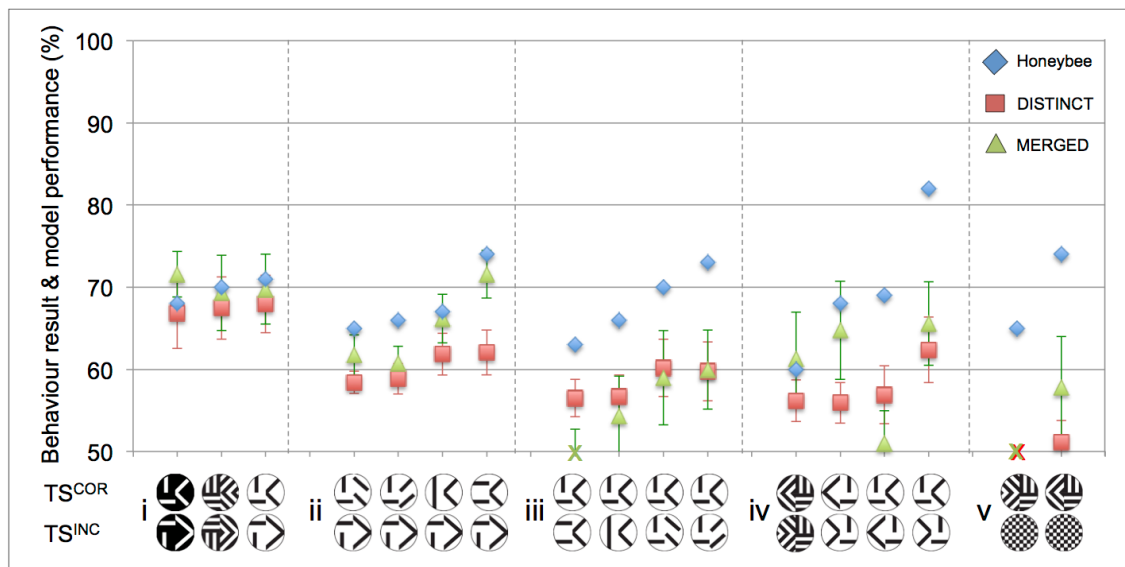


Figure 3.11 Summary of honeybee behaviour and model performance for generalisation of quadrant patterns. Blue diamonds: honeybee result, percentage of correct choice selections when tested with novel patterns of varying degrees of difference from the training CS+ / CS- patterns (here TS^{COR} and correct choice is the pattern the bees visited most often). Red squares: DISTINCT model performance when comparing each of the six CS+ patterns in a pattern set (a) against a novel TS^{COR} and TS^{INC} pattern pair. Green triangles: MERGED model results for the CS+ pattern sets compared against each TS^{COR} and TS^{INC} pattern pair. Error bars show standard deviation (these were not available for the behaviour results). For simple generalisations (i) where the novel TS^{COR} patterns had the similarly oriented bars to the

CS+ pattern set and TS^{INC} was similar to the CS- patterns the DISTINCT and MERGED model performances were almost identical to those of the real honeybee results. For the harder generalisations; (ii) TS^{COR} one quadrant incorrect – TS^{INC} all quadrants incorrect, (iii) TS^{COR} all quadrants correct – TS^{INC} three quadrants correct, (iv) mirror images and left-right reversals of CS+ layout, the DISTINCT model correctly generalised all pattern pairs but performed substantially worse than the real bees. The MERGED model failed most experiments in (iii) but did typically perform better than the DISTINCT model in (ii) & (iv). Both models failed to generalise correctly if the TS^{INC} was a chequerboard pattern whereas real honeybees typically rejected this novel stimulus. Figure adapted from my publication (Roper, Fernando et al. 2017)

3.5 Discussion

Apparently sophisticated cognitive abilities are often seen as a result of an equally complex neuronal architecture. However, here, this view is fundamentally challenged. Using a modelling approach, I investigated how bees' ability to discriminate and generalise could be explained by simple neural networks. I have shown that for patterns composed of multiple arrangements of achromatic bars, regularly used in honeybee behavioural experiments, bees may actually require very little sophistication in the neuronal architecture of their brain to discriminate them.

The honeybee LOSN responses are thought (Maddess and Yang 1997, Horridge 2000) to be the result of the summation of smaller receptive field orientation-sensitive neurons in the bee lamina or medulla (1st, 2nd optic ganglia), similar to those found in other insect medullas (McCann and Dill 1969, O'Carroll 1993, James and Osorio 1996, Maddess and Yang 1997, Okamura and Strausfeld 2007, Spalthoff, Gerdes et al. 2012). This collation of smaller subunits allows the LOSNs to encode a simplified summary of the oriented edges across the whole width of the bee eye. Although this means a bee cannot extract the exact retinotopic location or indeed orientation of individual edges through these neurons, my results show that, just eight of these large-field orientation-sensitive neurons would be sufficient for the discrimination and simple generalisation of

the described patterns. My models also demonstrate, even with their very simplified bee brain representation, that just a single layer of simple connections from the LOSNs to the mushroom body Kenyon cells would suffice to reproduce the empirical generalisation results between a given rewarding pattern (CS+) and the two test patterns (TS^{COR}, TS^{INC}). In fact my models may have had a more difficult challenge than that of real bees. During training the honeybees were exposed to both the CS+ patterns with a sugar water reward but also a non-rewarding (water) or even aversive solution (quinine) on the training distractor patterns (CS-), this differential training would allow the bees to learn both those features consistent with reward but also those pattern features that were to be avoided. There is empirical evidence to show that choice accuracy as well as the pattern features learnt by bees are affected by the training regime (e.g. absolute conditioning (no distractor pattern) vs. differential conditioning (Dyer and Chittka 2004, Giurfa 2004), and the penalty associated with a distractor (Chittka, Dyer et al. 2003, Avargues-Weber, de Brito Sanchez et al. 2010, de Brito Sanchez, Serre et al. 2015)).

Since it remains unclear how these different factors affect learning on the neuronal level, the theoretical models described here were restricted to an equivalent absolute conditioning protocol, with my virtual bees only having access to the CS+ pattern. Given that differential training typically yields better learning results (Giurfa, Hammer et al. 1999), it is all the more impressive that my simplified and experimentally disadvantaged virtual brains were able to facilitate largely similar results to actual bees. In addition, my models employed no form of learning. The Kenyon cell outputs of the models were achieved solely by the summation of either excitatory or inhibitory connections from the LOSNs (with synaptic weights of either 1 or -1 respectively). Here the simulated Kenyon cell outputs allowed the discrimination and generalisation of the tested patterns with approximately 50% activation of the Kenyon cell populations (due

to the reciprocal LOSN to Kenyon cell connection types, see Methods Chapter 2.3); I assumed, for comparison with my simple models, that some form of synaptic plasticity from the Kenyon cells to the mushroom body extrinsic neurons would allow the bees to associate the appropriate 50% active Kenyon cells to the CS+ pattern, and from these adjusted synaptic weights make the behavioural decisions. However, neuronal recordings of the mushroom body lip, which receives olfactory input, shows just ~5% activation of the Kenyon cells mediated by a feedback inhibitory network in the mushroom body calyces (Papadopoulou, Cassenaer et al. 2011). It may be that when honeybees visit a correct pattern synaptic plasticity in the Kenyon cells increases the firing rate, or reduces the response latency, of the Kenyon cells that fire, but potentially more importantly, it may inhibit those Kenyon cells that incorrectly fired for the CS-pattern (during differential training). In this case, the 5% of the Kenyon cells that are active (assuming the same value as for olfactory stimuli) would potentially be optimal to associate the CS+ pattern with reward. Additional research is required to see if this greater specificity would actually account for some of the bees' higher performances compared to that of my current models. It should be noted that ~50% of the olfactory projection neurons to the mushroom bodies are highly active when a particular odour is presented (Rossler and Brill 2013) providing a population coding response to a given odour, this differs considerably to that of the optic lobe neurons that typically have more specific firing rate tuning curve responses to particular stimuli. Due to issues with harnessing bees during visual learning tasks we currently lack the ability to record Kenyon cell responses for anything but the simplest visual stimuli (e.g. whole eye exposure to a single colour (Hori, Takeuchi et al. 2006)). Unfortunately this means we do not yet have empirical evidence for the Kenyon cell activation level for visual stimuli. New research using walking bees in virtual reality rigs (Paulk, Stacey et al.

2014) may allow these activation levels, and Kenyon cell response changes, to be recorded during visual learning paradigms. These findings will undoubtedly provide vital information for the next generation of theoretical models, which could be used to understand the trial-by-trial learning process of bees.

Despite the limitations mentioned above, my models still performed almost identically to the real bees when making simple generalisations (Fig 3.5, Fig 3.6) and only dropped in performance when the TS^{COR} and TS^{INC} patterns became very similar (Fig 3.7). Here the difference in training procedure almost certainly contributed to the typical 5-10% lower results in my absolute-like simulations to those of the differentially trained honeybees. Again, future behavioural and electrophysiological research may reveal how training paradigms affect the learning on the neuronal level, which would allow corresponding adjustments to the new theoretical models.

In addition, the poor concordance of the MERGED model results and the honeybees in the generalisation experiments may also result from the experimental paradigm that allowed the bees to fixate on the pattern at close range and make their final decision from a fixed perspective. This would, for these experiments, be very similar to the better-performing DISTINCT model with zero stimuli offsets. It is conceivable that honeybees have a combination of both DISTINCT and MERGED type LOSN to Kenyon cell configurations within their mushroom bodies. In this neuronally still simple scenario, attention-like processes could “selectively learn” the Kenyon cell responses that are good indicators of reward in a given experimental scenario. This might therefore account for some of the bees higher performance compared to that of my solely MERGED or DISTINCT models. Future work will investigate if there is an optimal distribution of distinct and merged LOSN connections to the Kenyon cells, or if

synaptic plasticity is able to adjust the proportion of each connection type for a particular task (see Chapter 6.2).

During the offset pattern discrimination simulations (Fig 3.3) I found that simply combining the neuronal firing rates of LOSNs from each eye would allow for pattern discrimination with an impressive horizontal location invariance of the perceived stimuli. By merging information from both eyes, a very coarse representation of the whole 270° bee eye horizontal field of view can be produced. Surprisingly, this non-retinotopic representation appears sufficient to discriminate quite complicated visual patterns, removing the need for the bees to have to store an image template or ‘photographic’ view of the pattern. This mechanism also has the advantage that very similar summed Kenyon cell responses can be achieved irrespective of how much of the pattern each eye views, as well as a representation that is less sensitive to small differences during generalisation experiments. However, despite the typically good discrimination results over large offsets and the ability to discriminate when patterns are only partially visible (Fig 3.3), my results show that this mechanism may well come at the expense of discriminating certain types of stimuli. Certain spiral and octagonal patterns (Fig 3.2) were not reliably discriminated by my MERGED model or by real honeybees (Zhang and Horridge 1992). Surprisingly, honeybees have been shown unable to discriminate a very simple pair of 90° cross patterns (CS- pattern rotated through 45°) (Srinivasan, Zhang et al. 1994) (Fig 3.12a), despite their apparent differences to a human observer. Simulations of these experiments once again showed the MERGED model’s similarity to the honeybee behavioural results, with a sub 60% discrimination performance on these simple cross patterns, whereas the DISTINCT model achieved over 70% accuracy. Interestingly both of the models, and honeybees, were able to discriminate a pair of 22.5° rotated cross patterns easily (CS- pattern

rotated through 90°) (Fig 3.12b). It may well be that in allowing the neuronal architecture of the honeybee brain to overcome horizontal location variance for common stimuli, it has compromised its ability to discriminate specific, arguably less important cue combinations.

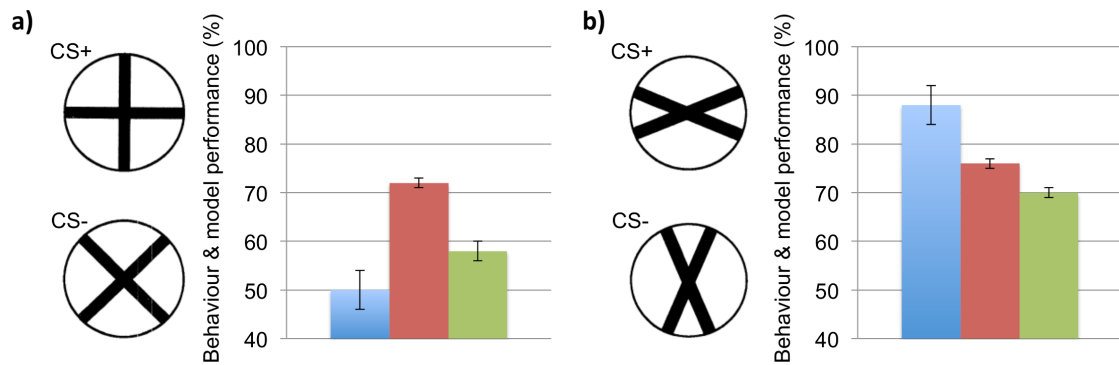


Figure 3.12 Honeybee behaviour and model performance for the discrimination of simple cross patterns. In the behavioural experiments (Srinivasan, Zhang et al. 1994) different groups of honeybees were differentially trained on a particular cross pattern pair, one rewarding (CS+) and one unrewarding (CS-). Blue: honeybee result, percentage of correct CS+ pattern selections after training. Red: performance accuracy of the DISTINCT model. Green: performance accuracy of the MERGED model. Error bars show standard deviation. (a) Discrimination of 90° cross and 45° rotation of this pattern. The DISTINCT model easily discriminates the patterns but honeybees cannot, and the MERGED model's performance is below 60% accuracy. (b) Discrimination of a 22.5° cross pattern and the same pattern rotated through 90°, both models and honeybees can discriminate these cross patterns.

In conclusion my research in this chapter shows that very simple neuronal connections, which would be easily accommodated within the miniature brain of a bee, are able to facilitate seemingly complex visual cognitive tasks. In addition the merging of visual information from both eyes, as seen in the mushroom bodies of bees (Ehmer and Gronenberg 2002), appears to be a very effective solution to partial occlusion and some degree of retinal location invariant pattern discrimination.

Chapter 4: Theoretical models of how honeybees could solve the ‘above and below’ conceptualisation task

4.1 Abstract

Honeybees exhibit remarkable visual cognitive abilities, such as the fine pattern discrimination and generalisation acuity discussed in the previous chapters, these capabilities provide obvious behavioural advantages when it comes to identifying rewarding floral resources in their natural environments. However, more surprising is honeybees’ apparent mastery of more complex cognitive tasks. Bees can be trained to identify a rewarding stimuli based on their ‘sameness’ or ‘difference’ to a previously seen pattern, they can count (up to four) and solve basic numerosity problems. Here I investigate another conceptual relationship task – the concept of ‘above’ and ‘below’. Bees are able to solve this task, identifying which of two presented stimuli contains the appropriate spatial organisation of a consistent referent pattern and a changing, and potential novel, target pattern. Simulations using my theoretical bee brain models while being presented with the ‘above and below’ stimuli initially showed an inability to choose the correct pattern in all but the simplest cases. However, a simple adaption to the models, allowing modelled bees to centralise their field of view directly in front of the referent shape drastically increased one of the model’s performances. This model was then able to solve the task without having to understand the underlying relationships between the referents and targets. It achieved average simulation accuracies of 80%, nearly identical to that of the empirical honeybee results.

4.2 Introduction

Over the last 100 years research into honeybee visual cognition has primarily focused on which visual features (colour, edge, orientation, symmetry) the bees are able to utilise in order to associate particular stimuli with reward (or punishment). However, over the last two decades, in large part due to the remarkable ability of the bees to adapt and learn almost any task presented to them, experimentalists have begun to ask if honeybees could possibly exhibit ‘higher-order’ cognition. These experiments, most often being adapted from those conducted on primates or birds, look to see if complex rules can be comprehended and followed. Successful examples performed on honeybees or bumblebees include, but are not limited to, social learning (Leadbeater and Chittka 2008, Leadbeater and Chittka 2009, Dawson and Chittka 2014, Smolla, Alem et al. 2016), counting and numerosity (Chittka and Geiger 1995, Dacke and Srinivasan 2008, Gross, Pahl et al. 2009), and conceptual learning tasks (‘sameness’ and ‘difference’ (Giurfa, Zhang et al. 2001), ‘larger than’ - ‘smaller than’ (Avargues-Weber, d’Amaro et al. 2014)). But should these discoveries be regarded as spectacular because bees manage to achieve human-like computations of visual image analysis and reasoning? Given that the bees’ brain contains less than a million neurons, could there be radically different explanations for how the bees solve these tasks compared to how we envisage large vertebrate brains solve the same problems?

For conceptual learning tasks, animals are typically exposed to a set of training examples where the rewarding stimuli all follow some standard format or sequence, the subjects are then tested on novel stimuli that may have nothing in common with the training set, other than obeying the same rule. One such conceptual learning task that

honeybees have been shown to comprehend is a spatial relationship problem called ‘above and below’ (Avargues-Weber, Dyer et al. 2011).

During the original ‘above and below’ behaviour experiments, honeybees were first pre-trained (Phase 1) within a Y-Maze (see Fig 1.2) to a consistent referent, either a black cross or a disc (Avargues-Weber, Dyer et al. 2011). This was performed to focus the bees’ attention on the referent shape. The initial 15 trials were conducted using absolute conditioning (Giurfa, Hammer et al. 1999), such that the second distractor pattern was always a blank white sheet of paper. After these pre-training trials, the bees were tested within the Y-Maze with the choice of the learnt referent shape, and a second distractor pattern selected from one of five target shapes, with neither of the stimuli providing reward. The bee’s first choice and number of subsequent touches on each pattern during the first 45 seconds of the test were recorded.

The second training stage (Phase 2) consisted of 50 training trials. One group of bees were trained such that target shapes (different to the selected referent shape) were always positioned above the referent shape on the patterns, and thus identified reward (sucrose solution was provided via a small feeder tube at the centre of the pattern), and correspondingly the target shapes below the referent led to an aversive quinine solution. A second group of bees was trained on the reciprocal condition, with the target shapes below the referent indicating reward. A different target shape was presented on the two patterns on each trial. After training, the bees were again tested, for 45 seconds without reward, with the above and below configurations using the target shape used in the Phase 1 discrimination test, which was unused during phase 2 training. This would therefore test the bees’ ability to correctly solve the ‘above and below’ relationship on completely novel patterns.

The empirical results suggest that the honeybees were able to utilise the spatial relationship between the referent and target shapes and thus learn to identify the rewarding patterns. By the end of training, the honeybees achieved ~80% correct choice accuracy (averaged over last 10 trials), and during the 45 second non-rewarded tests with novel target shapes the cumulative choices for the correctly configured patterns accounted for just under 70% of all choices ($n=20$; $t_{19}=11.2$, $p < 0.001$) (Avargues-Weber, Dyer et al. 2011).

As with the previous chapters (Chapter 2 and Chapter 3) here I investigate: can very simple neuronal models of the honeybee brain encapsulate appropriate rules, in this case for ‘above and below’, and transition between the training stimuli and test patterns. How much additional neuronal architecture or other requirements are necessary to accomplish the task, and finally how well do these models perform compared to the empirical behavioural results stated above.

4.3 Methods

4.3.1 Stimuli

In accordance with the honeybee behavioural experiments ((Avargues-Weber, Dyer et al. 2011) Experiment 2) the test stimuli for single experimental trials were composed of an ‘above’ and ‘below’ pair of patterns. Each achromatic pattern consisted of a white background (1065 x 1065 pixels) with a black ‘referent’, which in my simulations was always a 210 x 210 pixel cross, and a black ‘target’ that was either; concentric diamonds (290 x 350 pixels), a small horizontal bar (60 x 180 pixels), a vertical grating (290 x 290 pixels), a filled disc (180 pixels in diameter), or a radial three-sectored

‘trefoil’ pattern (235 x 235 pixels) (Fig 4.1a). For each pattern pair the same target was placed either above or below the referent cross, these shapes were aligned either with the crosses in the centre of the patterns, or the cross and target shapes vertical equidistance from the centre, with all shapes horizontally centred. In addition, for the phase 1 simulations, fourteen stimuli were produced with just the referent cross, positioned in different, non-central, locations on the pattern. A final set of stimuli consisted of each single shape (referent and targets) positioned centrally on the pattern, as well as a completely blank white pattern. All patterns were saved as 1065 x 1065 pixel PNG images.

4.3.2 Simulated experiments – phase 1

To represent the phase 1 (pre-training) experiments, I tested my models by simulating a similar absolute conditioning protocol to that used in the behavioural experiments (Avargues-Weber, Dyer et al. 2011). These simulations used the cross shape as the referent, versus a blank white image. I recorded simulation discrimination accuracies for when the rewarding pattern (CS+) had the cross in the centre of the pattern, and the correct test stimulus (TS^{COR}) had the same cross shape either in the centre of the pattern, or in 14 different non-central locations. These simulations used the blank white pattern as an absolute conditioning distractor (TS^{INC}). As in the original behavioural experiments (Avargues-Weber, Dyer et al. 2011), I subsequently tested how well the models could discriminate this same centred referent cross pattern, from each of five centrally positioned target shapes (bar, disc, diamond, grating, trefoil).

4.3.3 Simulated experiments – phase 2

In these simulations, I assumed that the ‘above’ configuration was rewarding (i.e. the target shape was always above the referent cross shape (CS+)). Two different configurations of test stimuli were used, those with the crosses aligned centrally and those with the crosses positioned the same vertical distance from the centre as the target shapes (hereon referred to as equidistance, see stimuli). In both configurations all the correct test stimuli (TS^{COR}) had the target above the referent and the incorrect distractor patterns (TS^{INC}) had the target below the referent. In any individual trial, the two test patterns always presented the same target shape.

To test the models’ ability to generalise between the patterns I produced a variety of stimuli configurations. Firstly, the CS+ pattern and TS^{COR} / TS^{INC} patterns presented the same target shapes. These were either aligned with all the crosses centrally located, or at the equidistance positions, or with the CS+ and test stimuli presenting the crosses in the different respective positions. The second set of simulations repeated these previous position configurations, but here, in each simulation the CS+ target was a different shape to the TS^{COR}/TS^{INC} targets. This was executed for every possible combination of CS+ and TS^{COR}/TS^{INC} target shapes, resulting in a total of 100 different pattern configurations.

4.3.4 Simulation procedure

To investigate how honeybees may respond to particular views of the ‘above and below’ experimental stimuli I evaluated three of my previous theoretical models, SEO_AB (Chapter 2), MERGED (Chapter 3) and DISTINCT (Chapter 3). In summary, these

models produce theoretical optical neuronal responses to presented stimuli; these are based on the two types of lobula (3rd optic ganglion) large-field orientation-sensitive neurons (LOSNs) discovered in honeybees (*Apis mellifera*) (Maddess and Yang 1997) (see Chapter 2.3.2 for LOSN response calculations). Each model uses the same eight LOSN outputs but these vary in the way the excitatory and inhibitory synaptic connections are configured between these lobula neurons and the models' Class II (clawed) Kenyon cells, which receive sensory input within the honeybee mushroom bodies (learning centres) (Strausfeld 2002). The MERGED model, in contrast to the other two models (DISTINCT, SEO_AB), combined LOSN inputs from both eyes onto single Kenyon cells.

Each simulation trial was composed of three patterns (CS+, TS^{COR}, TS^{INC}). The simulation Kenyon cell similarity ratio (KCSR) of each trial was calculated by comparing the particular model's Kenyon cell responses to the presented CS+, TS^{COR} and TS^{INC} patterns (see Chapter 2.3.4 for calculation details). Each pattern triplet configuration was simulated one thousand times to produce an overall experimental performance value (the minimum, maximum and standard deviation of all simulation KCSRs for that pattern triplet were also recorded). A model performance of ~50%, with individual trial KCSRs of <0.5, meant that there was an equal or greater similarity from the CS+ pattern to the TS^{INC} than TS^{COR} patterns, and therefore assumed to be my models' equivalent to the bees' inability to discriminate or generalise to the test patterns. For generalisations across target shapes (i.e. the CS+ and TS^{COR} / TS^{INC} presented different target shapes) the results of all pattern triplet combinations for a particular CS+ target shape and the four other target shapes were averaged (4,000 individual simulations). To identify if any particular target shape on the respective CS+ and TS^{COR}

/ TS^{INC} patterns would effect the simulation performances I also calculated individual experimental performances for each possible combination of the target shapes.

4.4 Results

4.4.1 Simulation results – ‘above and below’ phase 1

In the first set of simulations, I tested the SEO_AB, DISTINCT and MERGED models ability to discriminate a centrally located cross from a blank white pattern. All three models achieved average discrimination performances above 80% (DISTINCT: 84%±1%, MERGED: 88%±3%, SEO_AB: 87%±7%). In the second set of Phase 1 simulations I determined the models’ discrimination performances when presented with centrally positioned crosses, versus each of the five available target shapes (bar, diamond, dot, grating, trefoil), again aligned in the centre of the patterns. All models produced average discrimination performances in the range of 60-91% (DISTINCT: 59-78%, MERGED: 55-82%, SEO_AB: 80-91%), with the DISTINCT model outperforming MERGED on just the diamond and dot shapes, and the SEO_AB model consistently outperforming the other two models (Fig 4.1a).

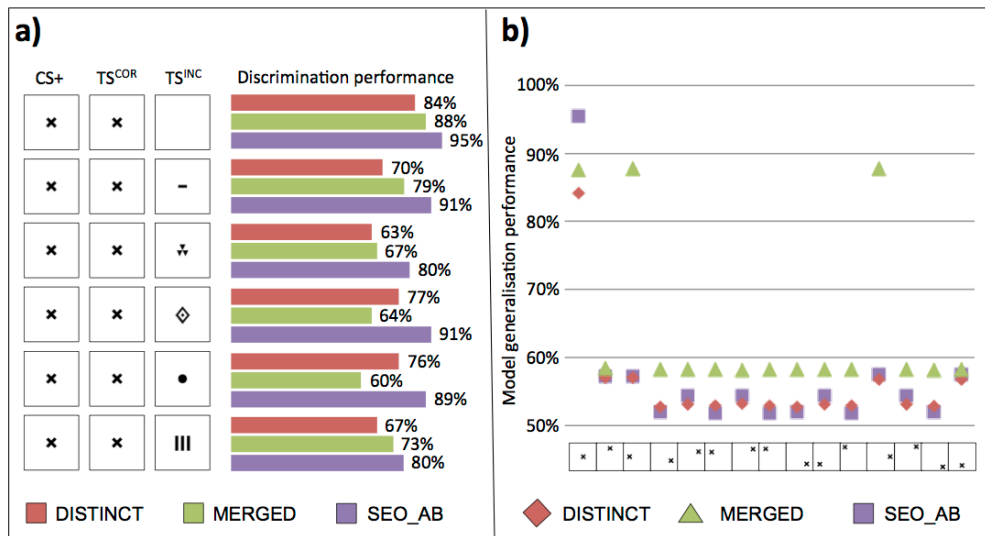


Figure 4.1 Model performance for discrimination of referent in ‘above and below’ phase 1 simulations. (a) Performance of models to discriminate the cross (referent) from a blank pattern and each target shape, all shapes positioned centrally on the pattern. (b) Performance of the models to discriminate a cross and blank pattern when crosses are in random positions on pattern, CS+ pattern had cross in centre.

For the final batch of Phase 1 simulations, the cross of the rewarding stimulus (CS+) was centrally located on the pattern, with the correct test stimuli (TS^{COR}) crosses being placed in non-central locations on the test patterns, TS^{INC} was always a blank white image. Here the DISTINCT model achieved average results for each of the cross locations ranging from just 52% to 58% (Fig 4.1b: blue diamonds). However, individual simulations for each location always returned very low accuracies of between 50-55%. The MERGED model performed marginally better, achieving averages of 58% to 59% during simulation on all but two configurations (Fig 4.1b: green triangles), with no individual simulation achieving less than 54%. This model did however achieve 88% accuracy for the two instances where the TS^{COR} pattern crosses were at the same height as the centrally located CS+ cross. The SEO_AB model simulations never achieved more than 58% accuracy with individual simulation KCSR results ranging from 0.52 to 0.58 (Fig 4.1b: purple squares).

Overall, all models were able to discriminate the cross referent shape from both a blank pattern and each of the five target shapes, with performances no lower than 60% accuracy. These were similar to the empirical honeybee results for phase 1 tests (~70% cumulative touches on the referent patterns (Avargues-Weber, Dyer et al. 2011)). Only the DISTINCT model was able to achieve simulation results of over 60% accuracy for the offset cross tests, and then, only when the cross was at the same height as the CS+ pattern's cross.

4.4.2 Simulation results – ‘above and below’ phase 2

In the first batch of Phase 2 simulations the models had to discriminate a centrally positioned cross with a target shape above it (CS+ and TS^{COR}) from a similarly positioned cross with the same target shape below it (TS^{INC}), repeated for each target shape (Fig 4.2a). The MERGED model failed to discriminate three out of the five target shape stimuli sets (trefoil, diamond, disk) with individual simulations having KCSRs of less than 0.5 (i.e. incorrectly identifying the TS^{INC} pattern as more similar to the CS+ pattern than TS^{COR}). The simulations for the remaining two target shapes averaged $\geq 60\%$ accuracy (bar: 65%, grating: 60%). The DISTINCT model's simulation averages for the different target shapes ranged from 62% to 67%. The SEO_AB markedly outperformed all other models with all individual simulation results in the region of $84 \pm 3\%$. When the stimuli were configured with the cross and target shapes positioned vertically equidistance from the pattern centre, the MERGED model again failed to discriminate the same three target shapes; it performed slightly better on the bar and grating patterns achieving simulations averages of 69% and 74% respectively (Fig 4.2b: green bars). The DISTINCT model failed to discriminate the dot target shapes, and only averaged 57%

on the diamond shape simulations (individual simulation KCSRs: 0.51 to 0.63). The other target shape simulations did however outperform the corresponding results on the centrally positioned cross simulations by 1-4% (Fig 4.2a,b). The SEO_AB model discriminated all the target shape simulations in this configuration, however the trefoil and diamond simulations performed less well using these equidistance stimuli achieving just 65% and 58% respectively, compared to 84% for both shapes on the centrally located cross patterns.

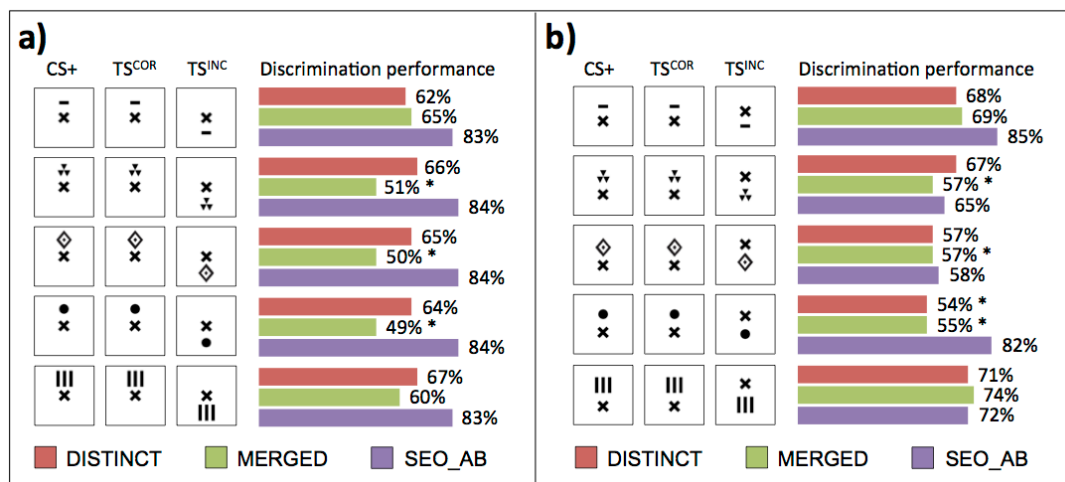


Figure 4.2 Summary of model performances for ‘above and below’ phase 2 simulations when target shape is the same on all patterns. (a) Referent centrally located in all patterns. (b) Referent and target shapes equidistance from centre.

The second set of simulation tasked the models with generalising from one target shape on the CS+ pattern to each of the five different target shapes on the test stimuli pair (Fig 4.3). The MERGED model failed to generalise between targets with the worst individual simulations always achieving a KCSR of 0.5 or lower, and averaging no more than 54% for any given target shape. The DISTINCT model produced similarly poor simulation results; only when the CS+ target was a diamond or dot, and the crosses were centrally located did the model simulations achieve an average performance of 60%. All other pattern combinations resulted in individual trials failing to achieve a KCSR of over 0.5. The SEO_AB model consistently achieved higher

simulation results, with the exception of the diamond shape on the CS+ pattern simulations. All TS^{COR} patterns were correctly identified on the equidistance cross configuration with average performances ranging from 55% to 62%. Where the target shape was a diamond on the CS+ patterns the simulations averaged 53%, interrogating the individual simulations of each target shape I found patterns that contained the bar target shape achieved just 49% (average of 1,000 simulations). Markedly higher simulation performances were achieved when the referent crosses were positioned centrally; here the lowest individual simulation trial for any target shape produced a KCSR of 0.73 with experiment performances for each of the possible CS+ targets ranging from 77% to 80%.

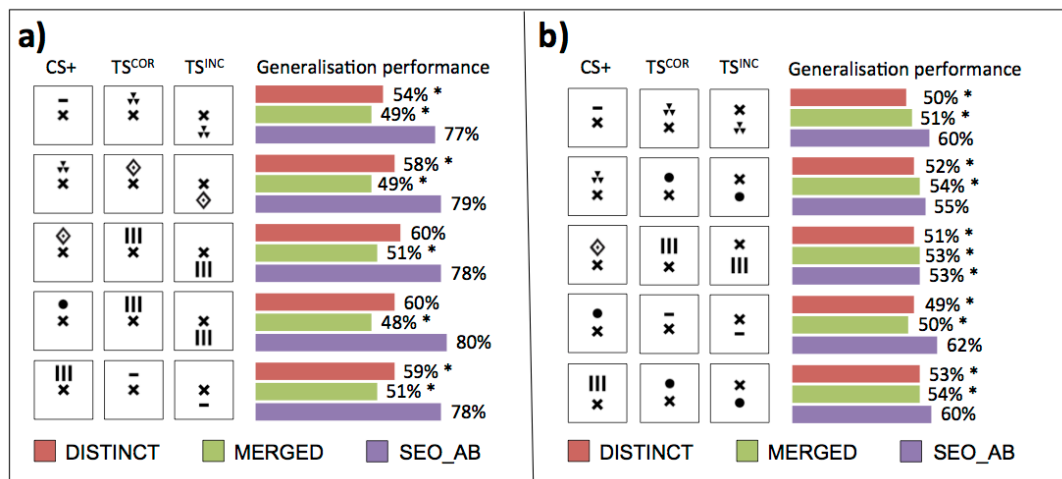


Figure 4.3 Summary of model performances for ‘above and below’ phase 2 simulations when target shape is different on the CS+ stimulus to those on the TS^{COR} / TS^{INC} stimuli. (a) Referent centrally located in all patterns. (b) Referent and target shapes equidistance from centre. Blue: DISTINCT, green bars: MERGED, purple bars: SEO_AB.

The remaining simulations were those where the CS+ and test stimuli pattern pairs were presented with the crosses in the different location configurations (CS+ crosses centred and TS^{COR}/TS^{INC} equidistance, or vice versa). When the same target shape was used for all patterns the MERGED model achieved simulation averages of 56% and 63% for the bar and grating shapes when the crosses were centrally located, and

similarly 57% and 63% respectively for these shapes on the equidistance patterns. Performance for the CS+ centrally located cross and trefoil target shape patterns was 56%. With the above exceptions, all other simulations for the matching target shapes failed to consistently achieve over 50% accuracy. When the CS+ and test stimuli pairs presented different target shapes none of the models succeeded in consistently generalising to the TS^{COR} pattern (Fig 4.4a, Fig 4.4b). Performances ranged from 31% to 45% for SEO_AB, showing a consistent preference for the TS^{INC} patterns. The DISTINCT and MERGED models performed 5-15% better, with simulation averages of 49-53% (individual simulation trial KCSRs ranged from, DISTINCT: 0.41 to 0.55, MERGED: 0.36 to 0.56).

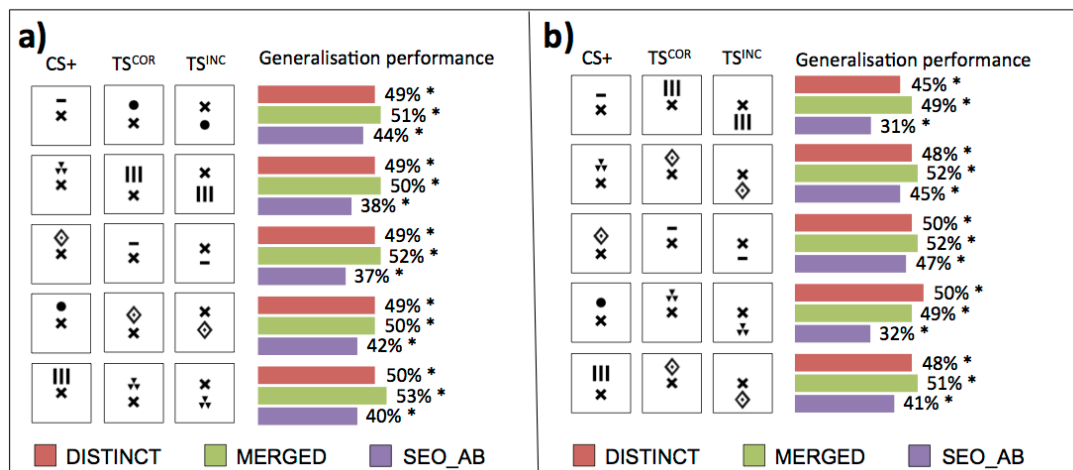


Figure 4.4 Summary of model performances for ‘above and below’ phase 2 simulations when referents are in different locations and target shape is different on the CS+ stimulus to those on the TS^{COR} / TS^{INC} stimuli. (a) CS+ referent centrally located, TS^{COR} / TS^{INC} shapes in equidistance positions. (b) CS+ referent at equidistance positions and test stimuli referents centrally located. Blue: DISTINCT, green bars: MERGED, purple bars: SEO_AB.

In summary, for the phase 2 stimuli experiments simulated here, only SEO_AB was able to consistently generalise to the correct ‘above’ pattern configuration irrespective of the target shapes used, however, this was only when the crosses were centrally positioned within all the patterns. All models failed the task when the CS+ and

test stimuli pairs had the referent crosses in different location configurations and the CS+ presented a different target shape to that of the TS^{COR} and TS^{INC} patterns.

4.5 Discussion

The ‘above and below’ experiments simulated in this chapter are often referred to as a conceptual, or spatial relationship, learning tasks. It is easy to presuppose that such a task would require a large vertebrate brain in order to be able to comprehend such advanced relationships. Indeed, the only (non-human) animals previously found to be able to solve the task had been birds (pigeons: (Kirkpatrick-Steger and Wasserman 1996)) and primates (chimpanzees (Hopkins and Morris 1989), baboons (Depy, Fagot et al. 1999), capuchins (Spinozzi, Lubrano et al. 2004)). The authors of the original ‘above and below’ honeybee study (Avargues-Weber, Dyer et al. 2011) sought to confute this ‘big brain’ assumption, and provided, for the first time, evidence of above/below spatial understanding in insects.

In this chapter I employed three theoretical bee brain models, previously discussed in chapter 2 (SEO_AB) and chapter 3 (DISTINCT and MERGED), and tested their ability to generalise over a large range of ‘above and below’ test patterns (5 target shapes and 2 position configurations = 100 stimuli trials). This was still a very simplified task compared to that conducted on real honeybees. The bees during their experiments were presented with 50 training pattern pairs where the referent and target shapes could be positioned in a large variety of different horizontal positions and heights on the patterns. Yet, even after the first five training trials the real honeybees had, on average, learnt to identify the rewarding pattern configuration above chance ($t_{19} = 2.8, p = 0.011$) (Avargues-Weber, Dyer et al. 2011).

In contrast, my models' performances were most often unimpressive, even with the simplified stimuli sets. When the test patterns had different cross configurations to that of the CS+ pattern (centrally located versus equidistance, or vice versa), the majority of the tests failed to produce consistent simulation performances of over 50% accuracy. This was also the case when I used the same target shape on both the CS+ and test patterns. These initial results suggest that the simple bee brain models presented here are insufficient for explaining how the bees can solve this spatial relationship task. It is possible that the lobula large-field orientation-sensitive neurons (Maddess and Yang 1997) I utilised in the models do not in themselves provide sufficient visual fidelity to discriminate the 'above and below' stimuli pairs. Equally, it could be that the single layer of excitatory and inhibitory synapses of these neurons onto the mushroom body Kenyon cells in my models are simply too rudimentary to allow more complex object relationships to be established (see (Kleyko, Osipov et al. 2015)). However, there is one other factor that has thus far been excluded from my investigation. In the original behaviour experiments (Avargues-Weber, Dyer et al. 2011), much like the other honeybee generalisation experiments (Giger and Srinivasan 1995, Giurfa, Hammer et al. 1999, Stach and Giurfa 2001, Stach, Benard et al. 2004), the authors determined an individual bee's final choice selection only when it either touched one of the two presented stimuli, or physically landed on a feeder. In my simulations I assumed that the bees would be making their choice from the initial decision chamber of the Y-Maze flight arena, viewing both patterns, and selecting to fly to the pattern that generated Kenyon cell responses most similar to those learnt during previously rewarding pattern views. So, if we presuppose that the honeybees were to fly down each of the Y-Maze arms before finalising on a choice, then a much simpler process could be employed to solve this task.

In line with my current modelling results (Fig 4.4), I hereon assume that the honeybees would be unable to make a correct choice from the Y-Maze decision chamber. The bees would therefore be forced to make a random selection and traverse down one of the two Y-Maze arms. Once near the end of the Y-Maze arm, a bee could fixate (slow scanning flight manoeuvres, typically 1-3 cm in front of a stimulus) on the pattern. The bee would now be able to consistently centre itself directly in front of each shape (referent and target), and in doing so would reduce any horizontal, vertical or distance invariance between visits; previously shown to enhance my models' performances (Fig 2.2, Fig 3.2). The bee should now be able to easily discriminate the referent from any of the other five target shapes; as demonstrated with all three of my models (Fig 4.1a), indeed the SEO_AB model achieved $\geq 80\%$ accuracies. With the referent identified, and aligned directly in front of the bee, the task of identifying if this pattern is the rewarding stimulus becomes identical to that of my consistently centred cross stimuli configurations (Fig 4.3a). The only difference is that, rather than the crosses having to be in the centre of the pattern, the bee now simply moves till the cross is in the centre of its field of view (see Fig 4.5). Simulations using the SEO_AB model showed, in these conditions, a consistent preference for the appropriately configured 'above' test stimuli, with overall averages just below 80% accuracy ($>70\%$ accuracy for each of the 25,000 individual simulations).

It is important to stress, that these simulation results were possible without any form of object relationship, or spatial representation being built into my models. In fact the SEO_AB model required absolutely no adaptations, being identical to that used in Chapter 2, and still only utilised just the four optic neuron outputs from each eye, and excitatory only synapses of these neurons onto a single layer of mushroom body Kenyon cells. Yet, despite this models extreme simplicity, these results are strikingly

similar to the empirical data recorded during the honeybees' training trials (~80% correct choice accuracy), as well as for the novel target unrewarded control tests (~70-75% cumulative touches on correct patterns) (Avargues-Weber, Dyer et al. 2011).

At this point, it is worth interjecting, and highlighting a discrepancy between the Chapter 2 results for the SEO_AB model simulations, and those simulation results reported here. In the previous chapter, I demonstrated the remarkable ability of the SEO_AB model to discriminate between two very similar horizontal grating patterns (Fig 2.4b, 2.4c), however, this same model failed to consistently generalise between pairs of similarly oriented gratings, even when using perpendicularly oriented grating patterns as the TS^{INC} distractors (Fig 2.5b). Yet in these 'above and below' simulations the SEO_AB model produced the highest average performances, even when tasked to generalise between different target shapes (Fig 4.3a). So how can the same model enable fine discrimination for one set of stimuli, and excellent generalisation for another? Detailed analysis of the LOSN responses for a given stimulus (see Chapter 2.3.2 for LOSN calculations), and the resultant Kenyon cell similarities between stimuli, provided an answer. Figure 4.5 shows an example of a 'above and below' stimuli triplet ($CS+$, TS^{COR} , TS^{INC}). I assume the bee learns the $CS+$ pattern while the cross is in the centre of its field of view, and that the bee would always identify and fly to the referent in the corresponding TS^{COR} and TS^{INC} patterns; in this way the bee's field of view is always centred on a cross (Fig 4.5, blue boxes). From this position the lower half of the pattern is identical on both the $CS+$ and TS^{COR} patterns (Fig 4.5 red boxes). This produces very similar LOSN responses, and therefore nearly identical Kenyon cell responses (the simulated responses include a small amount of noise, this was applied to account for both the slightly different LOSN responses to the same visual input observed during electrophysiological recordings (Maddess and Yang 1997), and

inevitable variability in synaptic neurotransmitter signalling). In contrast, the LOSNs responding to stimuli in the upper half of the patterns would not be identical, due to the different target shapes presented. Nonetheless, overall the similarities in this one half of the visual field, compared to no similarity at all between the CS+ and TS^{INC} patterns, is sufficient to produce $\geq 70\%$ simulation accuracies. This model is therefore once again doing fine discrimination, not generalisation, only here, with just one half of the patterns. It is conceivable that the bees could learn to associate only those Kenyon cells that receive input from the lower visual field with reward, but as I've demonstrated, this would not be absolutely necessary. When bees are trained on the 'below' configurations being rewarding, no change would be required to the model. In these instances the visual field above the crosses in the CS+ and TS^{COR} patterns would be identical, and similarly very different in the TS^{INC} stimuli, resulting in the same effect.

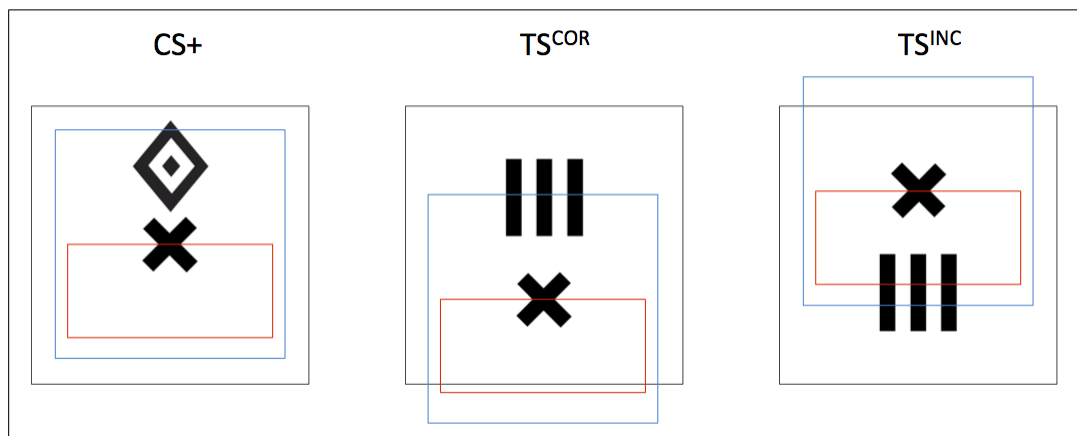


Figure 4.5 Schematic representation of the honeybee field of view when observing 'above and below' patterns. Blue boxes: field of view when bee positioned directly in front of referent cross shapes. Red boxes: lower half of visual field (in simulations this would encompass the entire lower half of blue box, it is shrunk here to be visible). The pattern portion visible within the lower half of the visual field (red boxes) of the CS+ and TS^{COR} stimuli would be virtually identical, allowing discrimination from the corresponding TS^{INC} viewpoint where part, or all, of the target shape would also be present.

The results presented in this chapter do not disprove that honeybees are using some form of spatial representation to solve the ‘above and below’ task. What they do provide is a number of predictions of honeybee behaviour that would be required if the bees are indeed using the simpler technique hypothesised here. (1) We would expect that the bees would be unable to identify the rewarding patterns from the decision chamber of the Y-Maze. This would culminate in them choosing to fly down the rewarding arm and unrewarding arm equally upon entering the Y-Maze, with no significant difference to chance over the 50 training trials. (2) We would expect the bees to initially fixate a small distance from the referent and target shapes on a pattern, and not to visit the feeder in the centre of the pattern directly. (3) If a bee were to fixate in front of the target shape first, it should then move to fixate in front of the current pattern’s referent. (4) After fixating at the rewarding pattern’s referent shape, the bees should choose to directly visit the current pattern’s feeder. (5) Similarly, a bee should traverse to the opposing arm after fixating at the referent of the unrewarding pattern.

In the following chapter (Chapter 5) I describe my replication of the experiments by Avargues-Weber et al. (Avargues-Weber, Dyer et al. 2011), incorporating high-speed videography. This allowed the tracking and subsequent analysis of the honeybees’ flight behaviour whilst they actually learnt the ‘above and below’ task. I was then able to assess how the observed honeybee behaviour correlated to my aforementioned hypotheses.

Chapter 5: High-speed videography analysis of honeybee flight trajectories provides new evidence on how bees solve the ‘above and below’ conceptualisation task

5.1 Abstract

Substantial research has been conducted to ascertain which visual features honeybees are able to discriminate, and how well they can generalise particular features to novel stimuli. However, little is known about how the bees actually manoeuvre in front of stimuli, which features they fixate, and how types of stimuli presented affect their flight paths or behaviour. Here, I explore if the physical characteristics of the honeybee flight trajectories could actually aid in solving a complex visual conceptualisation problem. Theoretical modelling of the bee brain when presented with stimuli from the ‘above and below’ spatial relationship task, showed it might be possible to solve the problem without having to ‘understand’ the underlying relationships between the pattern shapes. In this second stage of the study I used high-speed videography to capture the actual behaviour of real honeybee while learning the task. I analysed 150 flight paths of three bees recorded during the whole of their ‘above and below’ training regimes. By the end of training all three bees achieved $\geq 60\%$ correct choice accuracy for the rewarding patterns (last 10 trials). In over 80% of these flights the bees first fixated at the lowest shape on the pattern at the end of the initially chosen arm, if the bees were within the rewarding arm they directly visited the rewarding feeder in over 90% of such trials, if the bee was in the unrewarding arm it would inspect the pattern and abandon this incorrect arm without visiting the feeder 20-50% of the time. Two out of the three

honeybees tested were able to generalise to novel target shapes presented in the correct ‘above and below’ configurations during unrewarded tests. As with training trials, these bees fixated at the lowest shape on the patterns, and subsequently made their decisions based on a simple discrimination of this single observed shape, before choosing to visit the feeder, or not. This study shows that not all seemingly complex problems necessitate complex cognition, a fact that may be just as applicable for animals with big brains as for honeybees.

5.2 Introduction

In 1977 Wehner and Flatt published evidence of honeybees performing visual fixation flight manoeuvres when approaching within 1-3 cm of a vertically displayed stimulus (Wehner and Flatt 1977). In this situation, the bees would stabilise their head roll and pitch movements, and adjust their body axis to similar positions on each approach to a feeder. Subsequent behavioural work has shown that honeybees use optic flow in order to centre themselves while traversing a tunnel (Srinivasan and Zhang 1997) as well as stabilising their height to maintain a constant flight speed (or more specifically, constant speed of optic flow) (Baird, Srinivasan et al. 2006). Electrophysiology has been able to show how some of these behaviours are mediated, with identified neurons responding to neck muscle movements allowing a precise counter-rotation of the head in respect to the natural thorax roll during free flight (Hung, van Kleef et al. 2011), and numerous lobula (3rd optic ganglion) motion and direction sensitive extrinsic neurons are theorised to help in course correction and collision avoidance (Goodman, Fletcher et al. 1987, Ibbotson 1991). However, unlike the initial Wehner and Flatt experiments these are typically concerned with the flight dynamics themselves, not on the possible influence they may have on visual cognition. In the last few years, aided by the availability of

high-speed videography equipment, research has begun again on how bees approach and scan visual targets. These experiments have shown, as with the previous study, that the bee head is stabilised during free flight, with very fast yaw head saccades during turns (Boeddeker, Dittmar et al. 2010), as well as stabilisation during sideways translational movements during fixation scans (Boeddeker and Hemmi 2010), both of which would aid in keeping a stable image on the retina. Perhaps more revealing of how honeybees may adapt their flight behaviour to specific problems is recent publication by Morawetz et al. They showed that bees are both better and faster at discriminating colour cues which appeared in the lower half of a flight arena (i.e. within the ventral region of the bees visual field) than those same cues in the top half of the arena (Morawetz, Chittka et al. 2015). However, when all the feeders and corresponding cues were positioned at the top of the flight arena the bees would change their flight trajectory to fly directly towards the feeders and showed an increase in their accuracy and choice speed during the training, thus showing a direct adaption of their innate behaviour dependent on the specifics of the presented task. In this chapter, I investigate if honeybees might make similar behavioural changes during the training of the ‘above and below’ spatial relationship task, and if these changes could aid in the bees learning to solve the problem.

In the previous chapter (Chapter 4) I used theoretical bee brain models to simulate how honeybees might react to the ‘above and below’ stimuli. Due to the potential variability of the target and referent shapes positions on the experimental patterns, my models predicted that the bees would be unable to discriminate the correctly configured stimuli from the Y-Maze decision chamber. An alternative method for solving the task was consequently hypothesised; this involved a two-step process. First, the bee should fly down either Y-Maze arm to the displayed pattern, then fixate at

each of the presented shapes until it could determine which of the two shapes was the referent shape. In the second step, the bee should fly to, and fixate at, the identified referent. If the visual input while at this position was sufficiently similar enough to that of the learnt rewarding stimuli then it should go directly to the pattern's feeder, if not, immediately fly to the other Y-Maze arm and repeat the process.

Here, I replicate the 'above and below' experiments of Avargues-Webber et al. (Avargues-Weber, Dyer et al. 2011) with the addition of high-speed cameras to record the honeybee flight paths during each training trial, and determine if the honeybees' behaviour did indeed match that of the above hypotheses.

5.3 Methods

5.3.1 Apparatus

Honeybees (*Apis mellifera*) from two colonies were allowed to collect 20% sucrose solution (w/w) from a feeder located approximately 30 meters from the hives. Honeybees at the feeder were marked with coloured dots on the thorax and abdomen to uniquely identify them; those bees that regularly visited the site (every 5-10 minutes) were subsequently trained to visit a Y-Maze located five meters away from the main feeder. The Y-Maze was situated on a small table in open-air, but was sheltered from direct sunlight by a sunshade positioned 2 meters above the top of the apparatus.

The Y-Maze (see Fig 5.1) consisted of an entrance hole that led to a central decision chamber, from here two arms extended. Each arm measured 40 x 20 x 20 cm (L x H x W). Within each arm a removable back wall 20 x 20 cm was placed 15 cm from the decision chamber, this provided support for the stimuli and feeder tubes.

Unlike the original experiments no Perspex transparent cover was placed on the top of the Y-Maze flight arena; this was to allow for an unobstructed and undistorted view while taking high-speed video recordings. Two Yi (Xiaomi Inc. China) sport cameras were positioned side-by-side 10 cm above the entrance of the Y-Maze. Their field of view was adjusted such that they looked down into the arena at approximately 60° from horizontal, establishing in both cameras a wide-angle view of both arms. In the centre of the decision chamber, located on the Y-Maze floor, was a continuously running four-digit millisecond digital display (Adafruit Industries, LLC. USA) that allowed both cameras to be synchronised. This display was controlled via a microcontroller (Arduino Uno) housed outside the Y-Maze. Each Yi camera was configured to record at 120 frames per second at a resolution of 1280 x 720 pixels. Power to each camera was provided via USB cables from an externally powered USB hub, this also allowed video footage to be downloaded from the cameras' internal memory cards to a connected laptop computer (Apple MacBook Pro).

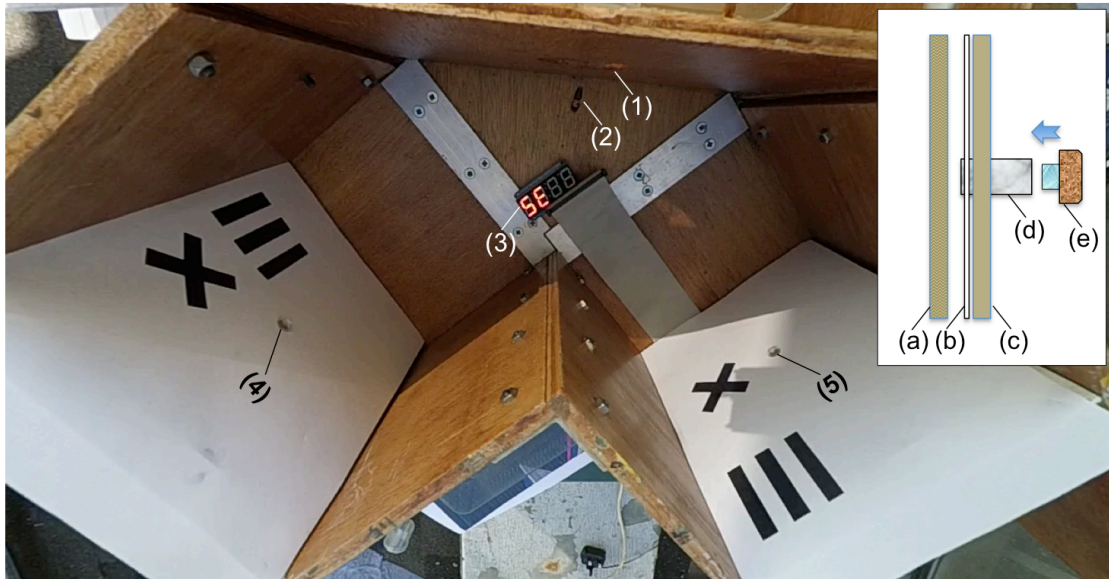


Figure 5.1 Y-Maze apparatus used for ‘above and below’ experiments. Main picture shows the view from one of the two Yi sport cameras. **(1)** Entrance hole that bees fly through to enter Y-Maze **(2)** Individual honeybee entering apparatus. **(3)** Millisecond timer used to synchronise the footage of both cameras. **(4, 5)** Feeding holes in the centre of patterns. **(4)** Example of ‘below’ configured stimulus with a cross referent and, in this case, a grating target shape. **(5)** Example of corresponding ‘above’ stimulus. Insert: side view schematic of the back wall at the end of Y-Maze arm. **(a)** Temporary cover plate added to hide the stimulus until the experimental trial was ready to be commenced. **(b)** Printed stimulus, discarded after each trial. **(c)** Removable back wall onto which the stimulus was attached; this had a 5mm diameter hole located in the centre. **(d)** Feeding tube pushed through printed stimulus flush into the removable back wall. **(e)** Stopper containing either 30 μ l of 50% sucrose solution (w/w) or saturated quinine solution, this was attached onto the back of the feeding tube.

Each stimulus (see below) was printed on A4 white UV-reflecting paper using a high-resolution laser printer. These were first cut to 20 x 24 cm (W x H) and then positioned in front of the 20 x 20 x 0.5 cm removable back wall (the additional height of the paper made it easier to align and adjust the pattern’s vertical position). The feeding tubes consisted of 5 mm diameter x 1 cm long flanged tubes; these were pushed flush through the centre position of the paper into a corresponding hole in the removable back wall. On the reverse of the wall a stopper containing either sucrose or quinine solution was attached to the feeding tube (Fig 5.1 insert). This technique was implemented to prevent sucrose solution being deposited on the entrance of the feeding tube during

refilling, thereby forcing the honeybees to crawl into the tube to determine if it contained a reward. A short pilot study with two honeybees demonstrated that the bees were able to detect the sucrose solution with their antennae if the tubes were filled from the front (Fig 5.2). For similar reasons, the stimuli were also disposed of after a single use, and the feeding tubes cleaned between trials to prevent odours being deposited by the bees and being subsequently used as an olfactory cue during learning. As there was no top cover on the apparatus, a blank brown cardboard cover-plate 20 x 20 x 0.5 cm was placed in front of each of the two stimuli to prevent a bee entering from the top of the Y-Maze and seeing the patterns or accessing the feeding tubes before a trial had begun.

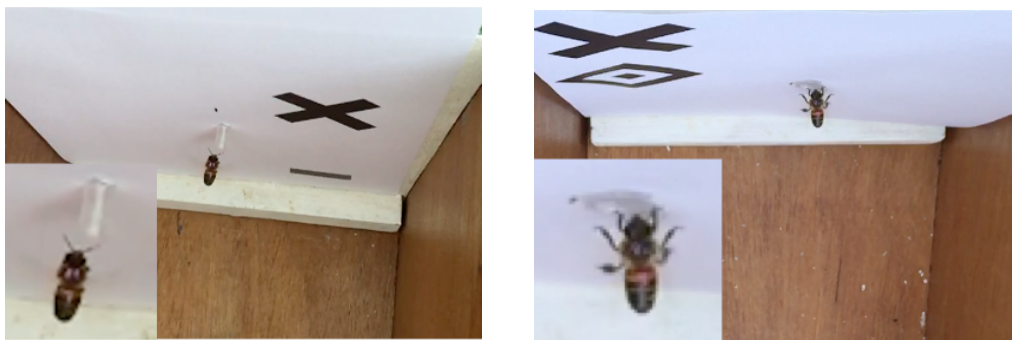


Figure 5.2 Pictures of honeybees approaching feeder tubes during the ‘above and below’ pilot study. **(Left)** bee that quickly scanned past the protruding unrewarding feeder tube and flew to the other Y-Maze arm. High-speed footage showed the bee antennae touching the tube before it departed. **(Right)** bee having to land and crawl into a flush feeder tube in order to determine if it is rewarding or not. Inserts: zoomed version of the respective bee bodies.

5.3.2 Stimuli

The stimuli for a single experimental trial were composed of two pairs of patterns, 20 x 22 cm (W x H) when printed and cut to size. Each achromatic pattern consisted of a white background with a black ‘referent’, which in these experiments was always a 4 x

4 cm cross, and a black ‘target’ that was either; concentric diamonds (5 x 6 cm), a small horizontal bar (1 x 3 cm), a vertical grating (5 x 5 cm), a filled circle (3 cm in diameter), or a radial three-sectored pattern (4 x 4 cm) (see Chapter 4, or (Avargues-Weber, Dyer et al. 2011) Experiment 2 for designs). For each pattern pair the same target was placed either above or below the referent cross, these were aligned with a variety of vertical and horizontal offsets from the pattern centres and with different vertical distances between the referents and targets. Ten variants were created per target creating in total fifty pattern pairs. In addition fifteen stimuli were produced with just the referent cross (randomly positioned), and, for both the referent and targets, one stimulus with each shape positioned centrally on the pattern.

5.3.3 Experiment trial procedure

Each trial consisted of the following setup. A rewarding stimulus (CS+) was placed onto the removable back wall and a clean feeding tube inserted with a stopper containing 30µl of 50% sucrose solution (w/w). The second, unrewarding, distractor stimulus (CS-) was fitted to its wall with another clean feeding tube leading to a stopper with 30µl of saturated quinine solution. The CS+ and CS- stimuli were pseudo-randomly (never more than four consecutive trials on the same arm) placed against the respective Y-Maze back walls to avoid the bees learning a side preference. The cover-plates were placed in front of these to prevent the stimuli from being seen. Both Yi cameras were started, such that there was an individual video file per camera, per trial. If the bee had already returned to the Y-Maze it was shoed away so that it had to re-enter the apparatus through the entrance hole. The two cover-plates were removed and an individual bee (only one bee was trained at a time to prevent multiple bees entering

the setup) was allowed to enter the decision chamber. From here, if the bee chose to enter the rewarding pattern's feeding tube, it crawled in, and could drink the sucrose solution ad libitum. If the bee chose the incorrect CS- pattern it entered the tube and tasted the quinine solution and was then allowed to fly to the other pattern to receive the reward. Typically the bees remained within the confines of the Y-Maze flying between the arms via the decision chamber; however it was possible for the bees to leave and re-enter the setup from the open top. Filming of a trial continued until the honeybee entered the CS+ feeding tube. After feeding the bee would depart for the hive, returning anywhere from 5 - 10 minutes to several hours later depending on weather conditions. This interval allowed for the next pair of stimuli to be inserted into the Y-Maze and the previous video files to be downloaded from the cameras onto the laptop.

5.3.4 Pre-training – ‘above and below’ phase 1

In total eleven honeybees were trained to visit the Y-Maze. Each individual bee was first trained using an absolute conditioning protocol (Giurfa, Hammer et al. 1999). The rewarding CS+ stimulus was always a black cross (referent) randomly positioned on the white background, the centrally located feeding tube led to 50% sucrose solution (w/w). These patterns were pseudo-randomly positioned into one of the two Y-Maze arms per trial. The other arm contained a fresh blank white sheet of paper with the feeding tube only providing quinine solution. The bee's first choice was recorded and acquisition curves produced by calculating the frequency of correct choices per block of 5 trials. After 15 training trials a discrimination test was introduced. In this test two patterns were used, one consisted of the normal cross shape, and the other contained one of the five target shapes; neither pattern was rewarding with both feeding tubes leading to

30µl of water. The bee entered as normal but was given 45 seconds to explore the new configuration. The number of visits to each feeding tube was recorded.

5.3.5 Main training – ‘above and below’ phase 2

In the second training phase, six of the initial eleven bees that completed phase 1 training were either subjected to a relational ‘above’ or ‘below’ conditioning protocol. For ‘above’ two patterns were presented in each Y-Maze arm on each trial, both patterns contained the cross referent shape and another shape selected from the four available target shapes (this excluded the shape used for that bee’s phase 1 discrimination test). In one pattern (CS+) the target would appear above the referent cross; this was configured so the central feeding tube lead to 50% sucrose solution (w/w). The other pattern (CS-) presented the target below the cross and its feeding tube led to saturated quinine solution. The target shape order was pseudo-randomised so that the same shape never appeared more than twice in a row and that there was no repeating order to the target presentations, all targets were shown ten times during initial training. Another group of individual bees were trained on the reversal of this protocol with the target below the referent being rewarding. After 50 training trials, the three bees that completed entire training regime were subjected to a 45 second non-rewarding control test. This maintained the above and below relationship used during training but presented the target shape that was used during that bee’s phase 1 discrimination test. After three subsequent training trials, a final non-rewarding control test was performed with the same cross and target shapes, but the ‘above’ and ‘below’ configurations were presented in the opposite arms of the Y-Maze to the first test. In each test the number of visits to each feeding tube were recorded.

5.3.6 Video analysis – annotation

The videos for each of the 50 training trials, for each bee, were replayed on a computer monitor in slow motion so that the particular flight trajectories of the bee could be observed and annotated.

The honeybees typically displayed three types of flight characteristics during a trial.

1. Direct flights: in these instances the bees would enter the flight arena and fly directly one or other of the feeding tubes. These flights would take less than a second until the bee had landed on the feeding tube (Fig 5.3a)
2. Brief inspection: here the bees would briefly fly towards one of the pattern shapes anywhere from 5 – 10 cm from the end of the arena arm displaying the pattern, before turning away. These types of flight manoeuvres would typically only last 1-2 seconds (Fig 5.3b).
3. Fixation scans: these were the most common form of flight manoeuvres observed during the experiments. The bees would approach a pattern shape and hover 1 – 3 cm from the shape, with a slow horizontal scanning motion. The bee might also quickly leave the pattern and then return and repeat the scan. These could last 5 – 10 seconds (Fig 5.3c).

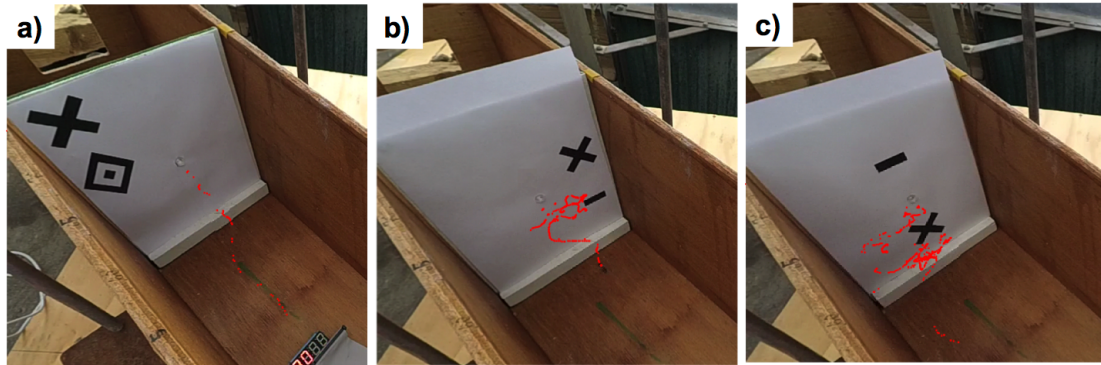


Figure 5.3 Tracking of honeybees approaching a pattern. **(a)** Direct flight: bees fly directly to the feeding tube. This flight took less than a second. **(b)** Brief inspection: bees move towards a particular pattern shape but do not spend very long at the shape, or view it from a distance (5-10 cm). In this instance the bee quickly approached the end of the bar, then flew away, flew back towards the edge of the bar and then flew to the feeding tube. This whole flight took less than 2.5 seconds. **(c)** Fixation scan: the bee flew towards the cross shape and made multiple flight transitions across the whole pattern, with additional smaller scans in front of the bottom edges of the cross. It then flew away from the pattern before approaching the feeding tube. This flight took ~7.5 seconds. Each red dot is the centre of the honeybee body in one frame of the video recording (approximately every 8ms).

The following types of behaviour were recorded during the video analysis:

- Side preference – upon entering the Y-Maze, whether the bee initially chose the left or right arm of the apparatus.
- Correct 1st arm – if the bee initially selected the arm that contained the correctly configured pattern (CS+ arm).
- Direct flights – if the bee flew directly to a feeder without fixating at the patterns, recorded for both CS+ and CS- arms.
- Initial fixation point – where on the pattern the bee visited first (bottom shape, top shape, centre (feeder)), and similarly the shape type (CS+ referent, CS+ target, CS+ feeder, CS- referent, CS- target, CS- feeder). This included both fixation scans and the less common brief inspections.
- Flight transitions – which transitions the bee made between the possible fixation locations (CS+ referent, CS+ target, CS+ feeder, CS- referent, CS- target, CS-

feeder). Both brief inspections and fixation scans of a location were recorded as a transition.

5.4 Results

5.4.1 Experimental issues (sample size and video analysis)

Due to the 2015 British summer being one of the wettest on record, as well as the long training protocols required for this experiment, many of the days in August and September allocated for this project were unsuitable for honeybee training. In total eleven bees, which regularly frequented the mass feeder, were selected and individually trained to visit the Y-Maze apparatus. Unfortunately, due to further thunderstorms during the training procedures, five of these eleven bees never returned to the Y-Maze during phase 1 pre-training, and a further two bees were lost whilst I was conducting the phase 2 training. One trained bee was excluded from subsequent video analysis because it always chose the left arm of the Y-Maze and almost always entered the left feeder tube, irrespective of the stimuli presented. This study therefore consists of the three bees that completed the full experimental protocol, including the non-rewarding control tests with novel target shapes. Two of these bees were conditioned with the ‘below’ pattern configuration being rewarding (named [Below_A] and [Below_B]), and the remaining bee trained on the ‘above’ condition (named [Above_A]).

It was initially presumed that detailed flight-path reconstruction of the honeybee flight trajectories would be necessary to assess how the bees were observing the ‘above and below’ stimuli. Paradoxically, given the effort establishing multiple camera views and video synchronisation, this was unnecessary for both the training and test trials. In just 9, out of the 150, recorded phase 2 training flights did the honeybees’ stop

approaching a pattern whilst midway down one of the Y-Maze arms and subsequently fly to the other arm. In all other cases the bees flew to the end of a Y-Maze arm and fixated a small distance from the presented stimuli. 488 of these fixation scans were directly in front of one of the referent shapes, target shapes, or feeder tubes. Out of all 150 training trials there were just 28 occasions where the bees appeared to fly towards a particular pattern shape but altered their flight direction without a full fixation scan. These simple and consistent flight behaviours allowed all 150 training trials and the six test trials to be analysed using just video annotations (see Methods).

5.4.2 Individual performances

During Phase 1 (pre-training) all three bees consistently achieved $\geq 60\%$ correct choices in each consecutive set of 5 trials (due to technical issues with the cameras the first 5 trial results for [Below_A] were not available) (Fig 5.4a). The bees were subsequently subjected to a differential non-rewarding control test. This consisted of a same styled cross pattern versus a pattern with one of the five novel target shapes. Two of the bees ([Above_A], [Below_B]) both visited the cross pattern first, upon finding no reward in the feeders they re-inspected the crosses, then entered the feeders again. [Below_B] subsequently left the arena. [Above_A] flew to the other arm, inspected the novel bar shape and entered that patterns feeder, again after no reward it left the arena. In contrast, [Below_A] first flew to the novel grating pattern and instigated numerous fixation scans at the bottom centre of this shape, after 5 seconds it eventually tried the feeder (containing 30 μ l of water). It then spent an additional 10 seconds making fixation scans of the bottom centre and bottom left bars of the grating before visiting the other arm. It fixated at different points of the cross shape for over 10 seconds but never entered the

feeding tube. After the 45 seconds allocated for the test the bee had to be repeatedly shoed out of the Y-Maze as it attempted to revisit each arm.

For phase 2, the two bees trained on the ‘below’ protocol showed a correct choice accuracy of 80% for the first 10 trials (Fig 5.4b). However, their performances did slowly drop throughout the training regime to 65±5%. The ‘above’ bee ([Above_A]) only achieved 60% correct choice accuracy at the very end of the training (last 10 trials), with preceding blocks of 10 trials averaging from 30-50%. Full flight transition details can be found at the end of the chapter (Section 5.6).

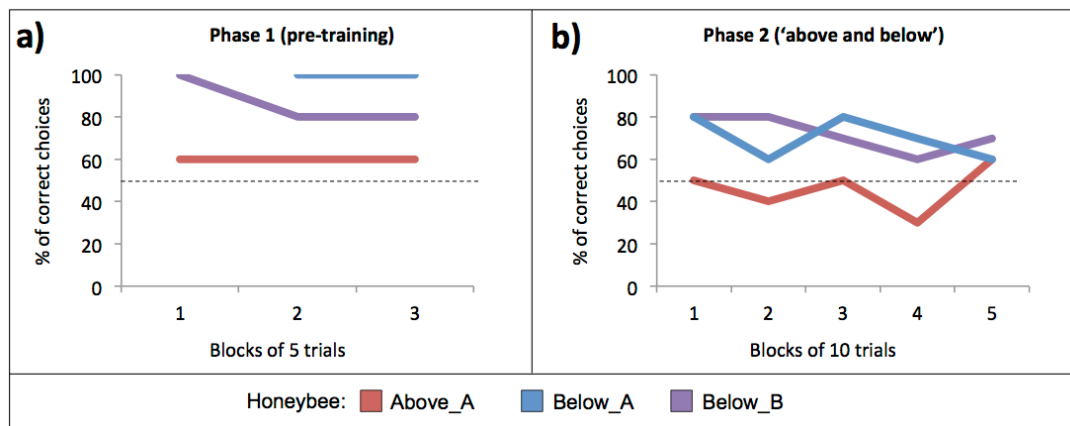


Figure 5.4 Individual honeybee performances for the ‘above and below’ experiments. **(a)** Phase 1 (pre-training): acquisition curves during an absolute conditioning protocol using a rewarding cross pattern and a blank distractor (percentage of correct choices as a function of blocks of five trials). **(b)** Phase 2 (‘above and below’ training): acquisition curve during training (percentage of correct choices as a function of blocks of ten trials). Bees had to, either, select the pattern where the target shapes were always below the crosses ([Below_A]: blue line, [Below_B]: purple line), or in the reverse configuration select the pattern where the targets were always above the crosses ([Above_A]: red line).

After the 50 training trials the bees were subjected to two 45 second non-rewarding control tests (with three refresher training trials between tests). [Above_A]’s first feeder tube choice was always that belonging to the correctly configured patterns. Accumulatively the bee chose these correct feeder tubes 71% of the time (novel target: bar, feeder visit sequence; 1st test: [+,+,+,+], 2nd test: [+,,-,-]). [Below_A] refused to

enter either of the feeder tubes during the entire 45 seconds of the 1st test (novel target: grating). During the 2nd test it entered the incorrect 'above' pattern's feeder tube just once. The other bee ([Below_B]) entered the feeder tubes of the correctly configured pattern as its first selection during both control tests. However, for this bee, accumulative feeder visits showed only a 50% and 60% preference for the correctly configured pattern after each of the two 45 second tests (novel target: diamond, 1st test: [+,-,-,+,-,-,+], 2nd test: [+,-,+,-,-]).

In summary, the bees' showed 64% choice accuracy for the correctly configured patterns. The choice accuracy remained at 63.3% for the last ten choices of training. Interestingly, choice accuracy during the entire training was significantly poorer for [Above_A], where overall more wrong choices were recorded (46% correct), while the other two bees ([Below_A], [Below_B]) resulted in clearly more correct than wrong choices (average of 73% correct choices). However, at the end of the training the bees performed consistently $\geq 60\%$ accuracy across all bees. In addition, at the end of training [Above_A] showed an overall preference for the correctly configured patterns when tested with a novel target shape (71%), whereas the results for the two bees trained on the reciprocal 'below' condition were less definitive.

5.4.3 Flight analysis

Analysis of the initial flight paths showed that the bees initially went to the left arm of the Y-Maze 57% of the time. For the last 10 training trials of each bee the overall average was 53%, with [Below_B] choosing each arm equally, however, [Above_A] and [Below_A] showed a consistent side preference for the right and left arms

respectively (see Fig 5.5). These preferences did not, however, show any correlation to their correct choice performance.

If a bee initially visited the Y-Maze arm containing the rewarding pattern, the bee subsequently chose the rewarding feeder in this arm an impressive $94\pm 6\%$ of the time. By the end of training (last 10 trials) all bees attained 100% correct choices in this situation. In contrast, if the bees initially chose the wrong Y-Maze arm they only disregarded the current feeder, traversing to the other (rewarding) arm, during 35% of such trials. Here there was a large disparity between the bees. The bee trained on the above protocol only rejected the wrong arm once in the first half of training, but in the last 10 trials the bee ignored the incorrect feeder and went to the rewarding Y-Maze arm in 43% of the initial incorrect arm visits. Whereas both 'below' conditioned bees ([Below_A], [Below_B]) rejected 67% of incorrect patterns during the first 25 trials, but conversely this dropped to 20% and 25% respectively for the last ten trials.

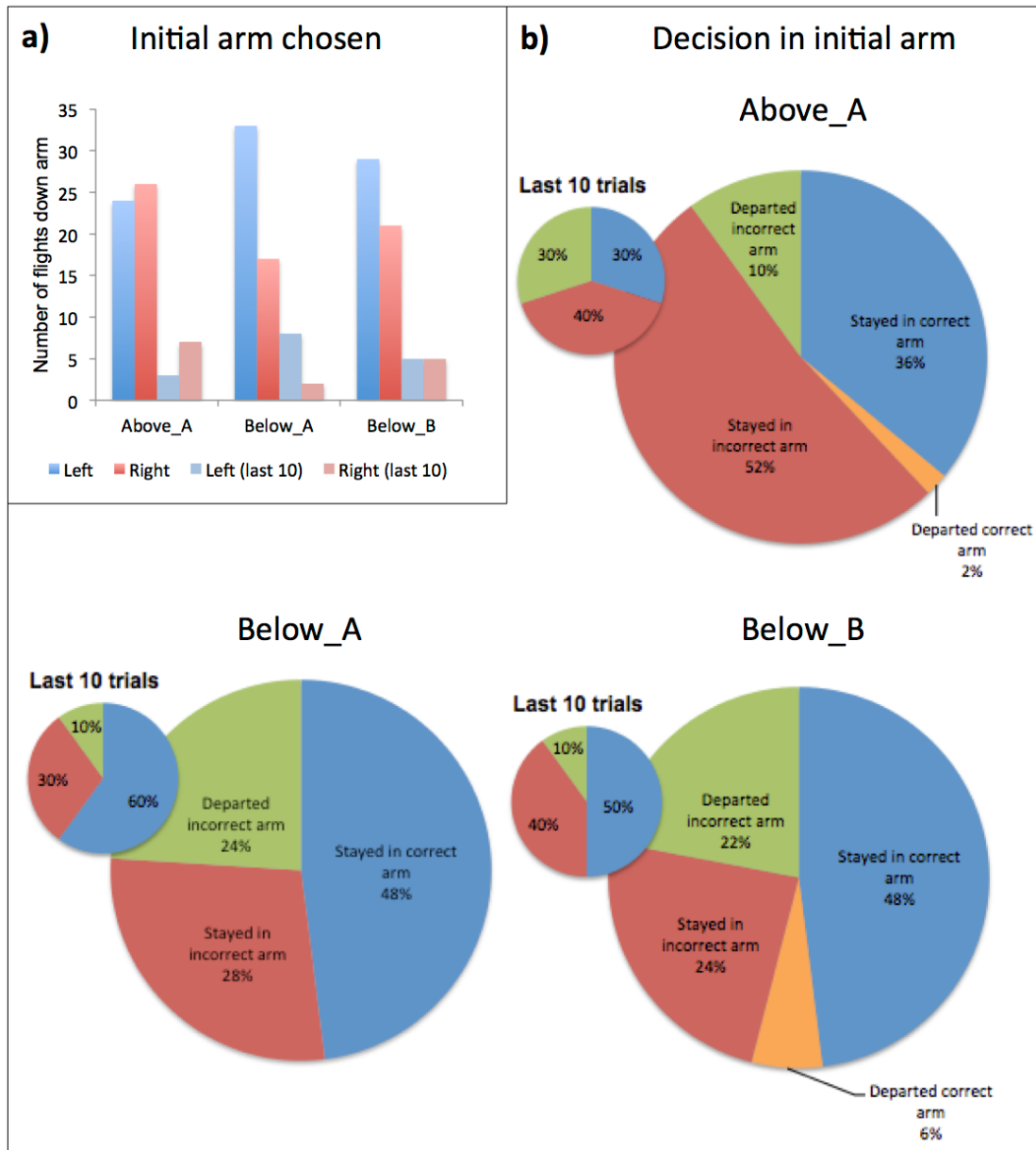


Figure 5.5 Honeybee initial arm choice and subsequent decision. **(a)** Number of times each bee chose the left and right Y-Maze arms, also shown number of choices in the last 10 trials. **(b)** Percentage of times the honeybees made a decision to stay or depart the initially chosen arm. If honeybees initially chose the rewarding arm they should have remained in that arm (blue), if they chose the unrewarding arm they should have departed that arm (green). Remaining in the unrewarding arm (red) or leaving the rewarding arm (orange) indicates the percentage of times the bees did not correctly solve the task. Insert shows percentages for last 10 trials.

Once the bees had approached a pattern, 77% of the stimulus scans commenced with a fixation of the bottom shape of the pattern (target or referent depending on the chosen arm). This behaviour consolidated towards the end of the training with 86% of

the last ten choices showing a fixation to the bottom shape. While this behaviour was overall less prominent in the [Below_A] compared to the other two bees, no such differences could be found towards the end of the training where [Below_A] again showed a high proportion of approaches and fixations at the bottom shape on the patterns (Fig 5.6).

Out of the last 30 trials (last 10 from each bee), on only two occasions did a bee's initial fixation on the bottom shape of the correct pattern, not immediately precede the bee going to the correct feeder (Table 5.1). In these exceptions, [Below_B] went to fixate at the top shape in the current pattern before entering the correct feeder, whereas [Below_A] visited the same shape on the other arm (top shape) before returning to this bottom shape again and finally choosing the correct feeder. Similarly, fixations on the bottom shape of the incorrect pattern were only followed by a fixation on that pattern's top shape, on two occasions.

After departing from the rewarding feeder tube, the bees would most often simply leave the flight arena, on a rare occasion they did briefly fixate on the bottom shape before leaving. Conversely, where bees chose incorrectly and were presented with quinine solution in the feeder, they would exit the feeding tube and proceed to fixate at length at both the bottom and top shapes, with repeated transitions between the presented shapes, they would also on occasion re-enter the incorrect feeder (Table 5.1). Only after these fixation scans would the bees finally leave this unrewarding arm and visit the other Y-Maze arm. Even during the last 10 trials of each bee, only four out of eleven visits to the wrong feeder were followed by a direct flight to the apposing arm.

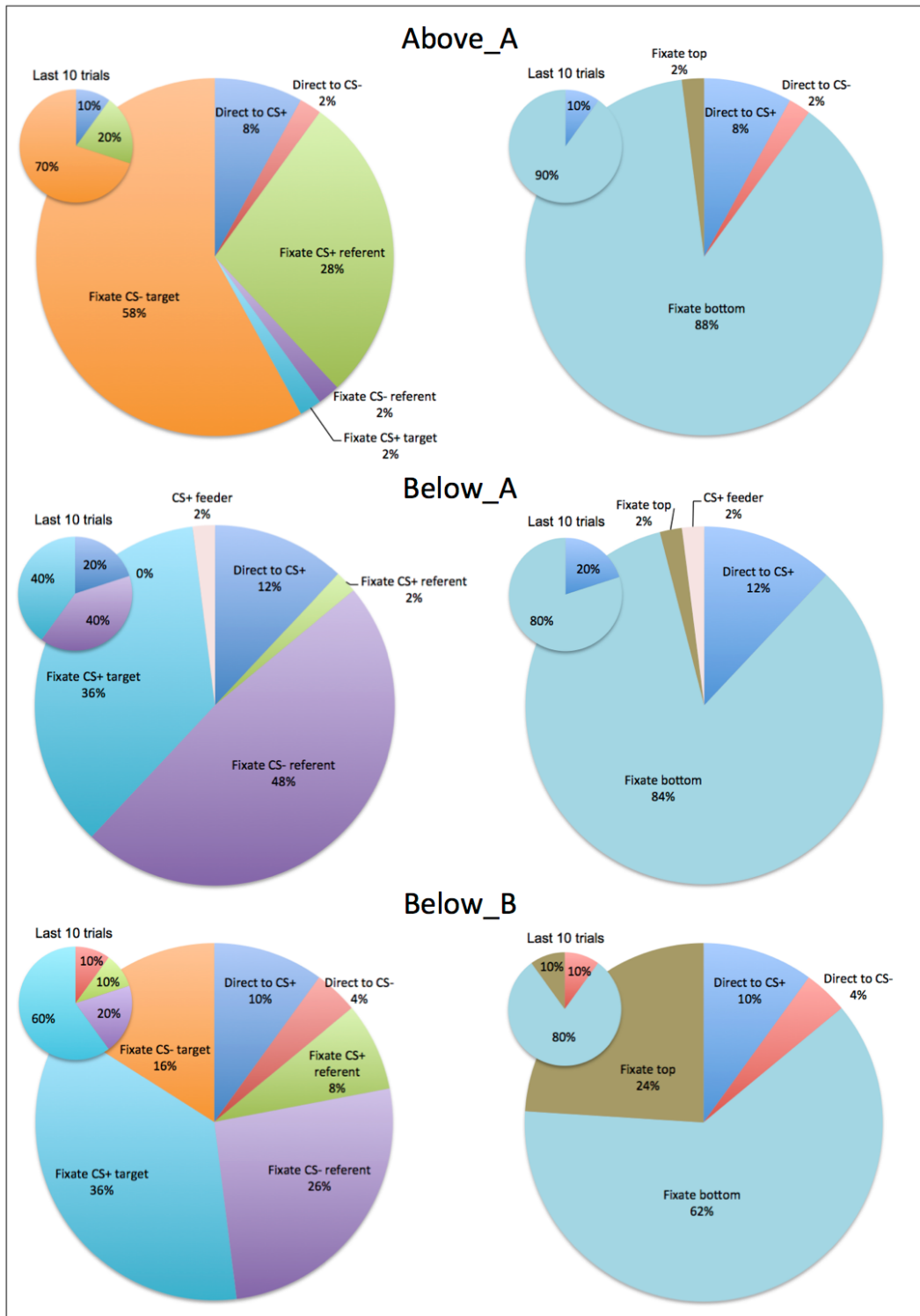


Figure 5.6 Honeybee initial fixation point during above and below experiments. All bees initially inspected the bottom shape of the pattern more often than the top shape or central feeding tube (right). This was independent of whether it presented the referent shape (cross) or one of the target shapes (left).

Transition	[Above_A]	[Below_A]	[Below_B]
Total fixation count	161	160	167
CS+ target => CS+ referent	7 => 0	39 => 4	37 => 4
CS+ referent => CS+ target	43 => 5	6 => 0	6 => 3
CS+ target => CS+ feeder	7 => 4	39 => 34	37 => 31
CS+ referent => CS+ feeder	43 => 35	6 => 5	10 => 6
CS- target => CS- referent	45 => 1	26 => 3	21 => 0
CS- referent => CS- target	16 => 3	25 => 10	19 => 6
CS- referent => CS+ arm	16 => 10	25 => 2	19 => 4
CS- target => CS+ arm	45 => 12	26 => 11	21 => 15
CS- feeder => CS+ arm	27 => 9	19 => 9	18 => 5

Table 5.1 Flight transition counts for honeybee ‘above and below’ experiments. Values (total number of fixations at 1st shape) => (number of transitions from 1st shape to fixate at 2nd shape).

5.4.4 Hypotheses comparison

The first and second hypotheses of my modelling work in Chapter 4 suggested that, the probability of the Y-Maze arm the bees initially chose upon entering the flight arena, being the correct rewarding arm, should be no more than chance. Additionally, I predicted that the bees would fixate at one, or more, of the different shapes on the patterns before making a final decision on which feeder tube to enter. In just 13% of the trials did the bees fly directly to a feeder, although of these, 80% were in fact the correct

choice. In all other trials, the bees first flew down one or other arms of the Y-Maze and fixated at either the referent or target shapes. Overall results showed that the bees went initially to the correct arm just 47% of the time, equally, during the last 10 trials of each bee, they also, on average, achieved only 47% correct arm choices.

The third hypothesis stated, “If a bee were to fixate in front of the target shape first, it should then move to fixate in front of the current pattern’s referent”. The flight transition analysis did not support this conjecture. Only 7% of all fixations in front of a target were followed by a flight and new fixation in front of the same pattern’s referent, a highly significant discrepancy to the hypothesis. Furthermore, this harsh discrepancy to the prediction was found across all bees, and was also independent of whether the target in question was on the CS+ or CS- stimuli.

The final two hypotheses declared that after a fixation at the referent of the rewarding pattern (CS+ referent) the bee should choose that pattern’s feeder (CS+ feeder). Correspondingly, if at the referent of the unrewarding pattern the bee should fly to the other Y-Maze arm. The [Above_A] bee (trained using ‘above’ protocol) did indeed traverse from the CS+ referent to the CS+ feeder after 81% of all its CS+ referent fixations. The two bees trained using the ‘below’ configuration also transitioned as expected $\geq 60\%$ of the time, however, in total they only fixated at the CS+ referents on 16 occasions out of all 327 fixation events ($< 5\%$). This compared markedly to [Above_A]’s 27% proportion of fixations on CS+ referent. A similar dichotomy was seen in the CS- referent fixations. In all three bees there were just 16-25 fixations of the CS- referent ($12 \pm 3\%$ of each bees’ fixations), [Above_A] transitioned 63% of the times to the opposing arm, whereas the other two bees ([Below_A], [Below_B]) transitioned just 8% and 21% of the times respectively.

Overall, the behavioural data collected supported hypothesis 1 and 2, refuted hypothesis 3, and showed a substantial variation, compared to the consistent behaviour anticipated from my modelling, depending on whether the bees were trained using the ‘above’ or ‘below’ protocols.

5.5 Discussion

There is evidence that bees are able to successfully learn to select the correctly spatially configured stimuli (Avargues-Weber, Dyer et al. 2011, Perry and Barron 2013). Here, I wished to investigate *how* honeybees solve the task. Despite the limited sample size (see Results) all of the bees analysed in the study achieved $\geq 60\%$ correct choices at the end of the training (last 10 trials). By careful analysis of the bees’ flight behaviour for all 150 training bouts I unveiled a new insight into the honeybees’ behaviour. Although confirming the core hypotheses formed in my previous modelling chapter (Chapter 4) that honeybees would not require the conceptualisation of ‘above’ and ‘below’ spatial arrangements to solve this task, the honeybees tested here found a simpler, but analogous, technique to that proposed by my models. This provides a sublime explanation of how honeybees, and potentially other animals, may approach the problem. Remarkably, it appears that the bees would need to employ nothing more than stereotypical flight trajectories, and the most simple of discrimination abilities.

Overall the analysis of the bees’ flight paths suggest that, other than a few instances, the bees could not (or chose not to) make the correct choice from the Y-Maze decision chamber, even though they were only a small distance (~15-20 cm) from the stimuli. A larger sample of examples would be required to see if there are any similarities in either the target shapes, or positions of the shapes on the patterns, when

bees choose to fly directly to a feeder. Nevertheless, this result is mostly consistent with my theoretical model research (Chapter 4), which suggested that the bees would need to approach and fixate at the patterns before making a final feeder selection. The next hypothesis was that after a bee approached a pattern it would identify the constant referent shape (in both my modelling and behaviour experiments this was always a cross shape) from the presented target shape. The bees showed a highly significant preference for first fixating at the shapes presented at the bottom of the patterns, not contrary to my models that had no predefined order in which order the shapes should be viewed. This is also not that unexpected as Morawetz et al. showed bees are better at discriminating cues in the ventral region of their field of view (Morawetz, Chittka et al. 2015), so it would make sense for bees to attend to these areas first. However, when bees first viewed the target shape, my models suggested that the bee should then move to fixate in front of the referent. This turned out not to be the case, with these particular transitions occurring only four times across all three bees. Fortunately, this behaviour also demonstrated a new strategy for solving the task. My modelling predicted that bees would use a consistent fixation point before making a decision, I assumed this to be the cross shape as it would provide a consistent discriminable feature (Chapter 4.5, Fig 4.5). However, if, as shown by the bees, the lowest shape on the pattern should be this fixed initial fixation point then my models can be reconfigured to centre their field of views at these lowest shapes. Since this task is now simply a discrimination task between a cross and potentially any of the other 5 target shapes, my modelling work in Chapter 4 (Fig 4.1a) predicts the bees should achieve anywhere between 70% to 85% during training dependent on the particular shapes presented and 63-77% and 80-91% during the final generalisation test depending on the model DISTINCT or SEO_AB respectively. The DISTINCT model's performance would be more invariant to the exact distance from

the observed shapes and therefore likely to be a better, or at least more consistent, indicator of reward. These DISTINCT results are indeed very reminiscent of the empirical results of the original honeybee experiments (Avargues-Weber, Dyer et al. 2011), if slightly higher than my own honeybee results (possibly due to reasons discussed later in this chapter).

Supportive to this assumption, is that during the honeybee training, after viewing the bottom shape of the rewarding pattern all three bees would subsequently chose the correct feeder (in all but four cases overall, and always during the last 10 trials). It appears that if presented with a shape at the bottom they previously found to be rewarding they could make an instant decision without inspecting the rest of the pattern. For the ‘above’ conditioned bee this is theoretically an easier assessment, as the bottom shape must always be a cross. For the ‘below’ conditioned bees they must recognise the four possible target shapes that could be displayed at the bottom of the rewarding pattern, or conversely learn if the shape is **not** a cross then it must be the rewarding stimulus. This may potentially explain the differences seen during the control tests between the two ‘below’ conditioned bees. [Below_A] when presented with the novel grating patterns during the first unrewarded control test refused to enter either of the feeding tubes, in this case neither the grating nor the cross would be associated with reward. This bee repeatedly returned to the decision chamber to fixate at the Y-Maze entrance (something not seen during training trials, as if it was unsure it was in the correct location), before re-inspecting each pattern. In contrast, [Below_B] exhibited a similar behaviour to that seen during the normal training trials. During the first test it entered the Y-Maze and chose the ‘below’ configured arm, fixated at the novel diamond shape then went to the feeder. In the second trial on numerous occasions it would approach the ‘above’ configured pattern (with the cross at the bottom) and then abandon

a feeder visit and return to the other arm, although interestingly within this correct arm it did fixate more at the top positioned cross shape, perhaps having already learnt that the diamond was not an indicator of reward.

When the bees initially entered the wrong Y-Maze arm and fixated at the bottom shape on the patterns, you would think the decision process would be the same as described above; is the pattern a cross, or known target shape (depending on the protocol), if not then fly to the other Y-Maze arm. Yet, in two thirds of such trials this did not occur. In these circumstances the bees most often flew and entered the incorrect feeder. It is possible that the bees simply choose to try this feeder since they were already close to it. Potentially being a more optimal strategy than expending energy flying to the other Y-Maze arm, only to have to return if it was incorrect. Indeed, the second 'above' bee, excluded from my analysis, in every trial went initially to the left arm, and almost always tried the feeder, if unrewarding it simply flew directly to the other feeder. However, this does not then explain why the bees would spend time fixating at the pattern shapes after they had already ascertained it was the wrong arm, a consistent behaviour seen even towards the end of the training. It may simply be that when observing a correct bottom shape the bees have high confidence that it is a rewarding stimulus, but when an incorrect shape is observed the bees would have a lower expectation that it was rewarding (as should be the case) but still insufficient certainty of an incorrect stimulus to breach some internal threshold, forcing the bee to try the feeder anyway. Although I used quinine solution as a punishment if the bees chose the wrong feeder, this may not have been a sufficient disincentive for bees to learn to avoid the negative patterns. The use of quinine itself was due to previous research (Avargues-Weber, de Brito Sanchez et al. 2010) that showed that the simple absence of reward reduced the effective learning rate of bees in Y-Maze binary choice

experiments, compared to association with a punishment (Chittka, Dyer et al. 2003). Previous honeybee studies have addressed this problem using a different training procedure (Si, Zhang et al. 2005, Stach and Giurfa 2005). In these protocols the bees were removed from the Y-Maze if they made a wrong choice, they would then have to fly outside the flight arena and return to the Y-Maze entrance to begin a new trial. In this way the bees not only had a further distance to fly, but could also make multiple wrong choices in a row. In doing so this may focus the bees' attention onto making accurate initial choice selections. Unfortunately, given the videography requirements of my experiment, the flight arena I used did not have a top cover, thus making this alternative procedure unachievable as the bees could simply fly back in. Hopefully, with the rapid development of high-speed camera sensors and miniature rigs, designed primarily for virtual reality capture systems, it should soon be possible to track the bees in a Y-Maze even with a top cover installed. It would therefore be interesting to see if the bees' performance and especially their behaviour change if they cannot simply fly to the other arm after incorrect choices.

The experiments replicated in this study were adapted from Experiment 2 of the original 'above and below' publication (Avargues-Weber, Dyer et al. 2011). Although no one would expect two studies to produce identical data, there were some notable differences between their results and my own (even accounting for my limited sample size). Avargues-Weber et al. found a marked improvement in performance of their bees towards the end of the training; with their bees reaching approximately 80% correct choice accuracy in the last two 5 trial blocks. Similar performances were seen in their Experiment 1, which used a long black bar as the referent. Perry and Barron (Perry and Barron 2013) who adapted this Experiment 1 also report performances of nearly 80% after just 30 training trials. In contrast, the three bees in this study only achieved 60-70%

at the end of their 50 training trials (although two bees reached 80% in the ‘below’ task in early training). However, there were some differences in the respective experimental setups. In the Perry et al. experiments the sucrose or quinine solutions were provided to the bees via small 5mm diameter tubes that protruded from the centre of the target shapes (although these were a common feature on both presented patterns so as not to be a useful indicator of reward). In the Avargues-Weber experiments similar protruding feeder tubes were used, in this case located in the centre of each pattern. Unfortunately, during a preliminary pilot-study using my apparatus I detected a problem with this arrangement. The first few bees trained in this setup would fixate very close to the patterns and the feeder tubes, high-speed recordings showed the bees antennae touching the tubes, and therefore potentially detecting the sucrose solution inside (Fig 5.2a). Bees would often depart the current arm even without landing at a feeder containing quinine solution, but most often land if the feeder contained sucrose. To prevent this I made two modifications. Firstly, the tubes were always centrally located in the patterns and were flush to the pattern face, secondly, that the tubes were always refilled via a small stopper attached to the feeding tubes from behind the stimuli and the respective removable back walls (Fig 5.1 insert). This procedure ensured that there was never any sucrose or quinine solution on the feeder tubes themselves, which in turn obligated the bees to crawl inside the tubes to get at the solutions (Fig 5.2b). Conveniently, this also allowed me to easily identify and record a definitive pattern choice, as well as the flush feeder tubes preventing the bees from being obscured during filming. It must be stressed, that this is not to say that the bees in the previous studies were detecting the sucrose before landing, or indeed that there were errors reporting feeder choices. The slightly lower performances I report here may simply be because the bees had to fly to a separate location to get reward after fixating on the pattern shapes, compared to Perry et

al. (Perry and Barron 2013); but beneficially, this again made determining the direct-to-feeder choices easier. Additionally bees had to be physically inside the feeder tubes, and consequently could not look directly at the stimuli, when they got reward. These factors being taken into account, the stimuli would still look identical to the bees in both setups, and the bees in this study were still able to solve, an arguably, more complicated training task; with two out of the three bees also generalising to novel target shapes.

Anecdotally, while I was analysing the flight videos for this chapter, I would determine which arm was the CS+ by identifying the cross in a pattern and then seeing if the target shape was above or below this cross. This appeared to be a fast and efficient way to solve the problem. In the same way it was assumed that, baboons (*Papio papio*) (Depy, Fagot et al. 1999) and tufted capuchins (*Cebus apella*) (Spinozzi, Lubrano et al. 2004) learnt to identify presented ‘above and below’ stimuli during their experiments, and subsequently articulating their decisions either by moving a joystick in a corresponding direction (baboons), or sliding their hand into an appropriate hole on each side of the apparatus (capuchins), in order to attain a reward. My experiments show that the bees have identified an alternative, but effective, way of solving the ‘above and below’ task. Instead of having to ‘understand’ the complexity of individual shapes (i.e. having to identify the constant referent shape from the different, and potentially novel, target shapes) and subsequently having to evaluate the spatial relationship between these objects, this whole problem can be paraphrased as: “if I approach a previously rewarding location and fixate at the lowest region of black on a white background, is this perceived stimulus sufficiently similar to that of a previously rewarding stimulus? If so, visit the feeding hole”. Although the primates in the mammalian studies cannot, obviously, fly to the bottom shape on the pattern, there seems no reason why their eyes cannot fixate on just the bottom shape of the presented

stimulus and, like the bees, simply determine if this shape is sufficiently similar to the referent (a long black bar in these experiments), or not. In the same way as the honeybees in my experiments, these primates may conceivably have learnt to determine the correct stimuli without using spatial relationships, instead utilising a much simpler discrimination task. In addition, since this method requires less of the patterns to be interrogated, it has the potential to also be faster than the solution that I used myself.

This study indicates that not all seemingly complex problems necessitate complex cognition. The ‘above and below’ task is often used as an example of a sophisticated relationship problem, where you have to identify multiple (potential novel) objects and assess how they are spatially aligned with each other. However, the honeybees in my experiment demonstrated this to be a relatively simple discrimination task. By following their innate behaviour and inspecting whatever stimuli was at the bottom of the patterns they could solve the task without ever needing to understand, or even recognising, that the problem had a more complicated underlying rule. This does not prove that honeybees can, or cannot, solve spatial relationship problems - but simply that this particular task can be very easily solved, at least when an appropriate choice strategy is used.

5.6 Individual flight transition details

Above A

Trial	CS+ Side	Target	1st arm	Correct	Flight Transitions
1	left	diamond	* left	1	cs- target, cs- feeder - BI, cs- target, cs+ feeder
2	right	grating	right	1	cs+ feeder
3	left	disc	left	1	cs+ cross, cs+ feeder
4	right	trefoil	left	0	cs- cross, cs- feeder, cs- target, cs+ target, cs+ feeder

5	left	grating	right	0	cs- target, cs- feeder, cs- target, cs- cross, cs+ cross, cs+ target, cs+ feeder
6	right	disc	left	0	cs- target, cs- feeder, cs+ cross, cs+ feeder
7	left	diamond	right	0	cs- target, cs- feeder, cs- cross, cs+ cross, cs+ feeder
8	right	grating	right	1	cs+ cross, cs+ feeder
9	left	trefoil	left	0	cs+ cross - BI, cs- target, cs- feeder, cs- cross, cs+ cross, cs+ feeder
10	right	disc	left	1	cs- target, cs- cross, cs- feeder - BI, cs+ cross, cs+ feeder
11	left	diamond	left	1	cs+ cross, cs+ feeder
12	left	grating	left	1	cs+ cross, cs+ feeder
13	left	disc	right	0	cs- target, cs- feeder, cs- cross, cs+ cross, cs+ feeder
14	left	trefoil	right	0	cs- target, cs- feeder, cs+ cross, cs+ feeder
15	left	diamond	right	0	cs- target, cs- feeder, cs+ cross, cs+ feeder
16	right	grating	left	0	cs- feeder, cs- cross, cs- target, cs+ cross, cs+ feeder
17	right	disc	right	1	cs+ cross, cs+ feeder
18	left	diamond	right	0	cs- target, cs- feeder, cs+ cross - BI, cs+ feeder
19	right	trefoil	left	0	cs- target, cs- feeder, cs+ cross, cs+ cross, cs+ feeder
20	left	diamond	left	1	cs+ cross, cs+ feeder
21	right	trefoil	left	0	cs- target, cs- feeder, cs- cross, cs- target, cs+ cross, cs+ feeder
22	right	disc	right	1	cs+ cross, cs+ feeder
23	left	grating	right	0	cs- target, cs- feeder, cs- target, cs- target, cs+ cross, cs+ feeder
24	left	trefoil	left	1	cs+ cross, cs+ feeder
25	right	diamond	right	1	cs+ cross, cs+ target - BI, cs+ feeder
26	right	grating	right	1	cs+ cross, cs+ feeder
27	left	disc	right	0	cs- target, cs- feeder, cs- cross, cs- target, cs+ cross, cs+ feeder
28	right	diamond	left	0	cs- target, cs- feeder, cs+ feeder
29	left	trefoil	right	1	cs+ cross, cs+ target, cs- target, cs- feeder, cs- target, cs+ cross, cs+ target, cs+ feeder
30	right	grating	left	0	cs- target, cs- feeder, cs+ cross, cs+ feeder
31	left	diamond	right	0	cs- target, cs- feeder, cs+ feeder
32	right	disc	left	0	cs- target, cs- feeder, cs- target, cs+ cross, cs+ feeder
33	left	trefoil	right	0	cs- target, cs- feeder, cs+ cross, cs- target, cs+ cross, cs+ feeder
34	right	trefoil	left	0	cs- target, cs- feeder, cs- cross, cs+ feeder
35	right	disc	left	0	cs- target, cs- feeder, cs- cross, cs+ feeder
36	left	trefoil	left	1	cs+ feeder
37	right	grating	left	0	cs- target, cs- feeder, cs- target, cs+ cross, cs+ feeder
38	left	diamond	left	1	cs+ feeder
39	right	diamond	right	1	cs+ cross, cs+ feeder
40	left	disc	right	0	cs- target, cs- feeder, cs- cross, cs+ cross, cs+ feeder
41	right	grating	left	0	cs- target, cs- feeder, cs- cross, cs+ cross, cs+ target, cs+ cross, cs+ feeder
42	right	trefoil	right	1	cs+ feeder
43	right	disc	right	1	cs+ cross, cs+ feeder

44	left	disc	right	1	cs- target, cs+ feeder
45	right	diamond	left	1	cs- target, cs+ feeder
46	right	grating	left	0	cs- target, cs- target, cs- feeder, cs+ cross, cs+ feeder
47	left	disc	right	0	cs- target, cs- feeder, cs- cross, cs+ cross, cs+ feeder
48	left	trefoil	right	0	cs- target, cs- feeder, cs- cross, cs+ cross, cs+ feeder
49	left	trefoil	right	1	cs- target, cs- cross, cs- feeder - BI, cs+ cross, cs+ feeder
50	right	grating	right	1	cs+ cross, cs+ feeder

Table 5.2 Individual flight transitions for honeybee Above_A. * left / * right – indicates honeybee only flew half way down an arm before turning and flying to the opposite arm. BI: Brief inspection.

Below_A

Trial	CS+ Side	Target	1st arm	Correct	Flight Transitions
1	left	bar	right	1	cs- cross, cs- target, cs+ target, cs+ feeder
2	right	diamond	left	1	cs- cross, cs- target, cs+ target, cs+ feeder
3	left	trefoil	left	1	cs+ cross, cs+ feeder
4	right	disc	* left	1	cs+ target - BI, cs+ feeder
5	left	bar	left	1	cs+ feeder - BI, cs+ target, cs+ feeder
6	left	trefoil	right	0	cs- cross - BI, cs- feeder, cs- target, cs+ target, cs+ feeder
7	right	diamond	right	1	cs+ target, cs+ feeder
8	right	bar	left	1	cs- cross, cs- feeder - BI, cs- target, cs+ target, cs+ feeder
9	left	trefoil	left	1	cs+ target, cs+ feeder
10	right	disc	right	0	cs- cross, cs- feeder - BI, cs- target, cs- feeder, cs+ feeder
11	right	diamond	left	0	cs- cross, cs- feeder, cs- target, cs- feeder, cs- cross, cs+ target, cs+ feeder
12	left	trefoil	left	1	cs+ target, cs+ feeder
13	right	bar	left	1	cs- cross, cs- feeder - BI, cs- target, cs+ target, cs+ feeder
14	left	diamond	left	1	cs+ target, cs+ feeder
15	right	disc	right	1	cs+ feeder
16	left	trefoil	right	0	cs- cross, cs- feeder, cs- target, cs+ target, cs+ feeder
17	right	disc	right	1	cs+ target, cs+ target, cs+ feeder
18	right	trefoil	right	1	cs+ target, cs+ feeder
19	left	bar	left	0	cs+ target, cs+ cross, cs- feeder, cs+ target, cs+ feeder
20	right	trefoil	left	0	cs- cross, cs- target, cs- feeder, cs- target, cs+ feeder
21	left	disc	left	1	cs+ target, cs+ feeder
22	right	bar	left	0	cs- cross, cs- feeder, cs+ target, cs+ cross, cs+ feeder
23	left	diamond	left	1	cs+ feeder
24	right	disc	right	1	cs+ feeder, cs+ cross, cs+ feeder
25	right	trefoil	left	0	cs- cross, cs- feeder, cs- target, cs+ target, cs+ feeder

26	left	diamond	left	1	cs+ feeder
27	left	bar	right	1	cs- cross, cs- target, cs- feeder - BI, cs+ feeder
28	right	trefoil	left	1	cs- cross, cs- target, cs+ target, cs+ feeder
29	left	diamond	left	1	cs+ target, cs+ feeder
30	right	disc	right	1	cs+ target, cs+ cross, cs+ feeder
31	left	bar	* left	0	cs- cross, cs- target, cs- feeder, cs+ target, cs+ feeder
32	right	disc	right	1	cs+ target, cs+ feeder
33	right	diamond	left	0	cs- cross, cs- feeder, cs- target, cs- feeder, cs+ feeder
34	left	trefoil	right	1	cs- cross, cs- target, cs- feeder - BI, cs+ target, cs+ feeder
35	left	diamond	left	1	cs+ target, cs+ feeder
36	right	bar	left	1	cs- cross, cs+ feeder
37	left	disc	right	1	cs- cross, cs- target, cs+ target, cs+ feeder
38	right	bar	right	1	cs+ target, cs+ feeder
39	left	disc	* left	1	cs- cross, cs- feeder - BI, cs+ target, cs+ feeder
40	right	trefoil	left	0	cs- cross, cs- target, cs- feeder, cs+ feeder
41	right	disc	* left	1	cs+ target, cs+ feeder
42	left	diamond	right	0	cs- cross, cs- target, cs- feeder, cs+ target, cs+ feeder
43	right	bar	left	0	cs- cross, cs- feeder, cs- target, cs+ target, cs+ feeder
44	left	trefoil	left	1	cs+ feeder
45	right	diamond	left	0	cs- cross, cs- feeder, cs- target, cs- feeder, cs+ target, cs+ feeder
46	left	disc	left	1	cs+ feeder
47	right	trefoil	left	0	cs- cross, cs- feeder, cs+ target, cs+ feeder
48	right	bar	right	1	cs+ target, cs+ feeder
49	left	diamond	left	1	cs+ target, cs+ cross, cs+ feeder
50	left	trefoil	left	1	cs+ target, cs+ feeder

Table 5.3 Individual flight transitions for honeybee *Below_A*. * left / * right – indicates honeybee only flew half way down an arm before turning and flying to the opposite arm. BI: Brief inspection.

Below_B

Trial	CS+ Side	Target	1st arm	Correct	Flight Transitions
1	right	bar	left	1	cs- target, cs+ feeder
2	left	trefoil	right	1	cs- cross, cs- target, cs+ target, cs+ feeder
3	right	disc	left	0	cs- target, cs- feeder, cs+ feeder
4	left	bar	left	1	cs+ target - BI, cs+ feeder
5	right	disc	left	0	cs- target, cs- target, cs- feeder, cs+ cross, cs+ feeder
6	right	bar	right	1	cs+ target, cs+ feeder
7	left	disc	left	1	cs+ cross, cs+ target, cs+ feeder

8	left	grating	left	1	cs+ cross, cs+ target, cs+ feeder
9	right	bar	left	1	cs- target, cs- feeder - BI, cs+ target - BI, cs+ feeder
10	left	trefoil	left	1	cs+ feeder
11	right	grating	right	1	cs+ feeder
12	right	disc	right	1	cs+ cross, cs+ feeder
13	left	trefoil	right	0	cs- cross, cs- feeder, cs- target, cs- feeder, cs+ feeder
14	left	grating	left	1	cs+ feeder
15	right	disc	left	1	cs- target, cs- cross, cs+ target, cs+ feeder
16	left	bar	left	1	cs+ target, cs- cross, cs+ feeder, cs+ target, cs+ feeder
17	right	trefoil	right	1	cs+ target, cs+ feeder
18	left	grating	right	0	cs- cross, cs- feeder, cs- target, cs+ feeder
19	right	disc	right	1	cs+ target - BI, cs+ feeder
20	left	grating	left	1	cs+ target, cs- cross, cs+ target, cs+ cross, cs+ feeder
21	left	disc	left	1	cs+ target - BI, cs+ feeder
22	right	trefoil	left	1	cs- cross, cs+ feeder
23	left	disc	right	0	cs- cross, cs- feeder, cs- target, cs+ target, cs+ feeder
24	left	trefoil	left	1	cs+ target, cs+ feeder
25	right	bar	left	0	cs- target, cs- feeder, cs- target, cs+ target, cs+ feeder
26	right	grating	left	1	cs- cross, cs- target, cs+ target, cs+ cross, cs+ feeder
27	left	disc	right	1	cs- cross, cs- target, cs+ cross, cs+ feeder
28	right	bar	left	0	cs- cross, cs- feeder, cs- target, cs+ target, cs+ cross, cs- feeder, cs+ feeder
29	right	trefoil	* left	1	cs+ target, cs+ feeder
30	left	grating	right	1	cs- cross, cs- target, cs+ target, cs+ feeder
31	left	disc	left	1	cs+ target - BI, cs+ feeder
32	right	trefoil	right	1	cs+ feeder
33	left	bar	right	0	cs- feeder, cs- cross, cs- target, cs+ target - BI, cs+ feeder
34	right	grating	right	1	cs+ target, cs+ feeder
35	right	trefoil	left	1	cs- cross, cs- target, cs+ target, cs+ feeder
36	right	disc	left	0	cs- target, cs- feeder, cs- target, cs- cross, cs+ feeder
37	right	bar	left	0	cs- target, cs- cross, cs- feeder, cs- target, cs- feeder
38	left	grating	right	0	cs- cross, cs- feeder, cs- target, cs+ target, cs+ feeder
39	right	bar	* left	1	cs+ feeder
40	right	trefoil	right	1	cs+ target, cs+ cross, cs+ feeder
41	left	grating	left	1	cs+ target - BI, cs+ feeder
42	left	trefoil	right	0	cs- feeder, cs- target, cs+ feeder
43	left	bar	right	0	cs- cross, cs- feeder, cs- target, cs+ target, cs+ feeder
44	right	grating	right	1	cs+ target - BI, cs+ feeder
45	right	trefoil	right	1	cs+ target, cs+ feeder
46	left	bar	left	1	cs+ target, cs- target, cs+ target, cs+ feeder

47	right	disc	right	1	cs+ target - BI, cs+ feeder
48	right	bar	* left	1	cs+ cross, cs+ target, cs+ feeder
49	left	trefoil	left	1	cs+ target - BI, cs+ feeder
50	right	bar	left	0	cs- cross, cs- feeder, cs+ target, cs+ feeder

Table 5.4 Individual flight transitions for honeybee *Below_B*. * left / * right – indicates honeybee only flew half way down an arm before turning and flying to the opposite arm. BI: Brief inspection.

Chapter 6: General discussions

In what follows, I pull together the modelling and behavioural findings from the previous four chapters to highlight how remarkably simple mechanisms within the honeybee brain appear to successfully process visual information over a diverse range of tasks.

6.1 Main findings

Over the course of this thesis I have described a large variety of achromatic pattern experiments that had previously been performed on honeybees. The lobula large-field orientation-sensitive neurons (LOSNs) (Maddess and Yang 1997) studied here have proved remarkably versatile at identifying almost all of the CS+ patterns taken from previous honeybee experiments, but equally interesting, is that they also failed on some of the experiments that bees themselves failed to discriminate. Obviously, the LOSNs will not be the only optic neurons that a honeybee needs; future work will need to ascertain what neurons in addition to these LOSNs might be necessary for symmetrical and non-symmetrical pattern discriminations (Giurfa, Eichmann et al. 1996, Lehrer 1999, Rodriguez, Gumbert et al. 2004), topological pattern recognition (Chen, Zhang et al. 2003), to name but a few. Nevertheless, despite these LOSNs providing virtually no useful retinotopic information, their functional capability within a miniature brain is astonishing; not only do they provide sufficient neuronal response specificity to discriminate fine angles ($\sim 30^\circ$ angle differences) as seen in bees (Sathes chandra, Geetha et al. 1998), but they can also discriminate the small changes in length of the

edge; allowing the discrimination of pairs of almost identical horizontal bars, until now thought to require an eidetic image memory (Giger and Srinivasan 1995). Furthermore when these LOSNs are wired into the mushroom body learning centres, using only a single layer of connections, their cognitive flexibility is substantially enhanced. By combining the LOSNs with different numbers of excitatory and inhibitory synapses onto the Kenyon cells (which is realistic given the structured layers of the mushroom bodies (Ehmer and Gronenberg 2002)) the models showed that fine discrimination (using Chapter 2 model: SEO_AB), stimuli size invariance (Chapter 2 model: EAI_AB), horizontal location invariance (Chapter 3 model: MERGED), but perhaps most notable, generalisation to more complicated oriented patterns composed of multiple orientations and edge lengths (Chapter 3 model: DISTINCT) was all possible with no ‘tweaking’ of the model parameters for particular stimuli. The honeybee brain truly does exemplify both simplicity and elegance. For example, the most straightforward model solution to horizontal location invariance – was simply combining sensory inputs from both eyes, and indeed the anatomical structure of the mushroom bodies shows this is not only possible but almost certain (Ehmer and Gronenberg 2002). However, this summation of inputs would render any chance of reconstructing a visual representation of the world impossible. My models still show that a large majority of the stimuli could be discriminated, but how could this be achieved?

Within the human medial temporal lobe (MTL) there exist neurons that fire selectively to images of particular human faces (Quiroga, Reddy et al. 2005). Some of the volunteers tested in these experiments have neurons that only respond to pictures of Jennifer Aniston, invariant to the rotation or view of this face. It is therefore easy to assume that a honeybee may learn to identify a particular flower species invariant to different views, and may even have a neuron that selectively fires for only one flower

species. Accordingly, every time the bee sees, for example, a daisy, a particular neuron fires, this may have been previously associated with reward and so the bee approaches, lands and feeds from the flower. But, does a honeybee require even this level of sophistication, given its miniature brain and specific behavioural requirements? My models show that very simple sensory inputs would allow the bee to discriminate a previously learnt rewarding stimulus from a multitude of other stimuli. Does the bee brain need to modify synaptic weights such that a particular neuron, or indeed a specific set of Kenyon cell responses only correspond to the exact features of a 'daisy', or simply evaluate if a given the stimulus has a sufficient Kenyon cell neuronal similarity to 'something' that was previously rewarding? In fact, there is no reason why different groups of Kenyon cell activations could not correspond to the same object. Imagine a honeybee in a Y-Maze; it may associate reward with a set of Kenyon cell responses (similar to the MERGED model configuration) while in free flight in the decision chamber, therefore choosing which arm to visit. However, these same Kenyon cells may not be a good indicator of reward close to the pattern, and a second set of responses may now be more similar to previous rewarding response when fixating at the patterns (like in the SEO_AB model), allowing a final decision of whether to land or not. Indeed this may explain why bees generalise to common features, rather than specific constant visual cues, after repeated training (Stach and Giurfa 2005). If a bee identifies a rewarding flower for the first time, the Kenyon cell responses, similar to both my SEO and EAI Kenyon cells, might initially be quite selective to that specific flower's visual cues, but with experience selectively prefer those responses that are inherently more generalised (as long as they still provided consistent indication of reward) and would therefore allow identification of conspecific flowers (see Chapter 2.5 discussion on discrimination of two horizontal bars). Once again simple mechanisms imposed by the

inherent structure of the miniature brain seem to produce an optimal adaption, in this case generalisation, without any necessity for neuronal complexity.

6.2 Model limitation and future work

LOSN responses

In this thesis I presented six very simple models (SEO_AB, SEO_ABC, EAI_AB, EAI_ABC, DISTINCT (same as EAI_AB) and MERGED). I found very little performance differences between the respective models using the two LOSNs based directly on the known LOSN responses (Maddess and Yang 1997) and theoretical three offset LOSN tuning curves, similar to that seen in dragonflies (O'Carroll 1993). The only notable exception was the EAI_AB model's worse performance during the very fine angle discrimination experiments (Chapter 2.4.2). Here, increasing the firing rates of the LOSNs, by progressively extending the length of the perceived oriented edges, produced ever better performance. Although some particular angles of oriented edges were never discriminated. This raises two questions; what effect would varying degrees of neuronal noise have on the models, and is there a functional advantage in having tuning curves with a large disparity of responses as seen between the type A (20-36Hz) and type B (3-14Hz) LOSN recordings?

For the former, within my models I applied a small amount of Gaussian noise to the LOSN and Kenyon cell synapses to account for variance in the synaptic neurotransmission and minor differences in the presentation of the stimuli. Electrophysiology on bumblebees has shown that neurons within the final layers of the lobula (layers 5-6) produce very precise phasic neuronal responses when presented with identical stimuli (Paulk, Dacks et al. 2009). Given the ~10-15Hz range of both the

LOSN types this high precision would be expected in order for these neurons to provide useful sensory data. I am currently researching how additional Poisson noise or perceptual noise (artefacts added to the presented stimuli) might affect the model performances, especially with the longer edge lengths and corresponding higher firing rates. Additional electrophysiology will eventually be required to fine-tune these parameters; of particular interest would be simultaneous multi-electrode recordings of both the type A and type B LOSNs during stimuli presentation, ideally with expanding bar lengths and abrupt changes in the orientations during a single presentation trial.

For the later, the disparity between LOSN base firing rates, a different approach is being employed. As a new collaboration within our lab (Bee Sensory and Behavioural Ecology Lab, Queen Mary University of London) we are undertaking a formal mathematical analysis of the lobula orientation-sensitive neurons. This is similar to the recent Fisher Information analysis used by Alexandre Pouget (Kanitscheider, Coen-Cagli et al. 2015, Kohn, Coen-Cagli et al. 2016). However, rather than a population correlation analysis, here we are interested in determining the very minimum number of neurons and optimal tuning curves that are able to produce ‘honeybee like’ discrimination and generalization abilities. These optimal models can then be directly compared and evaluated against the known LOSN responses.

Learning and decision-making

Dependent on particular experiment simulated I found that, in most cases, one or other of models tested performed very similar to that of the empirical results of real honeybees. The only exceptions were where both test stimuli were very similar to that of the training pattern (Chapter 3.4.2 Batch 3). In these cases all models either failed to

generalise to novel patterns, or performed much worse than the honeybees. These highlight key areas where my models need to be developed.

Firstly, lets assume that some combination of LOSN to Kenyon cell connections akin to SEO_AB, EAI_AB (DISTINCT) and MERGED model connections all exist within the honeybee brain. Which could easily be established given they all use the same LOSNs and either excitatory or inhibitory synapses onto the Kenyon cells. In the case of scale invariance (Chapter 2.4.1), horizontal offset (Chapter 3.4.1) and indeed generalisation of oriented bars and gratings (Chapter 2.4.4) I found that the Kenyon cell responses for the EAI_AB, MERGED, EAI_AB models respectively were very similar for all the variations of the experimental CS+ and TS^{COR} stimuli, whereas the contrasting models (SEO_AB, DISTINCT, SEO_AB) had very different neuronal responses for each pattern. It is easy to envisage a theoretical model that would simply disregard those Kenyon cells that did not provide a consistent response to the different rewarding CS+ stimuli. This would allow just those that did, to be utilized when discriminating between the final test stimuli. This would still not require the models to perceive the CS- training patterns.

In the case of discriminating two horizontal grating patterns we see a large discrepancy in the honeybee performance dependent on whether the honeybee was initially trained on a CS- vertical grating (honeybees' failed the discrimination) or with an incorrect CS- horizontal grating (honeybees could discriminate the two gratings). Here it is obvious that honeybees are using the CS- stimuli to learn and discriminate the patterns. Within a new theoretical model this could be accommodated by presenting both the CS+ and CS- stimuli and then, positively adapting an associated weight with each Kenyon cell dependent on if it fires consistently for the CS+ patterns (as above), or

degrading this weight if it fires for both CS+, CS- stimuli. Alternatively we envisage dual pathways, in one pathway Kenyon cells adapt a set of weights based on how consistently they activate for all CS+ stimuli, and an identical pathway with separate weights that are adapted for those Kenyon cells based on the firing for CS- patterns. In this case the model would choose the test stimuli that had the greatest reward expectation value (Kenyon cell activation * the CS+ weights) and least aversive value (Kenyon cell activation * the CS- weights). In both cases the relative importance of the CS+ and CS- contribution could be tailored dependent on the particular training task (see Chapter 3.5 discussion on the importance of training procedure and punishment associated with CS- stimuli).

It is these very enhancements discussed above that my colleague Fei Peng has been investigating by building biologically realistic models of the honeybee mushroom bodies. This work, based on the olfactory system, has already shown that changing the mushroom body synaptic learning rates associated with the presentation of rewarding and unrewarding odours can replicate known behavioural phenomena (peak-shift / positive and negative patterning) (Peng and Chittka 2017). My next step in understanding bee visual cognition is to replicate this more sophisticated mushroom body model but exchanging the olfactory inputs for the LOSN responses from this study. This will allow us to test if the perception of both the CS+ and CS- stimuli will produce experimental performances closer to that of real bees, or if additional visual information or cognitive mechanisms are still required to replicate the honeybee's abilities.

6.3 Thesis implications for behavioural experiments

Changing bee research emphasis from ‘Can’ to ‘How’

Over the four years of my PhD I have very much enjoyed reading past behavioural papers, meeting and collaborating with experimentalists, and indeed conducting my own behavioural experiments on bees. However, one thing is very clear; a lot of emphasis is placed on determining what interesting, and often remarkable, things that bees ‘can’ do. Bees can discriminate colours (v. Frisch 1914), can communicate the location of flower resources to nest mates (v. Frisch 1927), can exhibit social learning (see review (Leadbeater and Chittka 2014)) and can teach techniques to other individuals (Alem, Perry et al. 2016), they can even be trained elementary tool use (Loukola, Perry et al. 2017). All these provide useful information on the behavioural ability of bees; they may also narrow down the task into ‘what’ the bees do (i.e. the positional dynamics of the waggle dance), but not necessarily how to understand the actual bee cognition.

Since joining the Queen Mary University of London bee lab, which was then predominantly a behavioural lab, the cognitive modelling team has recruited both mathematicians and software engineers to model the bee brain. However, more importantly, this group now interacts with the experimentalists at every stage of a new project; from initial design of the stimuli, adaption of the experimental procedures, analysis of results, to the final modelling of the bee decision processes. What this has done is focus research attention very closely on understanding: what information (visual, social, contextual) does the bee need to solve the task, how does the behaviour change during learning, what factors might affect performance between individuals? This new emphasis on ‘how’ has meant that very simple experiments that an experimentalist might have previously considered trivial (i.e. the discrimination of a simple spiral and

cross patterns) are opening up whole new research areas; in the above example does the flight dynamics of fixating at the spiral differ to the cross? If so, does the shape therefore dictate the movement (and what visual inputs are directing this movement)? If this is the case, counter-intuitively, it raises the very tantalising question: does the very difference between flight behaviour caused by particular shapes allow discrimination without the bee even having to learn the visual inputs? These types of behaviour and theoretical research collaborations are providing a new way to investigate bee cognition.

A similar paradigm shift was made much earlier in the field of mammalian vision; in 1973 David Marr joined the Massachusetts Institute of Technology (MIT), and in the subsequent years before his unfortunate early death in 1980 he and his colleagues revolutionised the world of computational neuroscience. Marr, like many others of his time, began his theoretical work using the (then) cutting-edge electrophysiological and neuroanatomical research of the 1960s, in his case concentrating on the mammalian cerebral cortex (Marr 1969). However, during his investigations he realised there was a fundamental issue with this approach, “*The key observation is that neurophysiology or psychophysics have as their business to describe the behaviour of cells or of subjects but not to explain such behaviour. What are the visual areas of the cerebral cortex actually doing? What are the problems in doing it that need explaining, and at what level of description should such explanations be sought?*” (Marr 1982). In an attempt to answer these questions Marr moved to MIT and changed his research field to the new emerging area of machine vision and artificial intelligence. What revolutionised, and in many ways established, the basis for computational neuroscience was the realisation that, as well as neurophysiology or psychophysics understanding of the problem, there was also another level of understanding required to encapsulate the information-processing of the task at hand

(Marr and Poggio 1976, Marr 1977). This analysis would be independent of the physical system it would run on (i.e. the neurons and connectivity within a brain, or the hardware of a computer) but provided a measurable efficiency at how well a given information-processing ‘algorithm’ could solve particular tasks. This established the ‘Three Levels’ of cognitive analysis that will one day, hopefully, allow the full understanding of perceptual tasks (Level 1: Computational Theory, Level 2: Representation and Algorithm, Level 3: Hardware Implementation) (Marr 1982).

This same approach may prove vital to the study of bee cognition, as well as other invertebrate vision research. The Vision book written by Marr before his death is a must read for anyone interested in visual perception and provides first-hand insights into how these levels were developed and explored (Marr 1982). In insect cognition we will need to pay very particular attention to Level 1 “*what is the goal of the computation*” (Marr 1982), we may be able to theorise what the human brain needs to solve a given problem, but this is not the question. We need to make sure we ask what the problem, and underlying information theory ‘goal’, actually is from the bees’ perspective. As we have seen from both eidetic image discrimination (Chapter 2) and ‘above and below’ conceptualisation tasks (Chapter 5) the way we, as humans, approach the problem may be very different from that of the bees’. This Level 1 computational analysis, done correctly, will provide better insights into the possible representations that could be used by the bees to solve a task (i.e. Level 2), and of these which best suits the physical resources within the limited neuronal structures of the bee brain (i.e. Level 3). These three levels are however very much interconnected, such that new discoveries in electrophysiology or behavioural evidence may further influence how we characterise the ‘goals’ in Level 1; therefore close cooperation between bee experimentalists and theorists will undoubtedly aid progress within all three levels and within each discipline.

For those experimental groups that do not have existing collaborations with modellers there is still much that can be done to help explore the question of ‘how’ bee cognition may work.

Data availability

Throughout this thesis I have compared my model performances to that of the honeybee empirical results. These results are most often from unrewarded tests performed after the bees have been repeatedly exposed to training stimuli; they typically take the form of a single average performance for all of the honeybees tested. Followed by a statistical analysis to show if these results were significantly different to chance, and occasionally, an indication of variance between the tested bees. Fortunately, for my thesis this information was sufficient to compare my model performances with that of real bees. The next stage of this research, as discussed above, is to investigate how and the presence of CS+ and CS- stimuli may affect the learning and performance of bees. Most honeybee and bumblebee visual cognition experiments conducted since the turn of the century have trained individual bees within an enclosed flight arena, this allows the experimenter to precisely control which training patterns each solitary bee is exposed to. Earlier experiments would routinely mass train bees on the training patterns before testing, this meant there was no record of how many times a particular bee might have viewed the training stimuli, or what effect social cues or odours would have on its learning. It is now standard practice within behavioural publications on bees to provide a learning curve (a graph providing the number of correct choices the bees made per block of typically five or ten choices) before describing the actual test results. Figure 6.1a shows a typical example, displayed is the average performance of ten bumblebees learning a colour discrimination task, subdivided into blocks of ten choices, the error

bars showing the standard deviation of the results for each block. When attempting to model the learning of individual bees, initial interrogation of these results might suggest that bees' performance slowly increases during the first 50 – 60 trials and then stabilises at 90% accuracy. However, Figure 6.1b shows the individual performance of each bee during this task. This provides a clearer indication of the variation in learning, with some bees learning very fast, while others take much longer to reach the 90% accuracy level. This difference in the representation of how bees learn could have real implications on how any new model employing learning is evaluated.

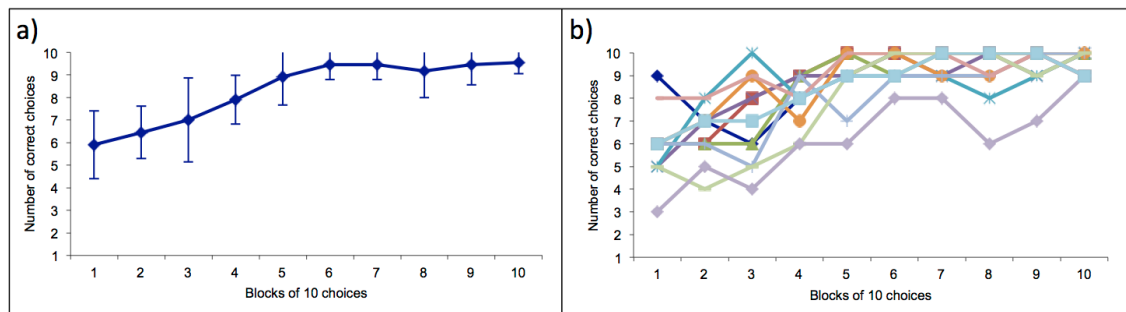


Figure 6.1 Example graphs displaying bumblebee discrimination task learning curves. **(a)** Average learning curve of bumblebees ($n=10$) learning to discriminate green and blue coloured chips. Number of correct choices per block of ten trials (total 100 trials). Error bars show standard deviation. **(b)** Individual learning curves for the same 10 bumblebees.

Publications today allow an almost unlimited amount of supplementary information to be uploaded and stored online. Therefore, it is strongly recommended that the full data sets of individual bee stimuli selections be provided. This is even more critical for generalisation experiments where the bees' choices could be influenced by particular stimuli. As modellers it is interesting to evaluate if all bees perform better or worse on particular CS+ and CS- stimuli, or whether an individual's exposure to previous stimuli may affect its subsequent choice selection on the next presented patterns. There is obviously a cost in formatting and preparing these data sets for open access, but the availability of this data to modellers such as myself is often as important as the final experimental test results. These data sets will in future allow new theoretical

models to be exposed to the exact same stimuli, in the same sequence, as real bees. We can then evaluate the model and honeybee performances to determine if previous experience, or simply differences in synaptic connectivity, can account for the variance we see in the empirical results.

Videography

In chapter 4 I investigated how bees might solve the spatial relationship task of ‘above and below’. The most significant finding from this work was that the ability of the models to succeed at the task was dependent on how the virtual bee was allowed to fixate at the patterns. This finding in turn led to the replication of the original ‘above and below’ behavioural experiment. High-speed video recordings revealed that the bees were solving the task by consistently fixating at the bottom shape of the pattern in whichever Y-Maze arm they entered, and making a simple discrimination of this shape to determine if to visit that arm’s feeding tube. However, this still only answered the question ‘what’ bees do.

Within our lab we have recently purchased a custom 3D flight arena video capture system (Pro Capture USA); with its three high-speed cameras and included software it is able to provide detailed tracking information as bees both approach and fixate at patterns. Again very simple experiments are providing vital, and often surprising, results as to how bees interrogate visual patterns. Within this thesis I provided a range of models that were able to replicate the honeybee behaviour performances at particular tasks. Some of these models were useful for generalisation (EAI_AB), others discrimination (SEO_AB) and others still for distance and horizontal location invariance of the stimuli (MERGED). Current behaviour experiments (utilising 3D tracking) are investigating which of these different models may be employed when the bees have a choice of features they can learn. Specific sets of stimuli have been

designed that provide both a discrimination feature (a shape presented on every CS+ pattern and a different shape on every CS- pattern) and a generalisation feature (different shape on each pattern but displaying the same feature type) (see Fig 6.2). The most interesting finding thus far, is that the bees' initial and secondary fixations are not just based on whether the pattern shape is the consistent discrimination or variable generalisation feature, but that the fixations also change dependent on the shapes presented, and also their relative locations. These fixation points in each particular stimuli set are largely consistent between the bees, suggesting some form of 'internal rules' that determine how the bees tackle each different task. The next step of this project is to use the 3D tracking data to replicate the bee-eye view (see (Sturzl, Boeddeker et al. 2010)) to understand if particular visual inputs are directing the bees flight dynamics and determining which stimuli features they preferentially learn.

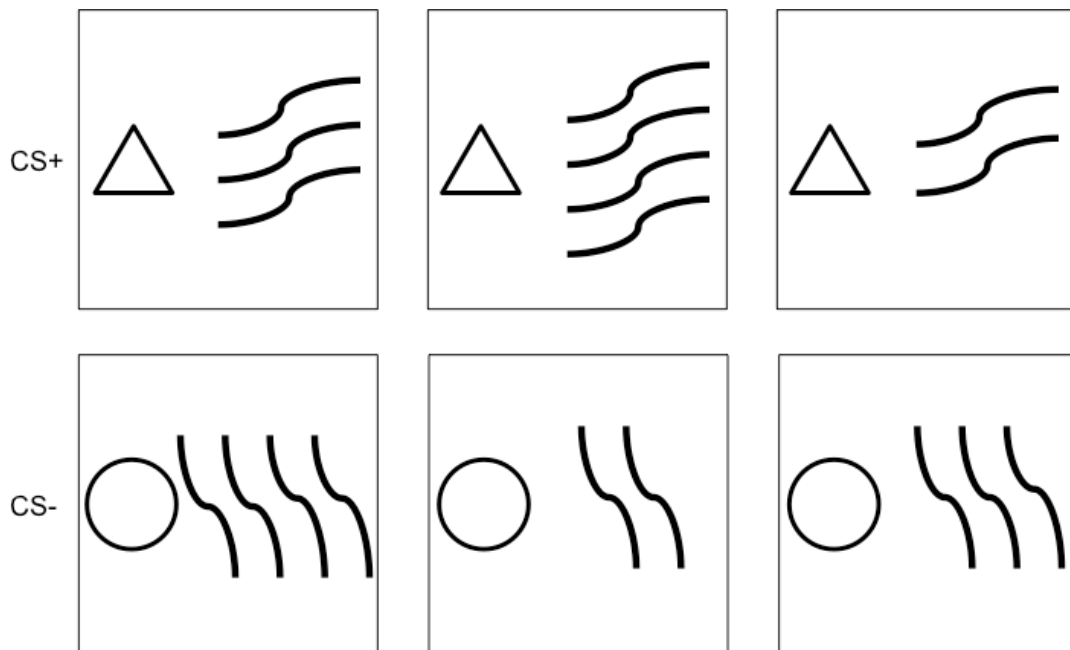


Figure 6.2 Example of combined discrimination and generalisation feature patterns. One CS+ and one CS- pattern are selected from a respective set of patterns and presented during each experimental trial. Here the CS+ patterns always display the exact same triangle shape (discrimination feature) on the left and an inclined wavy grating on the right, which can be composed of 2-4 lines (generalisation feature). The CS- always has a circle on the left and on the right 2-4 vertical wavy lines.

Due to the potential of being able to simulate the exact visual perception of bees, it is hoped, and strongly recommended, that all future free-flight bee experiments be recorded with multiple high-speed cameras, even when this isn't necessary for the current question being asked. The cost of these cameras is rapidly dropping and the cost of online storage for academic institutions is most often free (Dropbox, GitHub, etc.). The camera setup for my 'above and below' experiments was not ideal, with issues synchronising off-the-shelf action cameras and reconstruction of 3D coordinates, especially given the fish-eye distortions on these cameras. However, with increasing computer processing speeds and developments in machine vision processing, conversion of these video recordings into full 3d tracking data sets will become ever easier (with the raw video footage archived this process can always be performed in the future). Just as simple video recordings of the original 'above and below' experiment could have guided the development of my models in chapter 4, and prevented the need to replicate the experiments in chapter 5, so high-speed recordings of current experiments may provide a huge wealth of information for future cognitive modelling questions. Indeed, these new questions may have little in common with the original behavioural investigation, but nonetheless will be an incredibly useful resource, and save valuable time unnecessarily replicating required experiments.

6.3 Final thoughts

A substantial motivation for this thesis, and my PhD in general, is progressing our understanding of how the miniature brain of a bee is able to accomplish their remarkable visual recognition feats seen both in nature, and under experimental conditions. In this thesis I have provided novel insights into how the miniature

honeybee brain is, by virtue of its neuronal design, able to tackle complex discriminations, stimuli invariance, and even generalisation tasks. However, the research undertaken in Chapter 4 and Chapter 5 demonstrates another vital benefit of studying insects. Without this extremely focused modelling and behavioural study on *what* and *how* bees solve the ‘above and below’ conceptualisation task, we may not have identified such a seemingly obvious solution to this problem. This research now forces us to reassess previous experimental conclusions and ask the awkward question – just because we (humans) solve, what we perceive to be complex problems through a particular process, does this necessitate that other animals cannot solve the same task in a completely novel, and potentially much simpler way; even when the behavioural data seems to support our original hypothesis? With this said, there is no reason not to study other conceptual, social, or even tool use abilities in bees and other invertebrates. These studies, such as the one presented here, may provide novel insights into how different problems can be approached and solved. As electrophysiological techniques improve over the next few years, the miniature brain of the honeybee may have an even more vital role in computational neuroscience and animal cognition; the ability to investigate how these remarkable brains work during visual recognition and even ‘higher order’ learning tasks may have so much more to teach us.

Acknowledgments

Firstly I would like to thank my supervisors, Dr Chrisantha Fernando and Professor Lars Chittka, for the opportunity to work at Queen Mary University of London, and for all their amazing guidance and support. I'd also like to thank my PhD panel chair: Professor Peter McOwan, for his support and advice throughout my studies. I am also deeply grateful to my collaborator Dr Stephan Wolf for introducing me to the wonderful world of behavioural research, as well as his help and support during my PhD. I am also grateful to Fei Peng for the many hours of constructive and enjoyable discussion about the honeybee brain. Thanks to all the members of the Chittka lab, past and present, who have been there to help me with behavioural experiments and graciously sat through all my very long modelling presentations: Erika Dawson, Vivek Nityananda, Kate Hunt, David Barracchi, Sylvain Alem, Oscar Rodriguez, Clint Perry, Li Li, Cui Guan, Simon Emberton, Tristan William, James Makinson, Joseph Woodgate, HaDi MaBouDi, Vera Vasas and Marie Guiraud.

Finally, I would not have been able to get through these four years without the support of my family and friends. I am truly appreciative for all the encouragement that everyone has given me over these years. In particular, I would like to thank my friends: Gemma, Gavin, Rae and Theresa for their full support throughout my PhD and their very best attempts to keep me sane. Lastly, I want to pay a special thanks to my parents, Phil and Kath Roper, who have always stood behind me, supporting me no matter what crazy life adventures I choose to explore.

References

- Alem, S., C. J. Perry, X. Zhu, O. J. Loukola, T. Ingraham, E. Sovik and L. Chittka (2016). "Associative Mechanisms Allow for Social Learning and Cultural Transmission of String Pulling in an Insect." *PLoS Biol* **14**(10): e1002564.
- Avargues-Weber, A., D. d'Amaro, M. Metzler and A. G. Dyer (2014). "Conceptualization of relative size by honeybees." *Front Behav Neurosci* **8**: 80.
- Avargues-Weber, A., E. H. Dawson and L. Chittka (2013). "Mechanisms of social learning across species boundaries." *Journal of Zoology* **290**(1): 1-11.
- Avargues-Weber, A., M. G. de Brito Sanchez, M. Giurfa and A. G. Dyer (2010). "Aversive reinforcement improves visual discrimination learning in free-flying honeybees." *PLoS One* **5**(10): e15370.
- Avargues-Weber, A., A. G. Dyer and M. Giurfa (2011). "Conceptualization of above and below relationships by an insect." *Proc Biol Sci* **278**(1707): 898-905.
- Baird, E., M. V. Srinivasan, S. Zhang, R. Lamont and A. Cowling (2006). Visual Control of Flight Speed and Height in the Honeybee. *From Animals to Animats 9: 9th International Conference on Simulation of Adaptive Behavior, SAB 2006, Rome, Italy, September 25-29, 2006. Proceedings*. S. Nolfi, G. Baldassarre, R. Calabretta et al. Berlin, Heidelberg, Springer Berlin Heidelberg: 40-51.
- Berry, R. P. and M. R. Ibbotson (2010). "A Three-Dimensional Atlas of the Honeybee Neck." *Plos One* **5**(5).
- Bishop, L. G. (1970). "The spectral sensitivity of motion detector units recorded in the optic lobe of the honeybee." *Zeitschrift für vergleichende Physiologie* **70**(4): 374-381.
- Bitterman, M. E., R. Menzel, A. Fietz and S. Schafer (1983). "Classical conditioning of proboscis extension in honeybees (*Apis mellifera*)." *J Comp Psychol* **97**(2): 107-119.
- Blasdel, G. G. and G. Salama (1986). "Voltage-sensitive dyes reveal a modular organization in monkey striate cortex." *Nature* **321**(6070): 579-585.
- Boeddeker, N., L. Dittmar, W. Sturzl and M. Egelhaaf (2010). "The fine structure of honeybee head and body yaw movements in a homing task." *Proc Biol Sci* **277**(1689): 1899-1906.
- Boeddeker, N. and J. M. Hemmi (2010). "Visual gaze control during peering flight manoeuvres in honeybees." *Proc Biol Sci* **277**(1685): 1209-1217.
- Brill, M. F., M. Reuter, W. Rössler and M. F. Strube-Bloss (2014). "Simultaneous Long-term Recordings at Two Neuronal Processing Stages in Behaving Honeybees." *Journal of Visualized Experiments : JoVE*(89): 51750.
- Bulthoff, H. H. and S. Edelman (1992). "Psychophysical support for a two-dimensional view interpolation theory of object recognition." *Proc Natl Acad Sci U S A* **89**(1): 60-64.
- Chen, L., S. Zhang and M. V. Srinivasan (2003). "Global perception in small brains: Topological pattern recognition in honey bees." *Proceedings of the National Academy of Sciences* **100**(11): 6884-6889.
- Chittka, L. (2001). "Camouflage of Predatory Crab Spiders on Flowers and the Colour Perception of Bees (Aranida: Thomisidae / Hymenoptera: Apidae)." *Entomologia Generalis* **25**(3): 181-187.
- Chittka, L. and A. Brockmann (2005). "Perception space--the final frontier." *PLoS Biol* **3**(4): e137.
- Chittka, L., A. G. Dyer, F. Bock and A. Dornhaus (2003). "Psychophysics: bees trade off foraging speed for accuracy." *Nature* **424**(6947): 388.

Chittka, L., S. Faruq, P. Skorupski and A. Werner (2014). "Colour constancy in insects." J Comp Physiol A Neuroethol Sens Neural Behav Physiol **200**(6): 435-448.

Chittka, L. and K. Geiger (1995). "Can honey bees count landmarks?" Animal Behaviour **49**(1): 159-164.

Chittka, L., K. Geiger and J. A. N. Kunze (1995). "The influences of landmarks on distance estimation of honey bees." Animal Behaviour **50**(1): 23-31.

Chittka, L., J. Kunze, C. Shipman and S. L. Buchmann (1995). "The significance of landmarks for path integration in homing honeybee foragers." Naturwissenschaften **82**(7): 341-343.

Collett, T. S. and A. Kelber (1988). "The retrieval of visuo-spatial memories by honeybees." Journal of Comparative Physiology A **163**(1): 145-150.

Cuevas Rivera, D., S. Bitzer and S. J. Kiebel (2015). "Modelling Odor Decoding in the Antennal Lobe by Combining Sequential Firing Rate Models with Bayesian Inference." PLoS Comput Biol **11**(10): e1004528.

Dacke, M. and M. V. Srinivasan (2008). "Evidence for counting in insects." Anim Cogn **11**(4): 683-689.

Dawson, E. H. and L. Chittka (2014). "Bumblebees (*Bombus terrestris*) use social information as an indicator of safety in dangerous environments." Proc Biol Sci **281**(1785): 20133174.

de Brito Sanchez, M. G., M. Serre, A. Avargues-Weber, A. G. Dyer and M. Giurfa (2015). "Learning context modulates aversive taste strength in honey bees." J Exp Biol **218**(Pt 6): 949-959.

Denker, M., R. Finke, F. Schaupp, S. Grün and R. Menzel (2010). "Neural correlates of odor learning in the honeybee antennal lobe." European Journal of Neuroscience **31**(1): 119-133.

Depy, D., J. Fagot and J. Vauclair (1999). "Processing of above/below categorical spatial relations by baboons (*Papiopapio*)." Behav Processes **48**(1-2): 1-9.

Devaud, J. M., T. Papouin, J. Carcaud, J. C. Sandoz, B. Grunewald and M. Giurfa (2015). "Neural substrate for higher-order learning in an insect: Mushroom bodies are necessary for configural discriminations." Proc Natl Acad Sci U S A **112**(43): E5854-5862.

Dill, M., R. Wolf and M. Heisenberg (1995). "Behavioral analysis of *Drosophila* landmark learning in the flight simulator." Learning & Memory **2**(3-4): 152-160.

Dukas, R. (2004). "Evolutionary Biology of Animal Cognition." Annual Review of Ecology, Evolution, and Systematics **35**(1): 347-374.

Dukas, R. and D. H. Morse (2005). "Crab spiders show mixed effects on flower-visiting bees and no effect on plant fitness components." Ecoscience **12**(2): 244-247.

Durst, C., S. Eichmüller and R. Menzel (1994). "Development and experience lead to increased volume of subcompartments of the honeybee mushroom body." Behavioral and Neural Biology **62**(3): 259-263.

Dyer, A. G. and L. Chittka (2004). "Fine colour discrimination requires differential conditioning in bumblebees." Naturwissenschaften **91**(5): 224-227.

Dyer, A. G. and C. Neumeyer (2005). "Simultaneous and successive colour discrimination in the honeybee (*Apis mellifera*)." J Comp Physiol A Neuroethol Sens Neural Behav Physiol **191**(6): 547-557.

Dyer, A. G., C. Neumeyer and L. Chittka (2005). "Honeybee (*Apis mellifera*) vision can discriminate between and recognise images of human faces." J Exp Biol **208**(Pt 24): 4709-4714.

Dyer, A. G. and Q. C. Vuong (2008). "Insect Brains Use Image Interpolation Mechanisms to Recognise Rotated Objects." PLoS ONE **3**(12): e4086.

Ehmer, B. and W. Gronenberg (2002). "Segregation of visual input to the mushroom bodies in the honeybee (*Apis mellifera*)."
J Comp Neurol **451**(4): 362-373.

Galizia, C. G., S. L. McIlwrath and R. Menzel (1999). "A digital three-dimensional atlas of the honeybee antennal lobe based on optical sections acquired by confocal microscopy." Cell and tissue research **295**(3): 383-394.

Galizia, C. G., S. Sachse, A. Rappert and R. Menzel (1999). "The glomerular code for odor representation is species specific in the honeybee *Apis mellifera*." Nature neuroscience **2**(5): 473-478.

Ganeshina, O. and R. Menzel (2001). "GABA-immunoreactive neurons in the mushroom bodies of the honeybee: An electron microscopic study." The Journal of Comparative Neurology **437**(3): 335-349.

Giger, A. D. and M. V. Srinivasan (1995). "Pattern recognition in honeybees: eidetic imagery and orientation discrimination." Journal of Comparative Physiology A **176**(6): 791-795.

Giurfa, M. (2004). "Conditioning procedure and color discrimination in the honeybee *Apis mellifera*." Naturwissenschaften **91**(5): 228-231.

Giurfa, M., B. Eichmann and R. Menzel (1996). "Symmetry perception in an insect." Nature **382**(6590): 458-461.

Giurfa, M., M. Hammer, S. Stach, N. Stollhoff, N. Muller-deisig and C. Mizyrycki (1999). "Pattern learning by honeybees: conditioning procedure and recognition strategy." Anim Behav **57**(2): 315-324.

Giurfa, M., S. Zhang, A. Jenett, R. Menzel and M. V. Srinivasan (2001). "The concepts of 'sameness' and 'difference' in an insect." Nature **410**(6831): 930-933.

Goodman, L. J., W. A. Fletcher, R. G. Guy, P. G. Mobbs and C. D. J. Pomfrett (1987). Motion Sensitive Descending Interneurons, Ocellar LD Neurons and Neck Motoneurons in the Bee: A Neural Substrate for Visual Course Control in *Apis mellifera*. Neurobiology and Behavior of Honeybees. R. Menzel and A. Mercer. Berlin, Heidelberg, Springer Berlin Heidelberg: 158-171.

Gronenberg, W. (2001). "Subdivisions of hymenopteran mushroom body calyces by their afferent supply." J Comp Neurol **435**(4): 474-489.

Gross, H. J., M. Pahl, A. Si, H. Zhu, J. Tautz and S. Zhang (2009). "Number-based visual generalisation in the honeybee." PLoS One **4**(1): e4263.

Hammer, M. (1993). "An identified neuron mediates the unconditioned stimulus in associative olfactory learning in honeybees." Nature **366**: 59-63.

Hammer, M. (1997). "The neural basis of associative reward learning in honeybees." Trends Neurosci **20**(6): 245-252.

Heisenberg, M. (2003). "Mushroom body memoir: from maps to models." Nat Rev Neurosci **4**(4): 266-275.

Hertel, H. and U. Maronde (1987). Processing of Visual Information in the Honeybee Brain. Neurobiology and Behavior of Honeybees. R. Menzel and A. Mercer. Berlin, Heidelberg, Springer Berlin Heidelberg: 141-157.

Hopkins, W. D. and R. D. Morris (1989). "Laterality for visual-spatial processing in two language-trained chimpanzees (*Pan troglodytes*)." Behav Neurosci **103**(2): 227-234.

Hori, S., H. Takeuchi, K. Arikawa, M. Kinoshita, N. Ichikawa, M. Sasaki and T. Kubo (2006). "Associative visual learning, color discrimination, and chromatic adaptation in the harnessed honeybee *Apis mellifera* L." J Comp Physiol A Neuroethol Sens Neural Behav Physiol **192**(7): 691-700.

Hori, S., H. Takeuchi and T. Kubo (2007). "Associative learning and discrimination of motion cues in the harnessed honeybee *Apis mellifera* L." Journal of Comparative Physiology A **193**(8): 825-833.

Horridge, A. (2000). "Seven experiments on pattern vision of the honeybee, with a model." *Vision Res* **40**(19): 2589-2603.

Horridge, A. (2003). "Visual resolution of the orientation cue by the honeybee (*Apis mellifera*)." *J Insect Physiol* **49**(12): 1145-1152.

Horridge, A. (2003). "The visual system of the honeybee (*Apis mellifera*): the maximum length of the orientation detector." *J Insect Physiol* **49**(6): 621-628.

Horridge, A. (2006). "Visual discriminations of spokes, sectors, and circles by the honeybee (*Apis mellifera*)." *J Insect Physiol* **52**(9): 984-1003.

Horridge, G. A. (1997). "Pattern discrimination by the honeybee: disruption as a cue." *Journal of Comparative Physiology A* **181**(3): 267-277.

Horridge, G. A. (2000). "Visual discrimination of radial cues by the honeybee (*Apis mellifera*)." *J Insect Physiol* **46**(5): 629-645.

Horridge, G. A., S.-W. Zhang and M. Lehrer (1992). "Bees can Combine Range and Visual Angle to Estimate Absolute Size." *Philosophical Transactions of the Royal Society of London B: Biological Sciences* **337**(1279): 49-57.

Horridge, G. A. and S. W. Zhang (1995). "Pattern vision in honeybees (*Apis mellifera*): Flower-like patterns with no predominant orientation." *Journal of Insect Physiology* **41**(8): 681-688.

Hung, Y. S., J. P. van Kleef and M. R. Ibbotson (2011). "Visual response properties of neck motor neurons in the honeybee." *J Comp Physiol A Neuroethol Sens Neural Behav Physiol* **197**(12): 1173-1187.

Ibbotson, M. R. (1991). "Wide-field motion-sensitive neurons tuned to horizontal movement in the honeybee, *Apis mellifera*." *Journal of Comparative Physiology A* **168**(1): 91-102.

James, A. C. and D. Osorio (1996). "Characterisation of columnar neurons and visual signal processing in the medulla of the locust optic lobe by system identification techniques." *J Comp Physiol A* **178**(2): 183-199.

Kanitscheider, I., R. Coen-Cagli, A. Kohn and A. Pouget (2015). "Measuring Fisher information accurately in correlated neural populations." *PLoS Comput Biol* **11**(6): e1004218.

Kien, J. and R. Menzel (1977). "Chromatic properties of interneurons in the optic lobes of the bee." *Journal of comparative physiology* **113**(1): 35-53.

Kirkpatrick-Steger, K. and E. A. Wasserman (1996). "The what and the where of the pigeon's processing of complex visual stimuli." *J Exp Psychol Anim Behav Process* **22**(1): 60-67.

Kleyko, D., E. Osipov, R. W. Gayler, A. I. Khan and A. G. Dyer (2015). "Imitation of honey bees' concept learning processes using Vector Symbolic Architectures." *Biologically Inspired Cognitive Architectures* **14**: 57-72.

Kohn, A., R. Coen-Cagli, I. Kanitscheider and A. Pouget (2016). "Correlations and Neuronal Population Information." *Annu Rev Neurosci* **39**: 237-256.

Land, M. F. and L. Chittka (2012). Vision. *The Insects: Structure and Function*. A. E. Douglas, R. F. Chapman and S. J. Simpson. Cambridge, Cambridge University Press: 708-737.

Laska, M., C. G. Galizia, M. Giurfa and R. Menzel (1999). "Olfactory discrimination ability and odor structure-activity relationships in honeybees." *Chem Senses* **24**(4): 429-438.

Laughlin, S. B. and G. A. Horridge (1971). "Angular sensitivity of the retinula cells of dark-adapted worker bee." *Zeitschrift für vergleichende Physiologie* **74**(3): 329-335.

Leadbeater, E. and L. Chittka "Social Learning in Insects 2014; From Miniature Brains to Consensus Building." *Current Biology* **17**(16): R703-R713.

Leadbeater, E. and L. Chittka (2008). "Social transmission of nectar-robbing behaviour in bumble-bees." *Proc Biol Sci* **275**(1643): 1669-1674.

Leadbeater, E. and L. Chittka (2009). "Bumble-bees learn the value of social cues through experience." *Biol Lett* **5**(3): 310-312.

Lehrer, M. (1999). "Shape Perception in the Honeybee: Symmetry as a Global Framework." *Int J Plant Sci* **160**(S6): S51-S65.

Liu, G., H. Seiler, A. Wen, T. Zars, K. Ito, R. Wolf, M. Heisenberg and L. Liu (2006). "Distinct memory traces for two visual features in the Drosophila brain." *Nature* **439**(7076): 551-556.

Lodish, H. B., A.; Zipursky, S.L.; et al. (2000). "Molecular Cell Biology. 4th edition. New York: W. H. Freeman; 2000. Section 21.1, Overview of Neuron Structure and Function. Available from: <http://www.ncbi.nlm.nih.gov/books/NBK21535/>."

Logothetis, N. K., J. Pauls and T. Poggio (1995). "Shape representation in the inferior temporal cortex of monkeys." *Curr Biol* **5**(5): 552-563.

Loukola, O. J., C. J. Perry, L. Coscos and L. Chittka (2017). "Bumblebees show cognitive flexibility by improving on an observed complex behavior." *Science* **355**(6327): 833-836.

Maddess, T., M. P. Davey and E. C. Yang (1999). "Discrimination of complex textures by bees." *Journal of Comparative Physiology A* **184**(1): 107-117.

Maddess, T. and E. Yang (1997). "Orientation-sensitive Neurons in the Brain of the Honey Bee (*Apis mellifera*)." *J Insect Physiol* **43**(4): 329-336.

Marr, D. (1969). "A theory of cerebellar cortex." *J Physiol* **202**(2): 437-470.

Marr, D. (1977). "Artificial intelligence—A personal view." *Artificial Intelligence* **9**(1): 37-48.

Marr, D. and T. Poggio (1976). "Cooperative computation of stereo disparity." *Science* **194**(4262): 283-287.

Marr, D. (1982). "Vision. A computational investigation into the human representation and processing of visual information." *WH San Francisco: Freeman and Company* **1**(2).

McCann, G. D. and J. C. Dill (1969). "Fundamental Properties of Intensity, Form, and Motion Perception in the Visual Nervous Systems of *Calliphora phaenicia* and *Musca domestica*." *The Journal of General Physiology* **53**(4): 385-413.

McNeill, M. S., K. M. Kapheim, A. Brockmann, T. A. McGill and G. E. Robinson (2016). "Brain regions and molecular pathways responding to food reward type and value in honey bees." *Genes Brain Behav* **15**(3): 305-317.

Menzel, R. and M. Blakers (1976). "Colour receptors in the bee eye — Morphology and spectral sensitivity." *Journal of comparative physiology* **108**(1): 11-13.

Menzel, R. and A. W. Snyder (1974). "Polarised light detection in the bee, *Apis mellifera*." *Journal of comparative physiology* **88**(3): 247-270.

Michael F L, L. C. "The Insects: Structure and Function (5th Edition)."

Mobbs, P. G. (1984). "Neural networks in the mushroom bodies of the honeybee." *Journal of Insect Physiology* **30**(1): 43-58.

Morawetz, L., L. Chittka and J. Spaethe (2015). "Honeybees (*Apis mellifera*) exhibit flexible visual search strategies for vertical targets presented at various heights." *F1000Research* **3**.

Morse, D. H. (1981). "Prey Capture by the Crab Spider *Misumena vatia* (Clerck) (Thomisidae) on Three Common Native Flowers." *American Midland Naturalist* **105**(2): 358-367.

Mota, T., E. Roussel, J.-C. Sandoz and M. Giurfa (2011). "Visual conditioning of the sting extension reflex in harnessed honeybees." *Journal of Experimental Biology* **214**(21): 3577-3587.

Niggebrügge, C., G. Lebouille, R. Menzel, B. Komischke and N. H. de Ibarra (2009). "Fast learning but coarse discrimination of colours in restrained honeybees." Journal of Experimental Biology **212**(9): 1344-1350.

Nityananda, V., L. Chittka and P. Skorupski (2014). "Can Bees See at a Glance?" Journal of Experimental Biology.

O'Carroll, D. (1993). "Feature-detecting neurons in dragonflies." Nature **362**(6420): 541-543.

Okamura, J. Y. and N. J. Strausfeld (2007). "Visual system of calliphorid flies: motion- and orientation-sensitive visual interneurons supplying dorsal optic glomeruli." J Comp Neurol **500**(1): 189-208.

Olberg, R. M. (1981). "Parallel Encoding of Direction of Wind, Head, Abdomen, and Visual-Pattern Movement by Single Interneurons in the Dragonfly." Journal of Comparative Physiology **142**(1): 27-41.

Olberg, R. M., R. C. Seaman, M. I. Coats and A. F. Henry (2007). "Eye movements and target fixation during dragonfly prey-interception flights." J Comp Physiol A Neuroethol Sens Neural Behav Physiol **193**(7): 685-693.

Papadopoulou, M., S. Cassenaer, T. Nowotny and G. Laurent (2011). "Normalization for sparse encoding of odors by a wide-field interneuron." Science **332**(6030): 721-725.

Paulk, A. C., A. M. Dacks and W. Gronenberg (2009). "Color processing in the medulla of the bumblebee (Apidae: *Bombus impatiens*)." J Comp Neurol **513**(5): 441-456.

Paulk, A. C., A. M. Dacks, J. Phillips-Portillo, J. M. Fellous and W. Gronenberg (2009). "Visual processing in the central bee brain." J Neurosci **29**(32): 9987-9999.

Paulk, A. C. and W. Gronenberg (2008). "Higher order visual input to the mushroom bodies in the bee, *Bombus impatiens*." Arthropod Struct Dev **37**(6): 443-458.

Paulk, A. C., J. Phillips-Portillo, A. M. Dacks, J. M. Fellous and W. Gronenberg (2008). "The processing of color, motion, and stimulus timing are anatomically segregated in the bumblebee brain." J Neurosci **28**(25): 6319-6332.

Paulk, A. C., J. A. Stacey, T. W. Pearson, G. J. Taylor, R. J. Moore, M. V. Srinivasan and B. van Swinderen (2014). "Selective attention in the honeybee optic lobes precedes behavioral choices." Proc Natl Acad Sci U S A **111**(13): 5006-5011.

Peitsch, D., A. Fietz, H. Hertel, J. de Souza, D. F. Ventura and R. Menzel (1992). "The spectral input systems of hymenopteran insects and their receptor-based colour vision." J Comp Physiol A **170**(1): 23-40.

Peng, F. and L. Chittka (2017). "A Simple Computational Model of the Bee Mushroom Body Can Explain Seemingly Complex Forms of Olfactory Learning and Memory." Curr Biol **27**(2): 224-230.

Perry, C. J. and A. B. Barron (2013). "Honey bees selectively avoid difficult choices." Proc Natl Acad Sci U S A **110**(47): 19155-19159.

Pouget, A., P. Dayan and R. Zemel (2000). "Information processing with population codes." Nature Reviews Neuroscience **1**(2): 125-132.

Quiroga, R. Q., L. Reddy, G. Kreiman, C. Koch and I. Fried (2005). "Invariant visual representation by single neurons in the human brain." Nature **435**(7045): 1102-1107.

Ribi, W., E. Warrant and J. Zeil (2011). "The organization of honeybee ocelli: Regional specializations and rhabdom arrangements." Arthropod Structure & Development **40**(6): 509-520.

Ribi, W. A. (1975). "The neurons of the first optic ganglion of the bee (*Apis mellifera*)." Adv Anat Embryol Cell Biol **50**(4): 1-43.

Ribi, W. A. and M. Scheel (1981). "The second and third optic ganglia of the worker bee: Golgi studies of the neuronal elements in the medulla and lobula." Cell Tissue Res **221**(1): 17-43.

Ringach, D. L., M. J. Hawken and R. Shapley (1997). "Dynamics of orientation tuning in macaque primary visual cortex." *Nature* **387**(6630): 281-284.

Rodriguez, I., A. Gumbert, N. Hempel de Ibarra, J. Kunze and M. Giurfa (2004). "Symmetry is in the eye of the beholder: innate preference for bilateral symmetry in flower-naïve bumblebees." *Naturwissenschaften* **91**(8): 374-377.

Roper, M., C. Fernando and L. Chittka (2017). "Insect Bio-inspired Neural Network Provides New Evidence on How Simple Feature Detectors Can Enable Complex Visual Generalization and Stimulus Location Invariance in the Miniature Brain of Honeybees." *PLOS Computational Biology* **13**(2): e1005333.

Rössler, W. and M. F. Brill (2013). "Parallel processing in the honeybee olfactory pathway: structure, function, and evolution." *J Comp Physiol A Neuroethol Sens Neural Behav Physiol* **199**(11): 981-996.

Rybak, J. and R. Menzel (1993). "Anatomy of the mushroom bodies in the honey bee brain: The neuronal connections of the alpha-lobe." *The Journal of Comparative Neurology* **334**(3): 444-465.

Sathees chandra, B. C., L. Geetha, V. A. Abraham, P. Karanth, K. Thomas, M. V. Srinivasan and R. Gadagkar (1998). "Uniform discrimination of pattern orientation by honeybees." *Anim Behav* **56**(6): 1391-1398.

Schneirla, T. C. (1951). "Bees." *Ecology* **32**(3): 562-565.

Seelig, J. D. and V. Jayaraman (2013). "Feature detection and orientation tuning in the *Drosophila* central complex." *Nature* **503**(7475): 262-266.

Seidl, R. and W. Kaiser (1981). "Visual field size, binocular domain and the ommatidial array of the compound eyes in worker honey bees." *Journal of comparative physiology* **143**(1): 17-26.

Si, A., S.-W. Zhang and R. Maleszka (2005). "Effects of caffeine on olfactory and visual learning in the honey bee (*Apis mellifera*)." *Pharmacology Biochemistry and Behavior* **82**(4): 664-672.

Skrzipek, K.-H. and H. Skrzipek (1974). "The ninth retinula cell in the ommatidium of the worker honey bee (*Apis mellifica* L.)." *Zeitschrift für Zellforschung und Mikroskopische Anatomie* **147**(4): 589-593.

Smolla, M., S. Alem, L. Chittka and S. Shultz (2016). "Copy-when-uncertain: bumblebees rely on social information when rewards are highly variable." *Biol Lett* **12**(6).

Spalshoff, C., R. Gerdes and R. Kurtz (2012). "Neuronal representation of visual motion and orientation in the fly medulla." *Front Neural Circuits* **6**: 72.

Spetch, M. L. and A. Friedman (2003). "Recognizing rotated views of objects: interpolation versus generalization by humans and pigeons." *Psychon Bull Rev* **10**(1): 135-140.

Spinozzi, G., G. Lubrano and V. Truppa (2004). "Categorization of above and below spatial relations by tufted capuchin monkeys (*Cebus apella*)." *J Comp Psychol* **118**(4): 403-412.

Srinivasan, M. V. and M. Lehrer (1988). "Spatial acuity of honeybee vision and its spectral properties." *Journal of Comparative Physiology A* **162**(2): 159-172.

Srinivasan, M. V., M. Lehrer, S. W. Zhang and G. A. Horridge (1989). "How honeybees measure their distance from objects of unknown size." *Journal of Comparative Physiology A* **165**(5): 605-613.

Srinivasan, M. V. and S. W. Zhang (1997). Visual control of honeybee flight. *Orientation and Communication in Arthropods*. M. Lehrer. Basel, Birkhäuser Basel: 95-113.

- Srinivasan, M. V., S. W. Zhang and B. Rolfe (1993). "Is pattern vision in insects mediated by 'cortical' processing?" *Nature* **362**(6420): 539-540.
- Srinivasan, M. V., S. W. Zhang and K. Witney (1994). "Visual Discrimination of Pattern Orientation by Honeybees: Performance and Implications for 'Cortical' Processing." *Philosophical Transactions of the Royal Society of London B: Biological Sciences* **343**(1304): 199-210.
- Stach, S., J. Benard and M. Giurfa (2004). "Local-feature assembling in visual pattern recognition and generalization in honeybees." *Nature* **429**(6993): 758-761.
- Stach, S. and M. Giurfa (2001). "How honeybees generalize visual patterns to their mirror image and left-right transformation." *Animal Behaviour* **62**(5): 981-991.
- Stach, S. and M. Giurfa (2005). "The influence of training length on generalization of visual feature assemblies in honeybees." *Behav Brain Res* **161**(1): 8-17.
- Strausfeld, N. J. (2002). "Organization of the honey bee mushroom body: representation of the calyx within the vertical and gamma lobes." *J Comp Neurol* **450**(1): 4-33.
- Streinzer, M., A. Brockmann, N. Nagaraja and J. Spaethe (2013). "Sex and Caste-Specific Variation in Compound Eye Morphology of Five Honeybee Species." *Plos One* **8**(2).
- Sturzl, W., N. Boeddeker, L. Dittmar and M. Egelhaaf (2010). "Mimicking honeybee eyes with a 280 degrees field of view catadioptric imaging system." *Bioinspir Biomim* **5**(3): 036002.
- Su, S. K., F. Cai, A. Si, S. W. Zhang, J. Tautz and S. L. Chen (2008). "East Learns from West: Asiatic Honeybees Can Understand Dance Language of European Honeybees." *Plos One* **3**(6).
- Sun, X.-J., C. Fonta and C. Masson (1993). "Odour quality processing by bee antennal lobe interneurons." *Chemical Senses* **18**(4): 355-377.
- Sutherland, N. S. (1957). "Visual discrimination of orientation by octopus." *Br J Psychol* **48**(1): 55-71.
- Switzer, P. V. and W. Walters (1999). "Choice of lookout posts by territorial amberwing dragonflies, *Perithemis tenera* (Anisoptera : Libellulidae)." *Journal of Insect Behavior* **12**(3): 385-398.
- Szyszka, P., M. Ditzen, A. Galkin, C. G. Galizia and R. Menzel (2005). "Sparsening and temporal sharpening of olfactory representations in the honeybee mushroom bodies." *J Neurophysiol* **94**(5): 3303-3313.
- Szyszka, P., A. Galkin and R. Menzel (2008). "Associative and non-associative plasticity in Kenyon cells of the honeybee mushroom body." *Frontiers in Systems Neuroscience* **2**.
- Takemura, S.-y., C. S. Xu, Z. Lu, P. K. Rivlin, T. Parag, D. J. Olbris, S. Plaza, T. Zhao, W. T. Katz, L. Umayam, C. Weaver, H. F. Hess, J. A. Horne, J. Nunez-Iglesias, R. Aniceto, L.-A. Chang, S. Lauchie, A. Nasca, O. Ogundeyi, C. Sigmund, S. Takemura, J. Tran, C. Langille, K. Le Lacheur, S. McLin, A. Shinomiya, D. B. Chklovskii, I. A. Meinertzhagen and L. K. Scheffer (2015). "Synaptic circuits and their variations within different columns in the visual system of *Drosophila*." *Proceedings of the National Academy of Sciences of the United States of America* **112**(44): 13711-13716.
- Taylor, G. J., T. Luu, D. Ball and M. V. Srinivasan (2013). "Vision and air flow combine to streamline flying honeybees." *Sci Rep* **3**: 2614.
- v. Frisch, K. (1927). *Das Bienenvolk. Aus dem Leben der Bienen*. Berlin, Heidelberg, Springer Berlin Heidelberg: 1-4.
- v. Frisch, K. (1914). *Der farbensinn und Formensinn der Biene*. Jena, Fischer.

- van Hateren, J. H., M. V. Srinivasan and P. B. Wait (1990). "Pattern recognition in bees: orientation discrimination." Journal of Comparative Physiology A **167**(5): 649-654.
- Varela, F. G. and W. Wiitanen (1970). "The Optics of the Compound Eye of the Honeybee (*Apis mellifera*)." The Journal of General Physiology **55**(3): 336-358.
- Vergoz, V., E. Roussel, J. C. Sandoz and M. Giurfa (2007). "Aversive learning in honeybees revealed by the olfactory conditioning of the sting extension reflex." PLoS One **2**(3): e288.
- Wakakuwa, M., M. Kurasawa, M. Giurfa and K. Arikawa (2005). "Spectral heterogeneity of honeybee ommatidia." Naturwissenschaften **92**(10): 464-467.
- Wehner, R. (1967). "Pattern recognition in bees." Nature **215**(5107): 1244-1248.
- Wehner, R. and I. Flatt (1977). "Notizen: Visual Fixation in Freely Flying Bees." Zeitschrift für Naturforschung C **32**(5-6): 469-472.
- Witthöft, W. (1967). "Absolute Anzahl und Verteilung der Zellen im Hirn der Honigbiene." Zeitschrift für Morphologie der Tiere **61**(1): 160-184.
- Wolf, S. and L. Chittka (2016). "Male bumblebees, *Bombus terrestris*, perform equally well as workers in a serial colour-learning task." Animal Behaviour **111**: 147-155.
- Yacoub, E., N. Harel and K. Ugurbil (2008). "High-field fMRI unveils orientation columns in humans." Proc Natl Acad Sci U S A **105**(30): 10607-10612.
- Yang, E.-C., H.-C. Lin and Y.-S. Hung (2004). "Patterns of chromatic information processing in the lobula of the honeybee, *Apis mellifera* L." Journal of Insect Physiology **50**(10): 913-925.
- Zhang, S.-W. and G. A. Horridge (1992). "Pattern Recognition in Bees: Size of Regions in Spatial Layout." Philosophical Transactions of the Royal Society of London B: Biological Sciences **337**(1279): 65-71.